

Portland State University

**PDXScholar**

---

Environmental Science and Management  
Professional Master's Project Reports

Environmental Science and Management

---

Winter 2014

# Modeling Effective Shade to Prioritize Riparian Restoration Efforts in the Johnson Creek Watershed, OR

Brittany Sahatjian  
*Portland State University*

Follow this and additional works at: [https://pdxscholar.library.pdx.edu/mem\\_gradprojects](https://pdxscholar.library.pdx.edu/mem_gradprojects)



Part of the [Environmental Health and Protection Commons](#), and the [Environmental Indicators and Impact Assessment Commons](#)

**Let us know how access to this document benefits you.**

---

## Recommended Citation

Sahatjian, Brittany, "Modeling Effective Shade to Prioritize Riparian Restoration Efforts in the Johnson Creek Watershed, OR" (2014). *Environmental Science and Management Professional Master's Project Reports*. 42.

[https://pdxscholar.library.pdx.edu/mem\\_gradprojects/42](https://pdxscholar.library.pdx.edu/mem_gradprojects/42)

<https://doi.org/10.15760/mem.49>

This Project is brought to you for free and open access. It has been accepted for inclusion in Environmental Science and Management Professional Master's Project Reports by an authorized administrator of PDXScholar. Please contact us if we can make this document more accessible: [pdxscholar@pdx.edu](mailto:pdxscholar@pdx.edu).

# Modeling Effective Shade to Prioritize Riparian Restoration Efforts in the Johnson Creek Watershed, OR

---

Project report for the Masters in Environmental  
Management Program at Portland State  
University

**Brittany Sahatjian**

**3/12/2014**

# Table of Contents

|   |     |
|---|-----|
| Figures.....  | ii  |
| Tables.....   | ii  |
| Acknowledgments.....  | iii |
| Abstract.....   | iv  |
| 1.0 Introduction .....  | 1   |
| 2.0 Methods.....  | 8   |
| 2.1 Study Area.....   | 8   |
| 2.2 Overview of Methods .....                                   | 13  |
| 2.3 Data Derivation .....                                       | 15  |
| 2.3.1 Base Data .....   | 15  |
| 2.3.2 Restored Conditions.....                                  | 17  |
| 2.3.3 Sampling for Modeling Inputs.....                         | 23  |
| 2.3.4 Vegetation Density.....                                   | 30  |
| 2.4 Modeling .....  | 33  |
| 2.2.1 Solar Position .....                                      | 34  |
| 2.2.2 Potential Incoming Solar Radiation.....                   | 37  |
| 2.2.3 Solar Radiation Blocked by Vegetation and Topography..... | 39  |
| 2.2.4 Effective Shade.....                                      | 42  |
| 2.2.5 Model Execution .....                                     | 43  |
| 2.5 Effective Shade Analysis.....                               | 44  |
| 2.6 Restoration Prioritization.....                             | 45  |
| 2.7 Quality Control.....  | 48  |
| 3.0 Results.....  | 53  |
| 3.1 Effective Shade.....  | 53  |
| 3.2 Restored Conditions.....                                    | 57  |
| 3.3 Priority Rankings by Taxlot.....                            | 57  |
| 3.4 Priority Rankings by Subwatershed .....                     | 63  |
| 3.5 Priority Rankings by Jurisdiction .....                     | 69  |
| 4.0 Discussion.....   | 75  |
| 4.1 Summary of Findings.....                                    | 75  |
| 4.2 Model Assumptions .....                                     | 76  |

|                              |    |
|------------------------------|----|
| 4.3 Restored Conditions..... | 80 |
| 4.4 Priority Rankings .....  | 82 |
| 5.0 Conclusion.....          | 86 |
| References .....             | 90 |
| Glossary.....                | 95 |

## Figures

|  |    |
|--|----|
| Figure 1: Jurisdictional boundaries .....  | 10 |
| Figure 2: Subwatershed boundaries .....  | 11 |
| Figure 3: Total restorable area in watershed.....  | 20 |
| Figure 4: Example of restored conditions .....   | 21 |
| Figure 5: Radial sampling pattern .....  | 26 |
| Figure 6: Series of radial sampling patterns along a single stream. ....                     | 27 |
| Figure 7: Effective shade formula .....  | 34 |
| Figure 8: Polygon-to-point conversion .....  | 47 |
| Figure 8: Field measurements vs. modeling estimates of percent effective shade .....         | 53 |
| Figure 10: Current and Restored Effective Shade Estimates .....                              | 55 |
| Figure 11: Increase in Effective Shade under Restoration Scenario .....                      | 56 |
| Figure 12: Taxlot priority rankings chart.....   | 60 |
| Figure 13: Taxlot priorities eastern watershed.....  | 61 |
| Figure 14: Taxlot priorities: western watershed.....   | 62 |
| Figure 15: Subwatershed priority rankings chart.....   | 65 |
| Figure 16: Subwatershed rankings map.....  | 66 |
| Figure 17: Restorable acres within each subwatershed .....                                   | 67 |
| Figure 18: Percent of each subwatershed's restoration buffer deemed restorable .....         | 68 |
| Figure 19: Jurisdictional priority rankings chart.....                                       | 71 |
| Figure 20: Map of jurisdictional priority rankings.....                                      | 72 |
| Figure 21: Restorable acres within each jurisdiction .....                                   | 73 |
| Figure 22: Percent of each jurisdiction's restoration buffer that is deemed restorable. .... | 74 |

## Tables

|   |    |
|---|----|
| Table 1: Characteristics of most common riparian tree species planted in riparian restoration projects. | 23 |
| Table 2: Modeling input parameters derived from geospatial data.....                                    | 24 |
| Table 3: Effective Shade Summary Statistics .....   | 54 |
| Table 4: Summary statistics for taxlot priority rankings .....  | 59 |
| Table 5: Summary statistics for subwatershed priority rankings .....                                    | 64 |
| Table 6: Summary statistics for Jurisdictional rankings .....   | 70 |

## Acknowledgments

Thank you to Ryan Michie from ODEQ for helping me with every aspect of this project; without the training, resources, insight and guidance you provided this project would not have been possible. Thank you to my academic advisor Dr. Joseph Maser for providing me with the skills and encouragement to stay on track, stay organized, and stay focused. Thank you to Dr. Alan Yeakley for taking the time to serve on my MEM committee and for providing valuable insight, advice, and feedback. Thank you Robin Jenkinson, from the Johnson Creek Watershed Council, for helping me find a project that fit my interests, inviting me to attend Inter-Jurisdictional Committee meetings and events, and providing me with essential base data, guidance and feedback along the way. I'd also like to thank the Johnson Creek Watershed Council and Johnson Creek Watershed Inter-Jurisdictional Committee for allowing me to work with them and use them as a resource, making space for my project in their meeting agendas, providing essential guidance and feedback throughout the project, and for their genuine interest and involvement with the project in general.

## Abstract

The influence of stream temperature on the survival and reproductive success of anadromous salmonid populations has become an increasingly concerning issue in the Pacific Northwest. Enhancing the height, density and extent of riparian vegetation is widely accepted as one of the most effective strategies for reducing stream temperatures, while also providing numerous ancillary benefits. Effective shade is defined as the percentage of direct beam solar radiation attenuated and scattered by riparian vegetation before reaching the stream surface and is a commonly used criterion for choosing where to restore riparian vegetation. This project aims to prioritize sites for riparian restoration through effective shade modeling within the geographic extent of the Johnson Creek watershed. Modeling inputs included a limited set of channel morphology and riparian vegetation attributes and were sampled from high spatial resolution LiDAR derived raster datasets (3 ft.) using Python script programming tools. A separate raster was created to depict restored conditions, in which the height of all restorable riparian vegetation is set equal to 27 meters. Using the stream temperature model, Heat Source, effective shade simulations were performed along the mainstem Johnson Creek and all tributary streams over the duration of a single day in August. Model outputs provided effective shade and daily solar flux attenuation estimates under current and restored conditions, the difference of which represented the net benefit, in terms of shade, that would result from restoration. Model outputs were used to evaluate the current level of effective shade in the watershed and to prioritize restoration efforts at the taxlot, subwatershed and jurisdictional scale. Currently, effective shade is 73% on average for all streams in watershed. Under a restoration scenario, 544.9 acres would be restored resulting in the additional solar flux reduction of 209,118.9 watts/m<sup>2</sup>/d. Restoring only 22% of all taxlots or 21% of all restorable acres would accomplish 50% of the cumulative solar flux reduction. Restoring 38% of all taxlots or 55% of all restorable acres would accomplish 90% of the cumulative solar flux reduction. Prioritizing at the taxlot scale, as opposed to subwatersheds or jurisdictions, promotes a higher level of efficiency in the prioritization of restoration efforts. All taxlots should be further screened prior to final prioritization for opportunistic prospects such as landowner willingness, community support or proximity to existing restoration projects, and fundraising opportunities.

## 1.0 Introduction

### *Salmon and Stream Temperature*

Salmonid populations in the Pacific Northwest have dramatically declined since European settlement, primarily due to the degradation of coldwater habitat (Allen *et al.* 2007). Currently, six salmonid species are listed under the Endangered Species Act as threatened or endangered in Oregon alone (National Marine Fisheries Service (NMFS) 2013; US Fish and Wildlife Service (USFWS) 2013). Above all other water quality attributes, elevated water temperatures are particularly harmful to all life stages of salmonid species, causing weight loss, disease, competitive displacement or death (Beschta 1997; Oregon Department of Environmental Quality (ODEQ) 2006; Richter & Kolmes 2005). As water quality continues to degrade, the influence of stream temperature on the survival and reproductive success of anadromous salmonid populations has become an increasingly concerning issue in the Pacific Northwest (Allen *et al.* 2007; Chen *et al.* 1998; ODEQ 2006). As such, restoring thermal regimes is a major component of salmonid conservation and management (Richter & Kolmes 2005).

Every year, millions of dollars are spent on watershed restoration efforts aimed at increasing the abundance and resiliency of native salmonid populations in this region (OWEB 2007; Roni *et al.* 2010), yet many wild populations continue to decline causing policy makers, natural resource managers, and stakeholders to question the effectiveness of these efforts and continue their search for innovative and socio-economically feasible solutions (Beechie & Bolton 1999; Beschta 1997; Roni *et al.* 2002, 2008, 2010; Watanabe *et al.* 2005). By nature, salmonid populations are highly adapted to unique local conditions composed of spatially and temporally variable ecological processes and are known to exhibit large inter-annual fluctuations in abundance (Beechie & Bolton 1999; Richter & Kolmes 2005; Roni *et al.* 2002, 2010). When combined, these distinguishing features tend to confound management efforts and can impede attainment of restoration goals. The cumulative effects of human population growth,

competing societal priorities, and climate change are expected to further exacerbate the challenges associated with restoring salmon runs in the Pacific Northwest (Richter & Kolmes 2005). In sum, there is a growing need for cost-effective restoration strategies that will successfully promote and sustain salmonid populations in the Pacific Northwest.

### *Stream Temperature Regulations*

Water quality standards are established to protect the beneficial uses of state waters such as irrigation, recreation, hydropower or fish and aquatic life (CWA 40 CFR 131; Environmental Protection Agency (EPA) 1994; ODEQ 2011). In the Pacific Northwest, water quality policy is largely driven by the need to protect the beneficial use of fish and aquatic life from the effects of water quality degradation. Fish and aquatic life are typically the most sensitive beneficial use to water temperature, with anadromous salmonid species being particularly vulnerable to temperature changes (Boyd and Sturdevant 1997). The distribution, health, and survival of salmonid species, for example, is greatly influenced by stream temperature largely due to their cold-blooded, or ectothermic, nature (Bisson *et al.* 1992; Boyd and Sturdevant, 1997; Brungs and Jones, 1977; Fryer and Pilcher, 1974; ODEQ 1995). Temperature standards are designed to accommodate the temperature needs of all fish and aquatic life, including specific salmonid life stages (Nehlsen 1997; ODEQ 2008; Palmer 2009; Roni *et al.* 2010).

In Oregon, numeric stream temperature criteria, expressed as a 7-day moving average of daily maximum temperatures, are determined by ODEQ and approved by the EPA based on the upper optimal physiological temperature preferences known to support the biological processes required in salmonid spawning, rearing, and migration life stages (ODEQ 2008; Richter & Kolmes 2005). In general, stream temperatures between 18-25 °C that last anywhere from hours to months can cause thermal stress, leading to weight loss, disease or competitive displacement (Boyd and Sturdevant, 1997; Brungs and Jones, 1977; Fryer and Pilcher, 1974; ODEQ 1995). Given sufficient time, these same temperatures can



also cause thermally induced fish mortality for species that are poorly adapted to the prevailing conditions (Richter & Kolmes 2005). Streams that are found to violate water quality standards will be listed on the 303(d) list as water quality impaired and the formation of total maximum daily load (TMDL) allowances for pollutants of concern will be required (ODEQ 2008). TMDL's are developed by the Oregon Department of Environmental Quality (ODEQ) and submitted to the Environmental Protection Agency (EPA) for approval. TMDL's generally serve to identify the pollutant of concern, develop a loading capacity, identify pollutant sources and determine waste load allocations (ODEQ 2011). ODEQ will then work with implicated local or state agencies such as the Oregon Department of Agriculture (ODA), Oregon Department of Forestry (ODF), Oregon Fish and Wildlife Service (FWS) or city and county jurisdictional representatives, to implement the TMDL and attain the objectives.

### *Effective Shade Targets*

With respect to water temperature, heat is the pollutant of concern which can enter the stream as direct solar radiation (non-point sources) or heated effluent from point sources. A temperature TMDL defines the amount of thermal energy that can be discharged or allowed to enter into a water body without exceeding water temperature standards, and distributes allocations to point and nonpoint sources (Niemi *et al.* 2006; ODEQ 2011). For many streams, 100% of all heat loading originates from non-point sources due to a lack of adequate riparian vegetation and/or extensive channelization of the stream channel. In these circumstances, compliance with waste load allocations is attained through riparian restoration efforts.

Riparian vegetation provides a physical barrier between the stream and the sun that can attenuate and deflect incoming solar radiation (Boyd and Kasper 2003; Boyd and Sturdevant 1997). Although solar radiation is just a part of the heat budget for any given stream, it is the most important source of radiation in terms of temperature regulation, particularly in mid latitude regions during the summer

months (Allen *et al.* 2007; Beschta 1997; Boyd and Sturdevant 1997; Johnson 2003; Li *et al.* 2012). As such, enhancing riparian vegetation (canopy height, density, and buffer extent) is widely accepted as one of the most effective strategies for reducing stream temperatures, while also providing numerous ancillary benefits including erosion control, flood mitigation, water purification, improved channel complexity, formation of in-stream and riparian habitat and general ecosystem resilience (Chen *et al.* 1998; Gebhardt & Fischer 1999; Holmes *et al.* 2004; Johnson *et al.* 2007; Kentula 2007; Li *et al.* 2012; Niemi *et al.* 2006; ODEQ 2006; Teels *et al.* 2006). More specifically, riparian vegetation promotes the formation of habitat through large woody debris (LWD) recruitment, by creating narrower, more complex stream channels with reduced width to depth ratios, and by providing a microclimate along the streambank characterized by cooler air temperature, reduced wind speed, and higher relative humidity (Gergel *et al.* 2007; Opperman & Merenlender 2004).

**Effective shade**<sup>1</sup> is defined as the percentage of direct beam solar radiation attenuated and scattered by riparian vegetation before reaching the ground or stream surface (ODEQ 2006). In simple terms, effective shade is a function of solar positioning, geographic location, riparian vegetation and stream channel morphology. For example, the height of riparian vegetation controls the shadow length cast across the stream surface, solar positioning controls the timing and direction of the shadow, and the channel width determines the length of shadow necessary to shade the stream surface (Boyd & Kasper 2003). A strong predictive relationship has been observed between effective shade and stream temperature and, as such, it was selected by the Environmental Protection Agency (EPA) and ODEQ as a surrogate measure for stream temperature (Gebhardt & Fischer 1999; Li *et al.* 2012; ODEQ 2006). In general, surrogate measures are intended to provide managers with a cost-effective and workable tool for pollutant loading assessment and allocations (Gebhardt & Fischer 1999). When compared to stream temperature, effective shade is more stable over short periods of time, can be sampled and derived

---

<sup>1</sup> Note to reader: all text in bold is included in the Glossary at the end of this document.

from widely available remotely sensed data sources, is easily translated into quantifiable management objectives and is more sensitive and responsive to management changes (Chen *et al.* 1998; Gebhardt & Fischer 1999; ODEQ 2006). For streams that exceed water temperature standards due to a lack of adequate riparian vegetation, reach-specific **effective shade targets**<sup>2</sup> may be developed during the TMDL process to identify the level of shade needed to attain compliance with water quality standards for stream temperature (Sturdevant 2008). Attainment of effective shade targets is equivalent to attainment of non-point source (NPS) load allocations (ODEQ 2006). Consequently, a common approach to prioritizing restoration efforts aimed at stream temperature reduction involves the use of riparian vegetation, valued in terms of effective shade, as the **site suitability criteria**<sup>3</sup>.

### *Johnson Creek Watershed*

Johnson Creek and its tributaries experience annual warming beginning in late spring and lasting through the fall, largely due to anthropogenic non-point sources of heat loading. During this period, stream temperatures often exceed the criteria established to protect salmon and trout habitat during discrete life stages. Johnson Creek was 303(d) listed for temperature in 1998 due to observed exceedances of the biologically based numeric criteria for salmon and trout rearing (18° C) in the summertime of 1992. The Willamette Basin TMDL which was completed in 2006 further modified the listing for Johnson Creek. Two numeric criteria currently apply to Johnson Creek: salmon and trout rearing and migration (18° C) applies year round for most of the mainstem (river mile 0-23.7) while the criteria for salmon and steelhead spawning (13° C) applies October 15-May 15 from river mile 0.2-10.5.

---

<sup>2</sup> **Effective shade targets** define the level of effective shade required to attain desired stream temperatures and remain in compliance with water quality standards for temperature. In other words, they translate nonpoint source solar radiation loads into streamside vegetation objectives (ODEQ 2006).

<sup>3</sup> **Site suitability criteria** are ecological, socioeconomic, or physical attributes used to identify areas that are most deserving of restoration.

During TMDL development, natural background radiation under the system potential condition was found to consume all assimilative capacity in Johnson Creek and, as such, received 100% of the waste load allocation. This meant that all anthropogenic sources of heat loading, including degraded stream channel and riparian vegetation conditions, would need to be attenuated. Site specific shade targets were determined during TMDL development to be 80% on average for the mainstem (ODEQ 2006). Additionally, the 2006 TMDL states that the stream temperature and effective shade targets apply to both the mainstem and all tributaries since tributaries are known to contribute heat loading to the mainstem.

In 2012 and 2013, the Johnson Creek Watershed Inter-Jurisdictional Committee (JCW-IJC) placed temperature loggers throughout the watershed to determine the location, magnitude, and duration of temperature standard exceedances still occurring. Results of these efforts reveal that the mainstem and many tributaries continue to exceed temperature standards for salmon and trout rearing and migration (18° C) with the exception of a few well-shaded tributaries. As of 2013, the duration of temperature exceedances at each logger ranged from 2-113 days per year, with maximum recorded temperatures between 20-19.7° C. Only two locations (out of 41) remained in compliance year round.

Existing riparian vegetation in the watershed generally consists of mixed forest with some coniferous forest and shrub areas (Johnson Creek Watershed Council (JCWC) 2002). Many areas are dominated by blackberry, or young native plants and large mature trees (City of Portland 2005; JCWC 2002). While some of the smaller headwater creeks have extensive riparian vegetation, all other riparian areas are either narrow, minimal, or lacking (JCWC 2002). While numerous riparian restoration efforts have taken place in the watershed, temperatures continue to exceed the numeric criteria for salmon spawning and rearing. Additional riparian efforts are needed to achieve effective shade targets established in the TMDL and reduce stream temperatures. Confounding this issue is the fact that

financial resources are limited and effective shade data are lacking for the tributaries of Johnson Creek (ODEQ 2006). Combined, these factors make it difficult to prioritize areas for riparian restoration and allocate resources in a cost-effective manner.

### *Purpose of Project*

The purpose of this project is to assist the Johnson Creek Watershed Council (JCWC) in prioritizing areas for riparian restoration within the geographic extent of the Johnson Creek Watershed. Modeling effective shade along Johnson Creek and its tributaries, under current and restored conditions, will help to identify areas that produce the greatest benefit, in terms of shade, per unit restored.

There are two main objectives of the project: modeling effective shade under current and restored conditions and prioritizing areas for riparian restoration based on where the largest gains, in terms of shade, occur as a result of restoration. The first objective involves modeling effective shade for all Johnson Creek tributaries and mainstem using Heat Source, a data intensive heat transfer process model. The model will calculate solar flux at the stream surface and percent effective shade under both current and restored conditions, the latter of which will represent a theoretical restoration scenario characterized by user defined parameters. Effective shade estimates under current and restored conditions will be used to evaluate the current level of effective shade in the watershed, and to determine if restored conditions are sufficient to attain an average of 80% effective shade for all streams in the watershed. For the second objective, modeling results will be used to prioritize restoration efforts at the taxlot, subwatershed and jurisdictional scale, based on where the largest gains in **solar flux attenuation**<sup>4</sup> occur under restored conditions. The spatial extent of this study includes both the mainstem and all tributaries of Johnson Creek while, temporally, restoration objectives project out approximately 55 years.

---

<sup>4</sup> **Solar flux attenuation** is defined in this study as the amount of incoming direct beam solar radiation that is attenuated by riparian vegetation before reaching the stream surface.

## 2.0 Methods

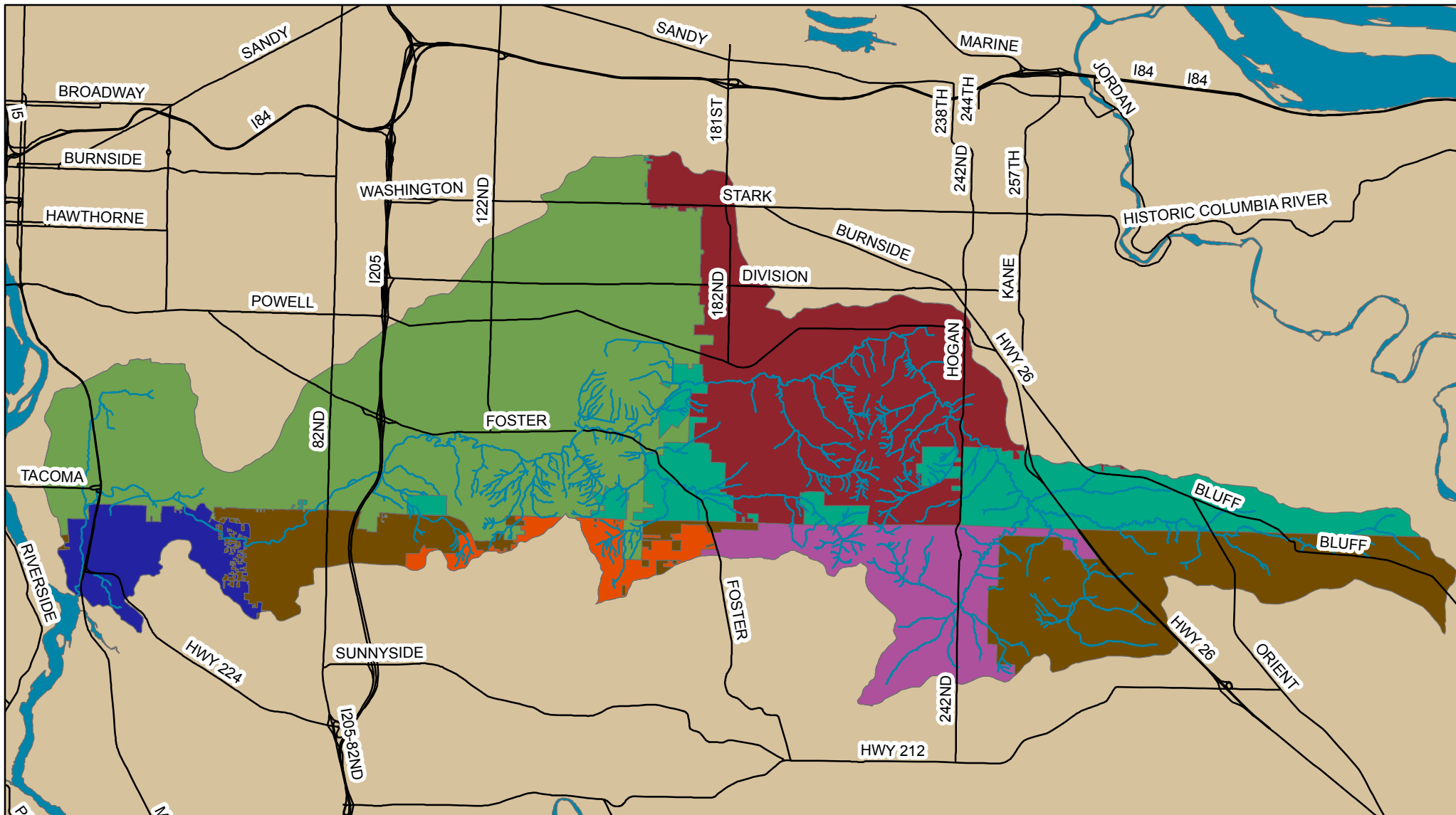
### 2.1 Study Area

#### *Geography*








The **study area** for this project includes all streams and near-stream vegetation within the Johnson Creek watershed, which encompasses two USGS 12-digit Hydrologic Units, Lower Johnson Creek (170900120103) and Upper Johnson Creek (170900120101). The Johnson Creek watershed occupies a relatively small but densely populated area of 54 square miles within the Willamette River Basin in Oregon. The watershed is home to 180,000 people and includes portions of the cities of Milwaukie, Portland, Gresham, Happy Valley and Damascus and Multnomah and Clackamas counties (see Figure 1). The creek itself travels 26 miles west from its headwaters at the foothills of the Cascade Range, near Boring, to its confluence with the Willamette River in Milwaukie. The creek is fed by numerous springs, surface runoff, and 50 inches of annual precipitation. Major tributaries include Badger, Kelley, Mitchell, Sunshine, Veterans and Crystal Spring creeks. A total of 40 subwatersheds, ranging from <1 to 7 mi<sup>2</sup> are recognized by the Johnson Creek Watershed Council (see Figure 2).

The geology of the watershed traces back to the Missoula floods and the Columbia River basalt group, which collectively deposited a thick layer of sediment underlain by thick basalt lavas. Large, flat, floodplains dominate the northern part of the watershed as a result of these historic floods (BES 2001). Most of the watershed's tributaries are located in the southern part of the watershed, where the topography is steep and varied (BES 2001). Elevation varies between 26-1100 feet above sea level and slopes generally range between 1-25%, with a few localized exceptions such as Mt. Scott and Powell Butte (10-30% slope).

Johnson Creek passes through heavily developed residential, commercial, and industrial areas before emptying into the Willamette River (Niemi *et al.* 2006). In general, the upper portion of the watershed is dominated by agricultural and rural residential land uses while the lower portion contains heavily developed urban areas (JCWC 2002).



### Jurisdiction

- |   |   |
|---|---|
|  Damascus     |  Milwaukie                         |
|  Gresham      |  Portland                          |
|  Happy Valley |  Clackamas County (unincorporated) |
|   |  Multnomah County (unincorporated) |

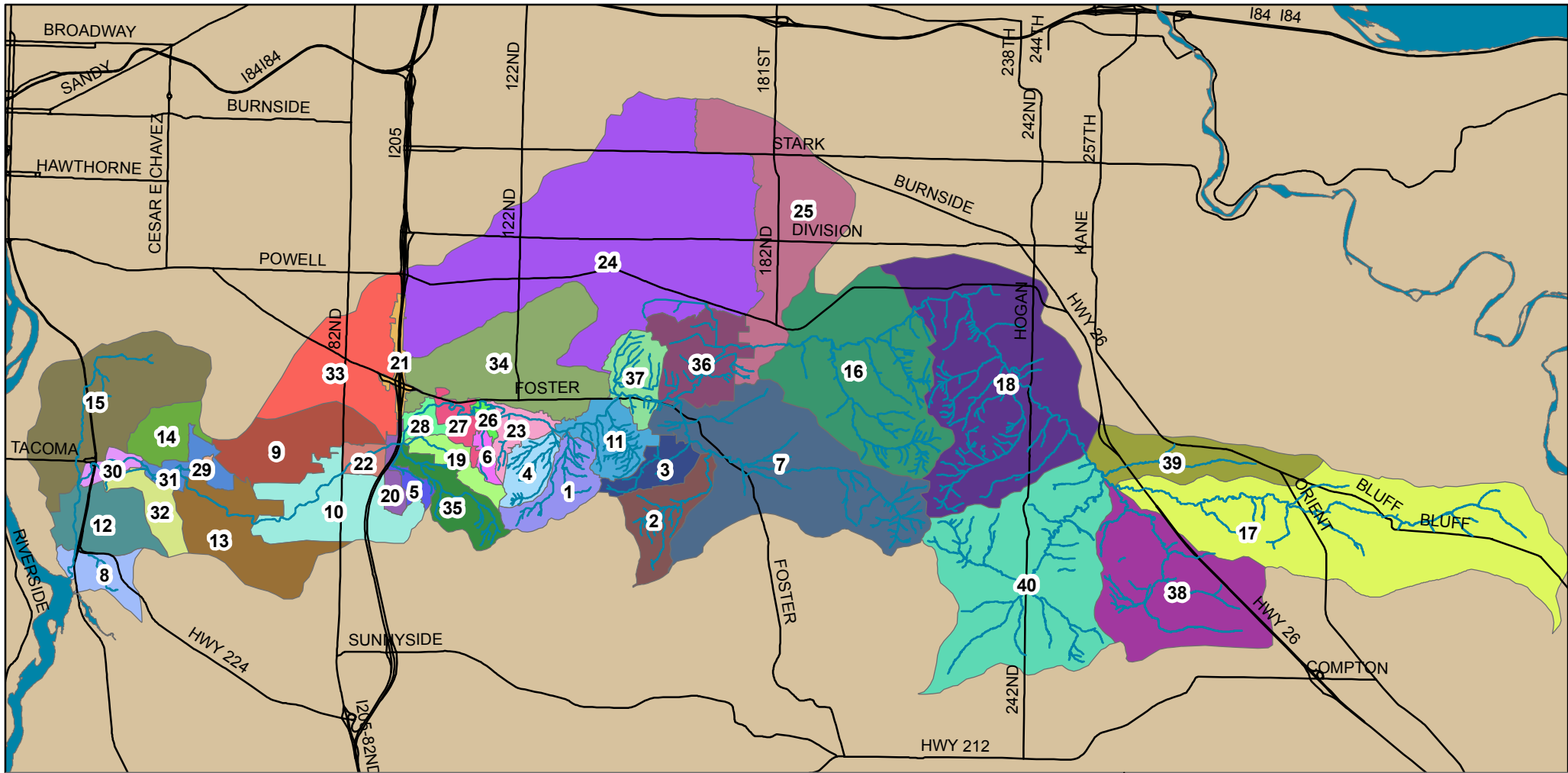
**Figure 1: Jurisdictional Boundaries in the Johnson Creek Watershed**

March, 2014

0 1.25 2.5 5 Miles







| Subwatersheds           |                            |                         |                       |
|-------------------------|----------------------------|-------------------------|-----------------------|
| Crystal Springs, 15     | Hogan, 18                  | South 205, 20           |                       |
| Ardenwald, 32           | Deardorff, 1               | Indian, 19              | Spring, 8             |
| Badger, 38              | East Clackamas Co, 10      | Kelley, 7               | Sunshine, 40          |
| Barbara-Welch, 11       | East Lents, 27             | Milwaukie, 12           | Three Bridges, 30     |
| Brentwood/Darlington, 9 | East Powell Butte, 36      | Mitchell, 2             | Tideman, 31           |
| Brookside, 26           | Eastmoreland/Woodstock, 14 | North 205, 21           | Veterans, 35          |
| Butler, 16              | Errol, 29                  | North Fork, 39          | Wahoo, 4              |
| Cedar, 23               | Freeway Land, 28           | North Powell Butte, 24  | West Clackamas Co, 13 |
| Clatsop, 3              | Frog, 6                    | Powellhurst-Gilbert, 34 | West Gresham, 25      |
| Cottonwood, 5           | Headwaters, 17             | SE 82nd Corridor, 33    | West Lents, 22        |
|                         |                            |                         | West Powell Butte, 37 |

**Figure 2: Subwatershed Boundaries in the Johnson Creek Watershed**

March, 2014



## *Disturbance History/ Ecological Integrity*

Gradual development of the watershed has adversely impacted the ecological integrity of the watershed. Before urbanization, the Johnson Creek watershed hosted a diverse array of habitats including forests, marshes and wetlands (BES 2001). As settlers arrived, the emergence of sawmills, agriculture, ranching and general industrial, commercial or residential development gradually began to diminish natural resources and degrade ecological functioning within the watershed (BES 2001). In the 1930's the Works Progress Administration (WPA) straightened, deepened, and lined the mainstem with rock in an effort to control flooding (BES 2001). Unfortunately, these and other flood control strategies have accomplished very little in terms of flood control, and have instead contributed to degraded streambank and wetland conditions (BES 2001). Native species of salmon and trout, once plentiful in Johnson Creek, were severely depleted by the 1980's; many of these native populations were eventually listed as threatened under the Endangered Species Act (ESA) during the late 1990's (BES 2001).

Beginning in the 1990's, fish surveys have periodically been performed to determine the species and extent of fish presence in the watershed (JCWC 2002, 2012). While salmon and trout species still inhabit Johnson Creek, their abundance has been reduced to a fraction of historic levels (JCWC 2012). There are three salmonid species listed as threatened under the ESA that are known to occur within the Johnson creek watershed: the Lower Columbia River Chinook Salmon Evolutionarily Significant Unit (ESU), Lower Columbia River Coho Salmon ESU, and Lower Columbia River Steelhead Distinct Population Segment (DPS). In addition, coastal cutthroat occurs within the watershed but is not listed under the ESA within the extent of the watershed. Recent fish surveys (2011) found native salmonid species occurring in nearly every tributary surveyed, even in small intermittent streams (JCW-IJC).

There is a clear need for riparian restoration in the Johnson Creek Watershed to protect salmon populations and meet TMDL requirements for stream temperature. Disturbance or removal of riparian

vegetation, channel modification, and alteration of the hydrologic regime resulting from historical development has greatly compromised ecological functioning within the watershed. Overall water quality and habitat conditions in the Johnson creek watershed are generally rated as poor, with problems related to sediment, bacteria, water temperature, streamflow, flooding and chemical contamination currently present (BES 2001; ODEQ 2005). Current in-stream and riparian conditions are characterized by extensive bank erosion, few pools, little to no LWD, homogenous channel bedform, substrate dominated by fine sediments and high levels of channel incision, all of which provide very little benefit to native salmonid populations in terms of habitat (BES 2001). Of particular relevance to this study, optimum salmon and trout habitat requires an average of 80% effective shade (JCWC 2012), yet as of 2002, effective shade on the mainstem of Johnson Creek averaged only 40% leaving ample room for improvement.

## 2.2 Overview of Methods

Prioritizing riparian restoration efforts using effective shade as the site suitability criteria typically involves a determination of current and restored conditions in terms of effective shade (Harris & Olson 1997; Landers 1997; Palmer *et al.* 2005; Tompkins & Kondolf 2000; USGS 2007). **Restored conditions** represent the condition of riparian vegetation at a climax life stage with buffer dimensions that will maximize solar flux attenuation (ODEQ 2006); this condition is achieved through riparian restoration efforts. Once restored conditions are determined, they are compared to current conditions to identify and prioritize areas performing below their ecological potential (Landers 1997; USGS 2007).

Current levels of effective shade can be estimated from aerial photos or remotely sensed vegetation data or directly measured using a solar pathfinder or gap light analyzer of hemispheric photos (ODEQ 2006). While it is unreasonable to rely on direct measurements when dealing with large spatial extents, estimates derived from high resolution data sources are far more convenient, practical and accurate

(Gergel *et al.* 2007). Consequently, modeling effective shade using data derived from high resolution spatial data sources has become a popular tool for watershed management applications. In addition, simulating effective shade under theoretical restored conditions is accomplished through modeling as well. In this study, effective shade modeling was performed under both current and restored conditions in order to compare the current level of effective shade provided by riparian vegetation to that provided under restored conditions and prioritize sites for restoration based on where the largest gains, in terms of shade, would occur as a result of restoration.

Various GIS based models have been developed over the past few decades to estimate effective shade, or some contingent parameter, as a function of the structure and orientation of riparian vegetation, channel width, directional flow of the stream, global position, time of day and time of year (Chen *et al.* 1998; Larson & Larson 1996; Li *et al.* 2012). The major difference between individual shade models is largely contained in the underlying set of algorithms used to calculate the heat energy balance. Shade models also vary in terms of their output and overall utility. Quigley (1981) developed the first algorithm to solve the temporally variable problem of shade cast by riparian vegetation as the sun travels along its daily arc (Li *et al.* 2012). Today, various similar algorithms exist that build upon this basic concept ranging from very simple to very complex (Li *et al.* 2012). More complex models incorporate additional variables, the data for which can be difficult and time consuming to collect, such as tree overhang, channel insulation and localized meteorological conditions (Johnson 2003; Li *et al.* 2012). In this study, effective shade was estimated as a function of one or more attributes concerning solar position (solar altitude and azimuth), riparian vegetation (height, width and density), geographic location (geographic coordinates, topography) and stream morphology (elevation and gradient) using the stream temperature model Heat Source (version 8.0).

## 2.3 Data Derivation

To assemble the necessary modeling inputs, the following attributes were sampled at 50m increments along all streams in the watershed:

- Physical attributes
  - Latitude/longitude
  - Topographic shade angle
  - Stream elevation
  - Stream gradient
- Riparian buffer attributes
  - Vegetation height
  - Bare earth elevation

All of the riparian vegetation and physical attribute data listed above was derived from LiDAR raster data (3 ft. pixel resolution) within a 30m wide buffer along both banks of all streams within the Johnson Creek watershed. Physical attribute data was sampled at each 50m longitudinal sampling node. In addition, riparian vegetation was sampled for every 50m of stream length using a radial sampling pattern that extends 30 meters outward in seven cardinal directions from the stream centerline. The radial sampling pattern will be further discussed in sections to come. Before sampling could be performed, however, base data to derive the modeling inputs from was acquired and/or created using the methods described below.

### 2.3.1 Base Data

A digitized stream layer, including the Johnson Creek mainstem and all tributaries, was developed by the JCWC in 2007 using a combination of LiDAR raster data (3 ft. resolution) and aerial photographs, and subsequently modified in 2009 to include additional data provided by the City of Gresham. This pre-

existing polyline stream layer was digitized using high spatial resolution imagery and, as a result, exhibited a high level of accuracy when overlain with current aerial photographs and LiDAR derived raster data. Subwatershed boundaries were delineated by the JCWC using this same digitized stream layer. Both the polyline stream layer and subwatershed boundary layer were acquired with the help of various members from the Johnson Creek Watershed Inter-jurisdictional Committee (JCW-IJC). Once acquired, the polyline stream layer was subdivided into many separate streams in ArcGIS, such that each stream was contained within a separate shapefile, and could be sampled and modeled separately. All streams less than 50 meters in length fell below the minimum length required for sampling and, as such, were excluded from the study. A total of 461 streams were delineated, 14 of which fell below the minimum length requirement resulting in a final count of 448 streams to be sampled and modeled.

LiDAR derived raster datasets for bare earth elevation (otherwise known as a Digital Elevation Model (DEM)) and vegetation height within the boundary of the watershed were acquired from three separate data acquisition flights (DOGAMI/ODF 2007; Puget Sound LiDAR Consortium (PSLC) 2004, 2005) and were pieced together by Ryan Michie. The majority (~90%) of LiDAR data came from the Portland/Mt. Hood data acquisition project, flown on March 16<sup>th</sup> -April 15<sup>th</sup> of 2007. A small portion of the watershed in the Milwaukie area came from the Portland Pilot study flown in March of 2004. Another small portion of the watershed in the Crystal Springs area came from the Lower Columbia Study, flown between January 10<sup>th</sup> and February 12<sup>th</sup> of 2005. Once combined, the final raster dataset for bare earth (DEM) and vegetation had a pixel resolution of 3ft.

The Datum used for all spatial data analysis was D\_North\_American\_1983\_HARN with a geographic coordinate system of GCS\_North\_American\_1983\_HARN and projected coordinate system of NAD\_1983\_HARN\_Lambert\_Conformal\_Conic. Jurisdictional (city, county, and metro) and 12<sup>th</sup> field Hydrologic Unit (HU) boundaries were derived from public RLIS data dated August 2013 (RLIS 2013).

Additional base data concerning taxlot attributes (such as land ownership and land use) and subbasin boundaries were provided by members of the JCW- IJC and used for post-modeling data analysis purposes.

### 2.3.2 Restored Conditions

A separate restored conditions raster was created to facilitate sampling and modeling of all streams under a **restoration scenario**. The restoration scenario is a scenario in which all shade restoration efforts that are likely to occur within the watershed are completed. Shade restoration is defined in this paper as the process of enhancing the height, extent, and density of riparian vegetation in order to reduce the amount of incoming solar radiation that reaches the stream surface (DeWalle 2008). The restored conditions raster was created by modifying the current-day LiDAR derived raster dataset (3 ft.) to depict the state of riparian vegetation in the watershed under the restoration scenario.

#### *Restoration Buffer*

First, a **restoration buffer** was delineated along all streams within the watershed, extending 15 meters to either side of the stream channel; this buffer represents the furthest distance from the stream in which restoration is likely occur. This buffer width has also been shown to provide an adequate level of shade to small streams in various studies (Chen *et al.* 1998b; DeWalle 2008; Fullerton *et al.* 2006; Washington State Department of Ecology (WSDOE) 2007; Watanabe *et al.* 2005). Buffer widths between 9-30m are generally considered adequate to provide shade benefits to smaller streams (DeWalle 2008; USGS 2007). Depending on the width of a stream, studies have shown that the percent effective shade ceases to increase as buffers become wider than 10-30m (Chen *et al.* 1998b; DeWalle 2010; Fullerton *et al.* 2006; Sridhar *et al.* 2004; Watanabe *et al.* 2005).

#### *Restorable vs. Un-restorable Area*

Using current day LiDAR raster data (3 ft.), each pixel of vegetation within the restoration buffer was classified as either: vegetation greater than or equal to 4m in height *or* vegetation less than 4m in height. Vegetation currently greater than or equal to 4 meters in height was classified as **un-restorable area** and remained unchanged under the restoration scenario, whereas vegetation currently less than 4 meters in height was classified as **restorable area** and was modified under a restoration scenario. A 4 meter height threshold for restorable area was chosen based on the assumption that most invasive species targeted for restoration, such as Himalayan blackberry (*Rubus discolor* and *Rubus procerus*), Japanese knotweed (*Polygonum cuspidatum*), or purple loosestrife (*Lythrum salicaria* L.), will fall under this threshold; all of the aforementioned species are common throughout the watershed (BES 2001; JCWC 2012) and can reach heights of 3-4 meters (Francis; King County 2013). Similarly, riparian vegetation was classified as restorable or un-restorable on a per-pixel scale since invasive species are often targeted for eradication and restorative purposes from equally small areas (BES 2001). Riparian vegetation within restored areas was assigned height, width and density dimensions typical of a climax life stage for native riparian tree species, which is characterized by the following conditions (ODEQ 2006):

- Vegetation is mature;
- Vegetation height and density are at or near the potential expected for the given plant community; and
- Vegetated buffer is sufficiently wide to maximize solar flux attenuation.

These same criteria are also used by ODEQ to determine “system potential effective shade” during TMDL development (ODEQ 2006). Characteristics of riparian vegetation within restored areas was determined from current data sources describing the optimal dimensions and species composition of a mature, native riparian community within the geographic study region. **Restored conditions** were



designed to represent the condition of riparian vegetation under the restoration scenario. Following the implementation of restoration activities that are likely to occur throughout the watershed, all vegetation in restorable areas are at a climax life stage and vegetation within un-restorable areas remain in the same state as current conditions.

All un-restorable area remained unchanged to control for the natural background growth of the vegetation that surrounds restored areas and to isolate the shade benefit of restoration efforts from the shade benefit of natural background growth. Isolating the shade benefit of restoration efforts will enable the performance of potential restoration sites under a restoration scenario to be compared to one another and prioritized according to where the largest benefit occurs due to restoration efforts alone. Where buildings and roads occurred within the restoration buffer, vegetation height also remained unchanged, since restoration is not likely to be feasible in these areas (see Figure 3 for example).

All areas with current vegetation greater than or equal to 4m in height, or occupied by buildings and/or roads are collectively referred to as the **“un-restorable” area**. Similarly, the total area within the restoration buffer occupied by vegetation currently <4 meters in height is collectively referred to as the total **“restorable” area** in the watershed (Figure 3).

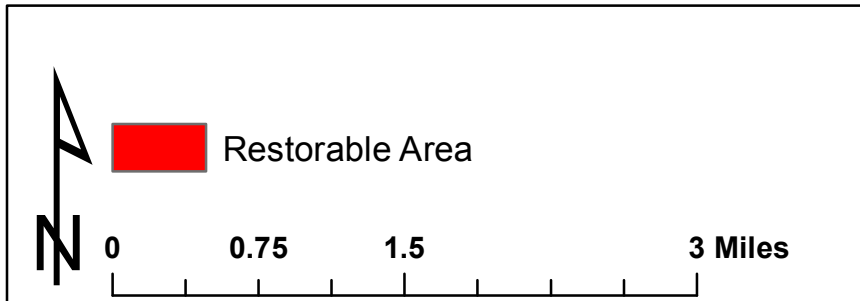
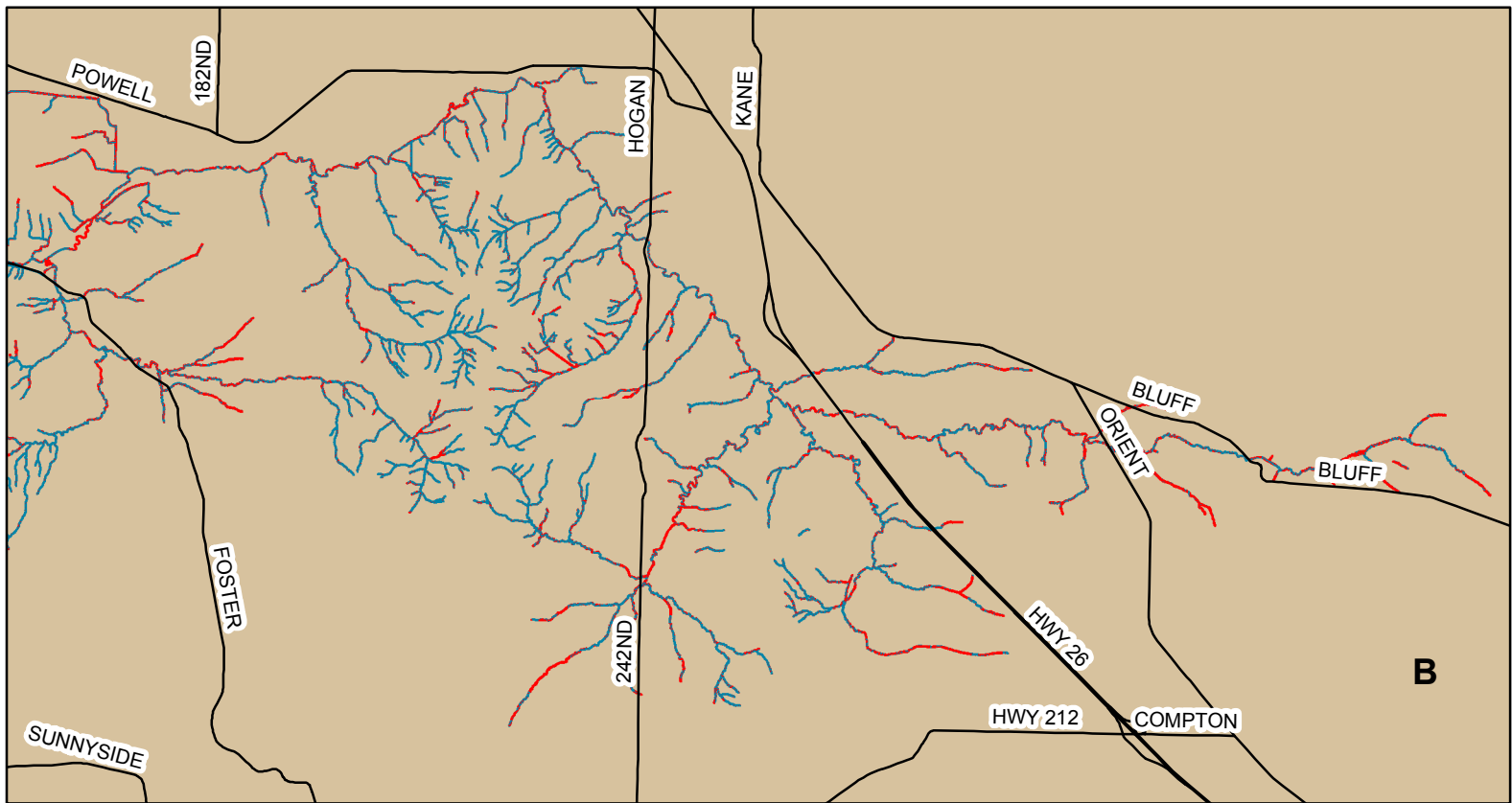
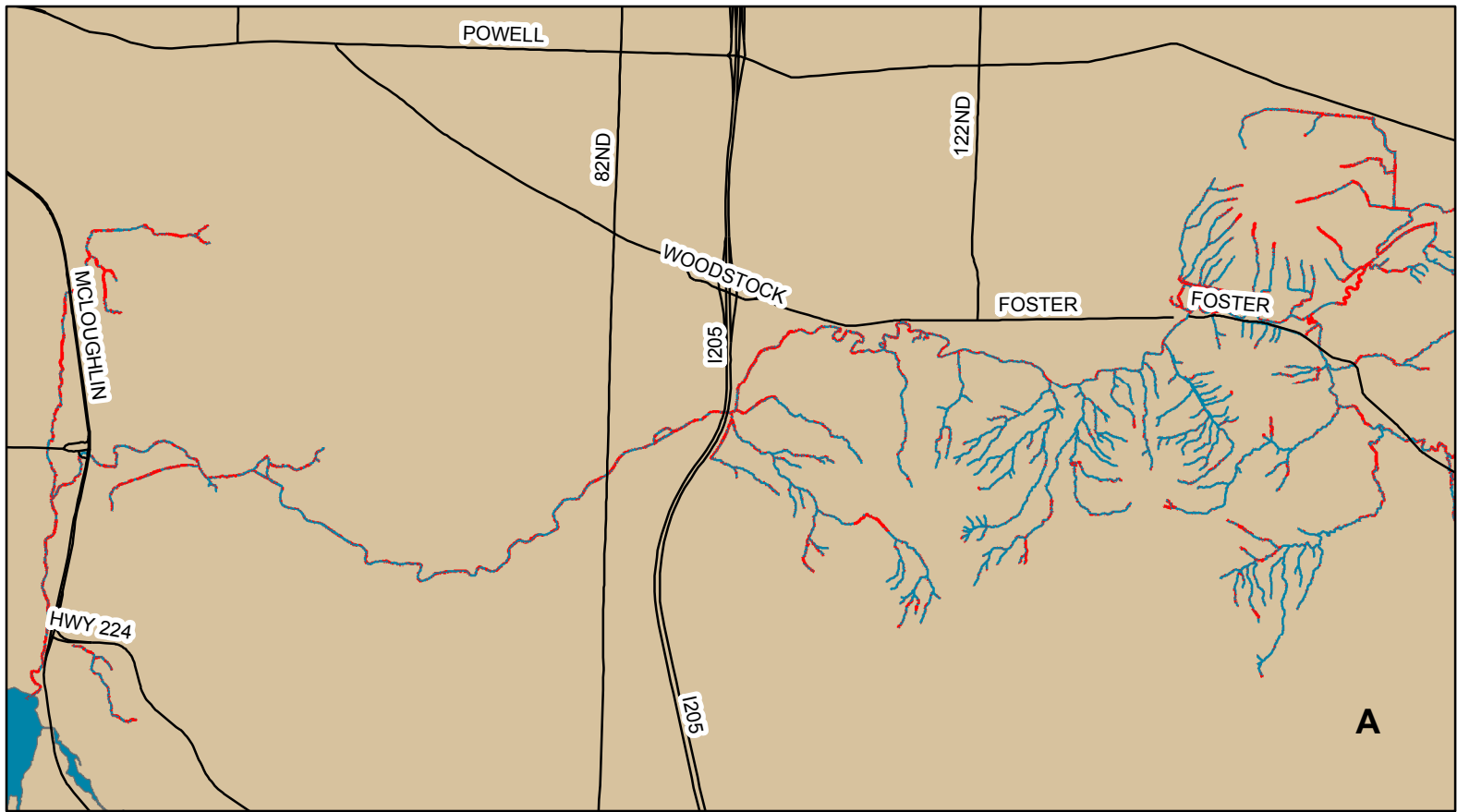


**Figure 3: Total Restorable Area**  
**A: Western Half of Watershed**  
**B: Eastern Half of Watershed**  
 March, 2014

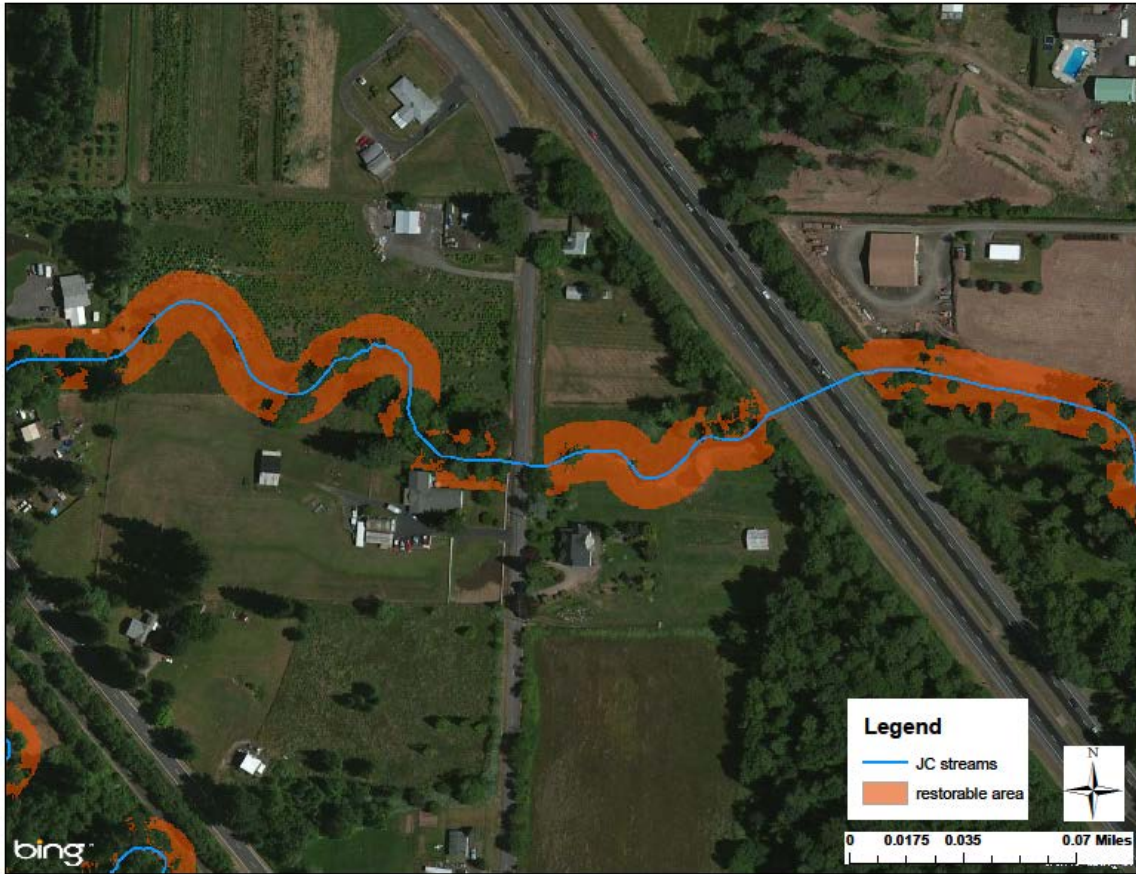


**Figure 4: Example of restored conditions**

*Area in orange corresponds to restorable area, or area within 15m of stream channel containing vegetation currently <4m in height.*

### *Height of Restored Vegetation*

The height of restored vegetation was determined from the average height at maturity for six of the most common riparian tree species planted for restoration purposes in the Johnson Creek watershed. A major assumption of this approach is that all tree species will be uniformly distributed within restored areas and throughout the watershed. Many other shade modeling studies have involved similar assumptions and generalizations regarding the dimensions of riparian vegetation in an effort to maintain model simplicity (Chen *et al.* 1998 a, b; Cristea and Burges 2010; Guoyuan *et al.* 2012; ODEQ 2006). In

their determination of system potential conditions for the Johnson Creek Watershed TMDL, ODEQ (2006) used a similar approach, in which each land cover class, or riparian community, was assigned a uniform value that represents the average height at maturity for that community, regardless of location within the watershed. Similarly, Greenberg *et al.* (2012) calculated the vegetation height for each stream reach modeled as the mean height of all vegetation within the riparian buffer for that reach.

The most common riparian tree species were identified using the Portland Plant List of Native Plant Communities: Mixed coniferous/deciduous riparian forest (ODOT 2011). They include: big leaf maple (*Acer macrophyllum*), red alder (*Alnus rubra*), Oregon ash (*Fraxinus latifolia*), black cottonwood (*Populus balsamifera var. trichocarpa*), Pacific willow (*Salix lucida ssp lasiandra*) and Western red cedar (*Thuja plicata*). Two additional tree species, black hawthorn (*Crataegus suksdorfii*) and quaking aspen (*Populus tremuloides*), were included in the Portland Plant list for this community but are not commonly planted for restoration purposes and as such, were excluded from the restored height calculation (Jenkinson, personal correspondence, February 19, 2013).

For each tree species, the height at maturity was derived from the USDA PLANTS database. The average of all values came to 26.6 meters and was rounded up to 27 meters for the final value. Cristea and Burges (2010) used similar values of 25-28m to characterize the average site potential tree height along streams dominated by cottonwood (*Populus sp.*), willow (*Salix sp.*) and red-osier dogwood (*Cornus sericea*). Similarly, Chen *et al* (1998b) found vegetation heights between 25-35m were necessary to bring tributary streams in the Upper Grande Ronde watershed into compliance with water quality standards (Chen *et al.* 1998b). The average *age* at maturity for each species was derived from a few different sources; the average age at maturity for all six tree species is estimated at 55 years old (Burns and Honkala 1990; Niemic *et al.* 1995; USDA 2013; WSDOE 2013); see Table 1 for further details.

**Table 1: Characteristics of most common riparian tree species planted in riparian restoration projects**

| Species  | Age at maturity | <sup>4</sup> Height at maturity (m) |
|--|-----------------|-------------------------------------|
| Big leaf maple ( <i>Acer macrophyllum</i> )                      | <sup>1</sup> 60 | 18                                  |
| Red alder ( <i>Alnus rubra</i> )                                 | <sup>1</sup> 65 | 27                                  |
| Oregon ash ( <i>Fraxinus latifolia</i> )                         | <sup>1</sup> 60 | 21                                  |
| Black cottonwood ( <i>Populus balsamifera var. trichocarpa</i> ) | <sup>1</sup> 60 | 30                                  |
| Pacific willow ( <i>Salix lucida ssp lasiandra</i> )             | <sup>3</sup> 30 | 16                                  |
| Western red cedar ( <i>Thuja plicata</i> )                       | <sup>2</sup> 55 | 45                                  |

<sup>1</sup>Source: Niemic et al. (1995)

<sup>2</sup>Source: Burns and Honkala (1990)

<sup>3</sup>Source: WSDOE Plant selection guide (accessed online 2013)

<sup>4</sup>Source: USDA Plants Database (accessed online 2013)

The final restored conditions raster depicted the state of riparian vegetation throughout the watershed following shade restoration activities that are likely to occur. All restorable area was restored to a height of 27m whereas all un-restorable area, including buildings and roads, was left unchanged. The restored conditions raster was used to derive the modeling inputs concerning riparian vegetation dimensions (height, width and density) under a restoration scenario.

### 2.3.3 Sampling for Modeling Inputs

All riparian vegetation and physical attribute data were sampled from LiDAR derived raster datasets (3 ft. resolution) using Ttools, an ArcGIS extension developed by ODEQ for use in conjunction with Heat Source, and the LiDAR Landcover Sampler, a python script created by Ryan Michie (ODEQ 2011). All of the above programming tools were pre-existing and previously utilized for other projects. Both Heat Source and Ttools are used extensively by ODEQ for purposes of water quality analysis (ODEQ 2012). The following table (Table 2) provides information on the sources and resolution of raster datasets used

to sample data concerning the height of riparian vegetation and physical attributes under both current and restored conditions.

**Table 2: Modeling input parameters derived from geospatial data**

| <b>Input Parameters</b>             | <b>Data Source</b>   | <b>Resolution</b> |
|-------------------------------------|--|-------------------|
| Stream length (km)                  | Derived from digitized stream channel-shapefile using Ttools; stream channel digitized using LiDAR derived raster data | 3 ft.             |
| Coordinates (lat/lon)               | Derived from DEM raster data using Ttools  | 3 ft.             |
| Gradient                            | Derived from DEM raster data using Ttools  | 3 ft.             |
| Elevation (meters)                  | Derived from DEM raster data using Ttools  | 3 ft.             |
| Topographic shade (in 3 directions) | Derived from DEM raster data using Ttools  | 3 ft.             |
| Bare earth elevation (mean)         | Derived from DEM raster data using LiDAR Landcover Sampler   | 3 ft.             |
| Vegetation height (mean)            | Derived from LiDAR raster data using LiDAR Landcover Sampler   | 3 ft.             |

### *Sampling Units*

Each stream was sampled for physical attribute and riparian vegetation data at a longitudinal sampling rate of 50 meters. Two different sampling units were used; one primarily for sampling physical attributes and one primarily for sampling riparian vegetation. Longitudinal sampling nodes occurring at 50m intervals along each stream were used to sample physical attribute data including elevation, gradient, geographic coordinates and topographic shade. While longitudinal sampling rates between 30-100m are commonly used for shade modeling purposes (Chen *et al* 1998b; Cristea and Burges 2010; Fullerton *et al.* 2006; Quinn *et al.* 1992; Watanabe *et al.* 2005) recent advances in remote sensing technologies

have enabled sampling at the finer scale of pixels (1-30m<sup>2</sup>) to become more prevalent (Allen *et al.* 2007; Greenberg *et al.* 2012; Johnson *et al.* 2007; Kentula 1997). However, these smaller sampling rates are accompanied by relatively large amounts of data and, as such, are often used for modeling areas much smaller than a watershed, such as a single stream reach.

At each of these longitudinal sampling nodes, the height of riparian vegetation and bare earth elevation were sampled using a radial sampling pattern (Figure 5). The radial sampling pattern involves multiple polygon-type sampling units (Figure 5) that radiate outward in seven cardinal directions from each longitudinal sampling node to a distance of 30m.

The following section begins with a description of the radial sampling pattern used for deriving riparian vegetation and bare earth elevation data and is followed by a description of the sampling pattern used to derive physical attribute data.

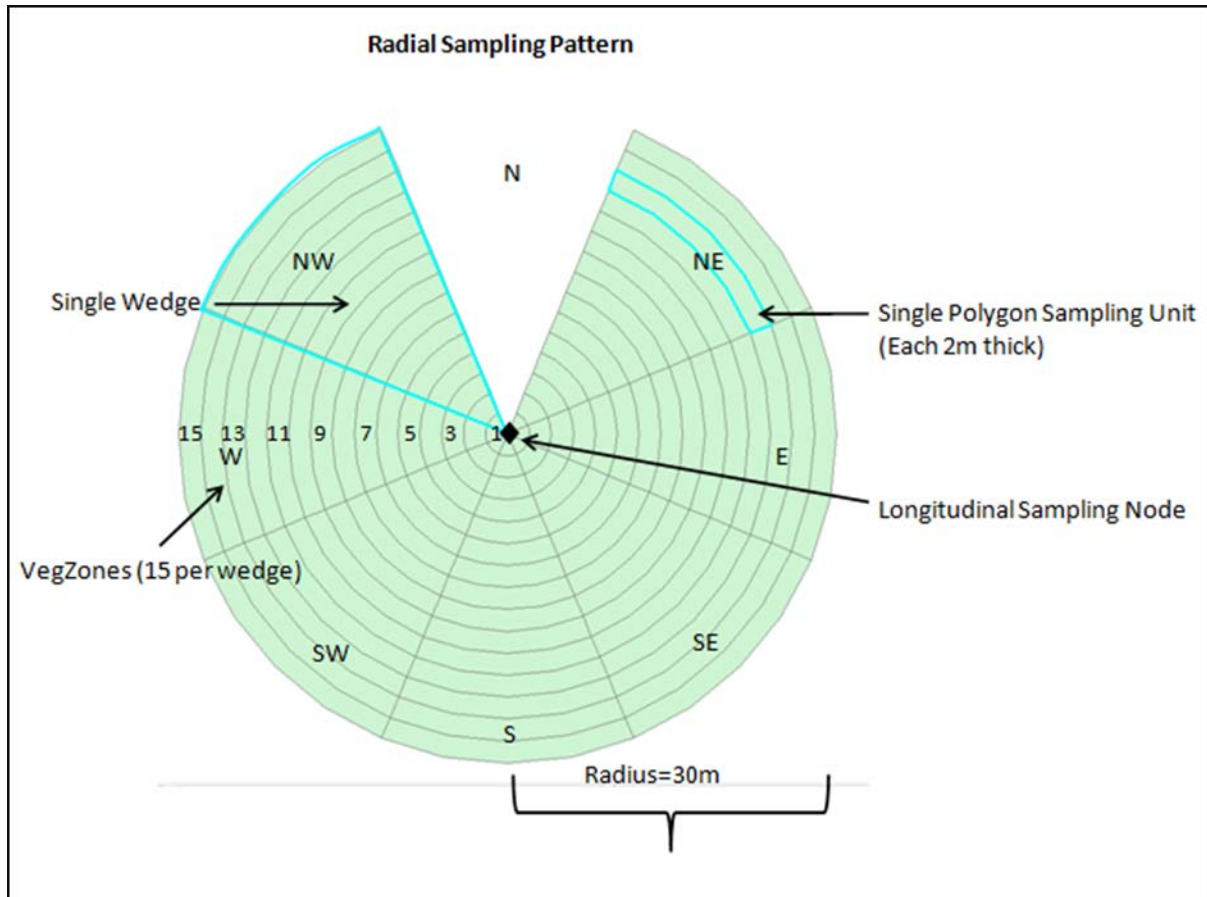


**Figure 5: Radial sampling pattern**

*Radial sampling of riparian vegetation and bare earth elevation occurs at each longitudinal sampling node (every 50 meters of stream length). Sampling extends 30 meters out from each sampling node at 2m increments, in seven cardinal directions. Each single polygon is assigned a unique identifying code based on its location both within the radial sample and along the stream. Northernmost wedges are excluded from modeling since the sun does not shine from that direction in the Northern hemisphere.*



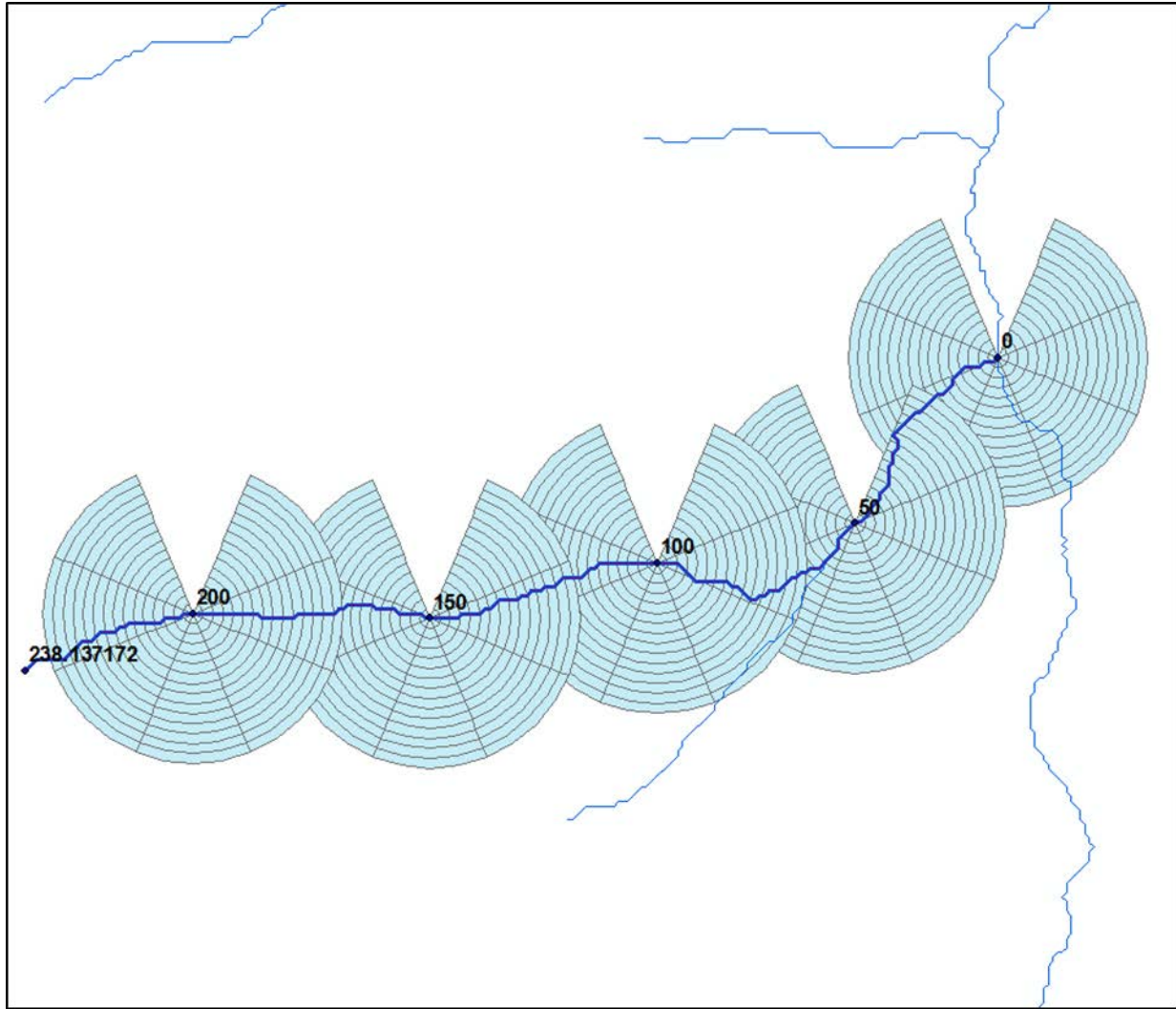


**Figure 6: Series of radial sampling patterns along a single stream.**

*Sampling occurs at a longitudinal sampling rate of 50 meters. Each longitudinal sampling node is labeled according to its stream length (m), with length 0 starting at the mouth of the stream. The last sample at the upper end of the stream (length=238.14m) falls short of 50 meters from the previous sample and is not included in the model.*

## *Vegetation Height and Bare Earth Elevation Sampling*

The following sampling pattern was used to sample riparian vegetation height and bare earth elevation from both current and restored condition raster datasets. At each longitudinal sampling node, radial sampling extended 30 meters out in every cardinal direction (north, northeast, east, southeast, south, southwest, west, northwest) creating a circle with eight “wedges”, or directional zones (Figure 5). Within each wedge, area samples were taken every 2 meters out from the stream channel, up to a distance of 30 meters, resulting in a total of 15 polygons sampled in each cardinal direction (Figure 5). Many other shade modeling studies have ignored lateral, or cross-sectional gradients in riparian vegetation, using evenly distributed and generalized blocks of vegetation along either side of the stream channel (Chen *et al.* 1998 a, b; DeWalle 2010; Greenberg *et al.* 2012; Li *et al.* 2012; Ryan *et al.* 2013). The lateral sampling rate of 2m used for this study will capture a greater level of lateral variation within the riparian buffer in comparison.

Samples that occurred within the North wedges were not included in the final model since the sun does not shine from that direction in the Northern Hemisphere and consequently, shadows will not be cast in a southerly direction (Boyd & Kasper 2003). Therefore, 105 polygons were individually sampled (excluding the North wedge) for near-stream vegetation height and bare earth elevation, at every 50 meters of stream length (Figure 5 and Figure 6).

Each individual polygon sampled was assigned an identifying code which is a function of the stream km, wedge zone, and veg zone associated with each polygon (see Figure 5). While these codes are unique to the stream they are associated with, they are not unique across streams (i.e. many streams will have codes in common but no individual stream will have duplicate codes occurring within it).

Within each polygon sampling unit, the current height of riparian vegetation was sampled from LiDAR derived raster data (3 ft. resolution) using the LiDAR Landcover Sampler. Summary statistics for

vegetation height and bare earth elevation were generated for each polygon including: minimum, maximum, range, mean, standard deviation, and sum. All vegetation height and elevation values within each polygon were averaged, resulting in a block of vegetation with uniform height and bare earth elevation as the final modeling input. In addition, a uniform density estimate for each polygon is included as a modeling input; methods used to estimate vegetation density within each polygon will be discussed in the following section.

The height of riparian vegetation under restored conditions was sampled from the restored conditions raster dataset using the LiDAR Landcover Sampler (Michie 2011), following the same radial sampling procedure used to sample current vegetation. Bare earth elevation was not re-sampled under restored conditions since it is assumed to remain unchanged from current conditions.

### *Elevation, Gradient, and Topographic Shade Sampling*

Physical attribute data was sampled at each longitudinal sampling node (every 50 meters of stream length). At each node, Ttools was used to derive the following physical attribute data from DEM raster data: geographic coordinates, maximum topographic shade angle, elevation and gradient. Ttools calculated elevation by sampling 25 pixels surrounding each node and defaulting to the lowest elevation found. Stream gradient was calculated from the elevation of each sampling node and the distance between nodes. Topographic shade is defined as the angle between the center of the stream and the highest topographic feature. Topographic shade angles were calculated at every 50 meter sampling node in three directions: east, south, and west. For each angle, Ttools sampled DEM pixels for elevation up to 10 km away from each longitudinal sampling node and recorded the maximum topographic shade angle found within this zone.

Sampling of physical attribute data (i.e. elevation, gradient, topographic shade) was not repeated for restored conditions since these values remained the same under both current and restored conditions;

the only difference between current and restored modeling input parameters was the height and density of riparian vegetation, the latter of which was estimated and not sampled (see following section for details).

#### 2.3.4 Vegetation Density

Almost all input parameters for Heat Source modeling were derived from raster data using Ttools and LiDAR Landcover Sampler (see Table 2) In addition to sampled modeling inputs, **vegetation density** values were estimated for each polygon. Vegetation density is required as a modeling input to calculate the transmissivity, or shade density, for each polygon, which is calculated using Beer's Law (Oke 1978) (see page 45 for equation). Heat Source, the model utilized in this study, defines vegetation density as an ocular estimate of the canopy closure and, as such, methods for estimating canopy closure were utilized to derive vegetation density modeling inputs (Boyd & Kasper 2003). **Canopy closure** is defined as the proportion of the sky hemisphere obscured by vegetation when viewed from a single point and is generally measured in terms of the size and frequency of gaps in the canopy (DeWalle 2008; Fujita *et al.* 2003; Jennings *et al.* 1999; Warren *et al.* 2013).

One common approach for estimating canopy closure or vegetation density involves delineation of polygons from aerial photographs that appear to contain relatively homogenous vegetative cover and assigning each polygon a uniform, generalized value (Boyd & Kasper 2003; Chen *et al.* 1998b; Cristea and Burges 2010; DeWalle 2008, 2010; Li *et al.* 2012). In this study, polygons were prohibitively small and numerous making this approach impractical.

The approach used for this study is similar to the 'crown position index' method (Baker 1950; Clark and Clark 1992; Dawkins & Field 1978; Smith 1986) as well as the 'vegetation height profile technique' (Brokaw & Grear 1991; Fujita *et al.* 2003; Hubbell & Foster 1986; Karr 1971; Nakashizuka 1995). Both the crown position index and vegetation height profile technique are used to evaluate various attributes

concerning canopy structure including gap distribution, gap frequency and light transmission through the canopy as a function of “canopy surface roughness” or the magnitude of variation in the vertical canopy height profile. The ‘crown position index’ and ‘vegetation height profile technique’ methods support the premise that vertical canopy height profiles can be used to estimate gap frequency and canopy closure-the approach used to estimate canopy closure in this study.

Canopy closure was estimated within each polygon using an index approach. For each polygon, an index of canopy spread was calculated based on the magnitude of variation, or spread, in the vertical canopy height profile. The objective of using this approach is to evaluate the size and frequency of gaps in the canopy of each polygon; the more variation there is in the vertical canopy height profile, the more gaps are assumed to occur. Once calculated, select index values were then assigned density (i.e. canopy closure) values based on how dispersed or compact the canopy profile was. Using paired index values and assigned density values, a formula for vegetation density was then derived to enable estimation of density within each polygon. The following steps illustrate how 1) canopy spread index values and 2) the final density formula were derived.

**Step 1)** Using the vegetation height data sampled within each polygon, an index of canopy spread was determined for each polygon using the following equation:

$$\frac{(max - mean)}{stddev}$$

Where *max* is equal to the maximum vegetation height (m), *mean* is equal to the mean vegetation height (m) and *stddev* is equal to the standard deviation of vegetation heights from the mean (m). Resultant index values ranged from 0 to 7, with 0 indicating a lack of gaps in the canopy and 7 indicating a large number of gaps in the canopy.

**Step 2)** After calculating the canopy spread index for each polygon, the density equation was derived using the point-slope formula for a linear line with two known coordinates. The two known coordinates were determined by assigning density values to the lowest and highest index values, 0 and 7. The lowest index value was assigned a density of 10% whereas the highest index value was assigned a density of 90%. For comparison, other studies were identified that used similar maximum or optimal density values (~85%) for effective shade modeling (Chen *et al.* 1998b; WSDOT 2007). The lowest density value of 10% was chosen instead of 5% or 0% since none of the polygons were completely barren or void of vegetation. The resulting coordinates were: (0, 90) and (7, 10) where  $x$  is equal to the canopy spread index and  $y$  is equal to the density (%). The following formulas were used to derive the density equation using these two known coordinates:

Slope formula:

$$m = \frac{y_1 - y_2}{x_1 - x_2}$$

$$m = \frac{90 - 10}{0 - 7} = \frac{-80}{7}$$

Point-slope formula:

$$(y - y_1) = m(x - x_1)$$

$$(y - 90) = \frac{-80}{7}(x - 0)$$

$$y = \frac{-80}{7}x + 90 = \rho$$

Where  $m$  equals the slope of the line,  $x$  is equal to the canopy spread index and  $y$  is equal to the density ( $\rho$  (%)). The density ( $\rho$ ) of vegetation within each polygon was estimated using this final equation.

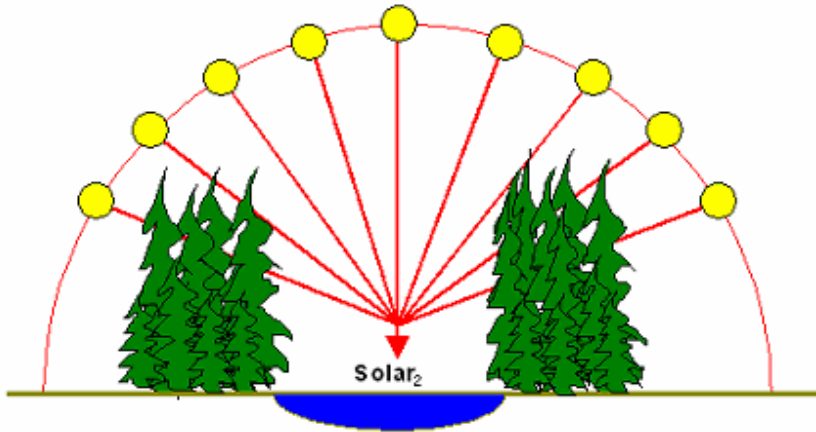
## 2.4 Modeling

Modeling was accomplished using Heat Source (version 8.0), a temperature model utilized by ODEQ to estimate stream network thermodynamics and hydrology. It was developed in 1996 by a graduate student, Mathew Boyd, as a Masters Thesis at Oregon State University in the Bioresource Engineering and Civil Engineering Departments and has been regularly updated through 2007 (Boyd & Kasper 2003; ODEQ 2006). Heat Source is recognized as a relatively data intensive stream temperature model utilizing high resolution inputs and producing equally refined outputs (Boyd & Kasper 2003; Watanabe *et al.* 2005). Heat Source uses multiple Microsoft Excel worksheets to store and configure model inputs and to chart and store model outputs. Using Python programming to calculate simulation algorithms, the model is capable of executing various modules including simulation of effective shade, comprehensive heat and mass transfer and water column temperature. The module utilized for this study, referred to as Shade-a-lator, is a solar routing routine from the sun to the stream surface used to simulate effective shade and stream surface solar exposure. Shade-a-lator is an implementation of the shade estimation method proposed by Chen *et al.* (1998 a,b) that computes a time series of effective shade as a function of solar position (solar altitude and solar azimuth), riparian vegetation (height, width and density), geographic location (latitude, longitude, and topography), and stream morphology (stream gradient and elevation).

Effective shade estimates are calculated using a relatively simple and straightforward algorithm (Figure 7). Heat Source simulates the sun's daily path across the sky based on the season and time of day) to determine the potential amount of incoming direct beam solar radiation that would reach the stream surface without shading or obstructions of any kind to attenuate or scatter the incoming radiation (i.e. vegetation or topography) ( $Solar_1$ ). The amount of incoming direct beam solar radiation actually received at the stream surface ( $Solar_2$ ) is estimated as a function of solar position (solar altitude and azimuth), riparian vegetation (height, density and width), elevation, gradient and topography.

### Effective Shade Defined

**Solar<sub>1</sub>**\* – Potential daily direct beam solar radiation load adjusted for julian day, solar altitude, solar azimuth and site elevation.



$$\text{Effective Shade} = \frac{(\text{Solar}_1 - \text{Solar}_2)}{\text{Solar}_1}$$

Where,

**Solar<sub>1</sub>**: Potential Daily Direct Beam Solar Radiation Load  
**Solar<sub>2</sub>**: Daily Direct Beam Solar Radiation Load Received at the Stream Surface

\* Represents potential **solar insolation** without any interference from vegetation or topography.  
 Source: *Heat Source Methodology (Boyd & Kasper 2003)*

**Figure 7: Effective shade formula**

### 2.2.1 Solar Position

Solar positioning variables, including solar altitude<sup>5</sup> ( $\theta_{SA}$ ) and solar azimuth<sup>6</sup> ( $\theta_{AZ}$ ) were calculated using the algorithms provided below.

#### *Solar Declination*

$$\delta = \sin^{-1} \left[ \sin \left( \theta_{OB} \cdot \frac{\pi}{180^\circ} \right) \cdot \sin \left( \theta_{AL} \cdot \frac{\pi}{180^\circ} \right) \right] \cdot \frac{180^\circ}{\pi}$$

<sup>5</sup> Solar altitude comprises the vertical position of the sun relative to a stream segment and is defined as the angular distance of the sun above or below the horizon (Boyd and Kasper 2003).

<sup>6</sup> Solar azimuth comprises the horizontal position of the sun relative to the stream segment. It is defined as the angular distance clockwise along the horizon from a specified location to the intersection with the circle drawn from the zenith, through a body on the celestial sphere (Boyd and Kasper 2003).



Where  $\delta$  is equal to solar declination,  $\theta_{OB}$  is equal to the obliquity of the elliptic (degrees) and  $\theta_{AL}$  is equal to the apparent longitude of the sun (degrees). For equations used to derive  $\theta_{OB}$  and  $\theta_{AL}$ , please refer to the Heat Source Methodology (Boyd and Kasper 2003).

### *Hour Angle*

$$0^\circ \geq \theta_{HA} \leq 360^\circ$$

$$\theta_{HA} = \frac{t_s}{4} - 180$$

Where  $\theta_{HA}$  is equal to the hour angle (degrees) and  $t_s$  is equal to solar time (minutes). For equation used to derive  $t_s$ , please refer to the Heat Source Methodology (Boyd and Kasper 2003).

### *Solar Zenith- Uncorrected for Refraction (Ibqual 1983)*

$$\theta_{SZ'} = \cos^{-1}(A) \cdot \frac{\pi}{180^\circ}$$

Where  $(-1 \leq A \leq 1)$ ,

$$A = \sin\left(\theta_{lat} \cdot \frac{\pi}{180^\circ}\right) \cdot \sin\left(\delta \cdot \frac{\pi}{180^\circ}\right) + \cos\left(\theta_{lat} \cdot \frac{\pi}{180^\circ}\right) \cdot \cos\left(\delta \cdot \frac{\pi}{180^\circ}\right) \cdot \cos\left(\theta_{HA} \cdot \frac{\pi}{180^\circ}\right)$$

Where  $\theta_{SZ'}$  is equal to the solar zenith (uncorrected for refraction; in degrees),  $\theta_{lat}$  is equal to latitude (degrees),  $\delta$  is equal to solar declination (degrees), and  $\theta_{HA}$  is equal to hour angle (degrees).

### *Atmospheric Elevation (Ibqual 1983)*

$$\alpha = 90^\circ - \theta_{SZ'}$$

Where  $\alpha$  is equal to atmospheric elevation (degrees) and  $\theta_{SZ'}$  is equal to the solar zenith (uncorrected for refraction; in degrees).

### *Refraction Correction Coefficient*

If  $\alpha > 85^\circ$  then,

$$C_R = 0^\circ$$

If  $5^\circ > \alpha \leq 85^\circ$  then,

$$C_R = \frac{\frac{58.1}{\alpha \cdot \frac{\pi}{180^\circ}} - \frac{0.07}{\left(\alpha \cdot \frac{\pi}{180^\circ}\right)^3} + \frac{0.000086}{\left(\alpha \cdot \frac{\pi}{180^\circ}\right)^5}}{3600^\circ}$$

If  $-0.575 > \alpha \leq 5^\circ$  then,

$$C_R = \frac{1735 + \alpha \cdot \left(-518.2 + \alpha \cdot (103.4 + \alpha \cdot (-12.79 + \alpha \cdot 0.711))\right)}{3600^\circ}$$

If  $\alpha \leq -0.575$  then,

$$C_R = \frac{-20.774}{\tan\left(\alpha \cdot \frac{\pi}{180^\circ}\right) \cdot 3600^\circ}$$

Where  $C_R$  is equal to the refraction correction coefficient (degrees), and  $\alpha$  is equal to atmospheric elevation (degrees).

### *Solar Zenith (corrected for refraction)*

$$\theta_{SZ} = \theta_{SZ'} - C_R$$

Where  $\theta_{SZ}$  is equal to the solar zenith (corrected for refraction; in degrees),  $\theta_{SZ'}$  is equal to the solar zenith (uncorrected for refraction; in degrees) and  $C_R$  is equal to the refraction correction coefficient (degrees).

### *Solar Altitude (corrected for refraction)*

$$\theta_{SA} = 90^\circ - \theta_{SZ}$$

Where  $\theta_{SA}$  is equal to solar altitude (degrees) and  $\theta_{SZ}$  is equal to the solar zenith (corrected for refraction; in degrees).

### *Solar Azimuth (Ibqual 1983) ( $0^\circ > \theta_{AZ} \leq 360^\circ$ )*

$$\theta_{AZ} = \frac{\sin\left(\theta_{lat} \cdot \frac{\pi}{180^\circ}\right) \cdot \cos\left(\theta_{SZ} \cdot \frac{\pi}{180^\circ}\right) - \sin\left(\delta \cdot \frac{\pi}{180^\circ}\right)}{\cos\left(\theta_{lat} \cdot \frac{\pi}{180^\circ}\right) \cdot \sin\left(\theta_{SZ} \cdot \frac{\pi}{180^\circ}\right)}$$

Where  $\theta_{AZ}$  is equal to solar azimuth (degrees),  $\theta_{lat}$  is equal to latitude (degrees),  $\theta_{SZ}$  is equal to the solar zenith (corrected for refraction; in degrees), and  $\delta$  is equal to solar declination (degrees).

### **2.2.2 Potential Incoming Solar Radiation**

The potential amount of incoming direct beam solar radiation ( $\Phi_{SRB1}$ ) above topographic features, or before interception by topography, is estimated as a function of Julian day ( $JD$ ), solar altitude ( $\theta_{SA}$ ), and stream elevation ( $z_s$ ). Julian day and stream elevation are measured or known variables whereas solar position is calculated in Heat Source using algorithms provided in the previous section (2.2.1) Julian day ( $JD$ ) refers to a continuous numeric count of calendar days (1 to 365). The following algorithms were used to estimate potential amount of incoming solar radiation at each stream sampling node:

### *Global Solar Radiation flux at the edge of the atmosphere (Wunderlich 1972)*

$$\Phi_{SRG} = \frac{\Phi_{SRC}}{r^2} \sin \theta_{SA}$$

Where  $\Phi_{SRG}$  is equal to global solar flux (watts/m<sup>2</sup>),  $\Phi_{SRC}$  is equal to the solar constant (watts/m<sup>2</sup>),  $r$  is equal to the radius vector (radians) and  $\theta_{SA}$  is equal to solar altitude (degrees).

### *Solar Constant (Dingman 2002)*

$$\Phi_{SRC} = 1367 \text{ watts/m}^2$$

Where  $\Phi_{SRC}$  is equal to the solar constant (watts/m<sup>2</sup>).

### *Radius Vector (Wunderlich 1972)*

$$r = 1 + 0.017 \cdot \cos\left(2 \cdot \frac{\pi}{365}\right) \cdot \left(186 - JD + \frac{t_{DST}}{24}\right)$$

Where  $r$  is equal to the radius vector (radians),  $JD$  is equal to Julian day (1-365) and  $t_{DST}$  is equal to daylight savings time (day fraction).

### *Atmospheric Transmissivity (Ibqual 1983)*

$$T_A = 0.0685 \cdot \cos \left[ \left( 2 \cdot \frac{\pi}{365} \right) \cdot (JD + 10) \right] + 0.8$$

Where  $T_A$  is equal to air mass transmissivity and  $JD$  is equal to Julian day (1-365).

### *Optical Air Mass Thickness (Ibqual 1983)*

$$M_A = \frac{35 \cdot e^{(-0.0001184 \cdot z_s)}}{\sqrt{1224 \cdot \sin \left( \theta_{SA} \cdot \frac{\pi}{180^\circ} \right) + 1}}$$

Where  $M_A$  is equal to air mass thickness,  $z_s$  is equal to stream elevation (m), and  $\theta_{SA}$  is equal to solar altitude (degrees).

### *Estimate-Potential Incoming Direct Beam Solar Radiation (above Topographic Features) (Wunderlich 1972, Martin and McCutcheon 1999)*

$$\Phi_{SRB} = \Phi_{SRG} \cdot T_A^{M^A}$$

Where  $\Phi_{SRB}$  is equal to an estimate of the potential incoming direct beam solar radiation (above topographic features; watts/m<sup>2</sup>),  $\Phi_{SRG}$  is equal to global solar flux (watts/m<sup>2</sup>),  $T^A$  is equal to air mass transmissivity and  $M^A$  is equal to air mass thickness.

### *Diffuse fraction (Chen 1994)*

$$D_F = (0.938 + 1.071 \cdot C_I) - (5.14 \cdot C_I^2) + (2.98 \cdot C_I^3) - \left( \sin \left( 2\pi \cdot \frac{(JD - 40)}{365} \right) \right) \cdot (0.009 - 0.078 \cdot C_I)$$

Where  $D_F$  is equal to the diffuse fraction of solar radiation,  $C_I$  is equal to the clearness index and  $JD$  is equal to Julian Day (1 to 365).

### *Potential Incoming Direct Beam Solar Radiation (above Topographic Features) (Chen 1994)*

$$\Phi_{SRB1} = \Phi_{SRB} \cdot (1 - D_F)$$

Where  $\Phi_{SRB1}$  is equal to potential incoming direct beam solar radiation (above topography; watts/m<sup>2</sup>),  $\Phi_{SRB}$  is equal to the estimate of potential incoming direct beam solar radiation (above topography; watts/m<sup>2</sup>) and  $D_F$  is equal to the diffuse fraction of solar radiation.

### **2.2.3 Solar Radiation Blocked by Vegetation and Topography**

Topography is oftentimes the first barrier encountered by incoming direct beam solar radiation (Boyd and Kasper 2003). If the solar altitude ( $\theta_{SA}$ ) is greater than the topographic shade angle ( $\theta_{T_z}$ ), or the angle between the center of the stream and the highest topographic feature, then topographic shade is not occurring. However, if the solar altitude ( $\theta_{SA}$ ) is less than the topographic shade angle ( $\theta_{T_z}$ ), topographic shade is occurring and incoming direct beam solar radiation ( $\Phi_{SRB2}$ ) is assumed to be zero.

#### *Direct Beam Solar Radiation below Topography*

When topographic shade is occurring ( $\theta_{SA} \leq \theta_{T_z}$ )

$$\Phi_{SRB2} = 0$$

When topographic shade is not occurring ( $\theta_{SA} > \theta_{T_z}$ )

$$\Phi_{SRB2} = \Phi_{SRB1}$$

Where  $\Phi_{SRB2}$  is equal to direct beam solar radiation below topography (watts/m<sup>2</sup>),  $\Phi_{SRB1}$  is equal to potential incoming direct beam solar radiation (above topographic features; watts/m<sup>2</sup>),  $\theta_{SA}$  is equal to solar altitude (degrees) and  $\theta_{T_z}$  is equal to the topographic shade angle (degrees).

#### *Direct Beam Solar Radiation below Vegetation*

The amount of incoming solar insolation attenuation by the riparian vegetation within each polygon sampled depends on the height ( $H_{poly}$ ), width ( $W_{poly}$ ) and density ( $\Psi_{poly}$ ) of riparian vegetation within each polygon. As previously discussed, these data are sampled at each longitudinal sampling node, in 105 individual and consecutive polygon sampling units that radiate out from each sampling node in seven cardinal direction (northeast, east, southeast, south, southwest, west, northwest) (Figure 5).

In addition, solar flux attenuation within each polygon is determined by the path length that radiation must travel through the polygon and a light extinction coefficient. Path length varies with solar altitude ( $\theta_{SA}$ ), solar azimuth ( $\theta_{AZ}$ ), and the width of each vegetation polygon ( $W_{poly}$ ). Attenuation of direct beam solar radiation as it travels through each block of vegetation is estimated using Beer's Law (Oke 1978) to determine the amount of solar radiation leaving each polygon ( $A_{poly}$ ); as previously mentioned, this value depends on the density of vegetation within each polygon.

Direct beam radiation is routed through riparian vegetation polygons beginning at the outermost polygon and working inward to the stream center. The calculated amount of radiation that passes through each polygon is routed to the next innermost polygon and factored into its solar flux attenuation estimate; the process is repeated until solar flux estimates for all polygons are complete and the final amount reaching the stream surface can be determined.

**Step 1:** Within each polygon, the following formula is used to calculate the length of the shadow cast by the vegetation within each polygon (SL):

$$SL_{poly} = \frac{H_{poly} + Z_{poly}}{\tan\left(\theta_{SA} \cdot \frac{\pi}{180^\circ}\right)}$$

Where  $SL_{poly}$  is equal to the shadow length for each riparian vegetation polygon,  $H_{poly}$  is equal to the mean height of vegetation within each polygon,  $Z_{poly}$  is equal to the bare earth elevation within each

polygon, and  $\theta_{SA}$  is equal to the solar altitude. If the shadow length cast from a polygon is greater than the distance to the stream, then shade is occurring.

**Step 2:** The following formulas are used to calculate 1) the path length (PL) over which the direct beam solar radiation must travel through each polygon and 2) the shade density ( $\Psi$ ), or transmissivity, of each polygon:

If  $SL_{poly} \geq W_{poly}$  then:

$$PL_{poly} = \frac{W_{poly}}{\cos\left(\theta_{SA} \cdot \frac{\pi}{180^\circ}\right)}$$

$$\Psi_{poly} = 1 - \text{Exp}\left(\frac{\text{Log}(1 - VD_{poly})}{10} \cdot PL_{poly}\right)$$

If  $SL_{poly} < W_{poly}$  then:

$$PL_{poly} = 0$$

$$\Psi_{poly} = 0$$

Where  $W_{poly}$  is equal to the width of each polygon,  $PL_{poly}$  is equal to the path length over which direct beam solar radiation must travel through each polygon,  $VD_{poly}$  is equal to the vegetation density in each polygon and  $\Psi_{poly}$  is equal to the shade density of each polygon.

**Step 3:** The amount of direct beam solar radiation received by each polygon is then calculated as a function of shade density and the direct beam solar flux leaving the previous zone using the following formula:

For polygons #15 (outermost) to #1 (innermost)

First polygon (outermost; #15):

$$A_{prev} = \Phi_{SRB2}$$

$$A_{poly} = A_{prev} \cdot (1 - \Psi_{poly})$$

Next polygon:

$$A_{prev} = \Phi_{SRB3}$$

Where  $A_{poly}$  is equal to the solar flux leaving a polygon,  $A_{prev}$  is equal to the solar flux leaving the previous (outer) polygon (watts/m<sup>2</sup>),  $\Phi_{SRB2}$  is equal to direct beam solar radiation below topography (watts/m<sup>2</sup>),  $\Psi_{poly}$  is equal to the shade density in each polygon, and  $\Phi_{SRB3}$  is equal to the direct beam solar radiation below vegetation (watts/m<sup>2</sup>).

The direct beam solar radiation received at the stream surface of each longitudinal sampling node is determined by the cumulative solar flux contributed by all 7 of the innermost polygons (veg-zone 1 from each wedge):

$$\Phi_{SRB4} = A_{NW\ poly(1)} + A_{W\ poly(1)} + A_{SW\ poly(1)} + A_{S\ poly(1)} + A_{SE\ poly(1)} + A_{E\ poly(1)} + A_{NE\ poly(1)}$$

Where  $\Phi_{SRB4}$  is equal to the direct beam solar radiation received at the stream surface (watts/m<sup>2</sup>),  $A_{direction\ poly(1)}$  is equal to the innermost polygon (veg-zone 1) within each wedge, and *direction* is equal to the cardinal direction of each wedge (Figure 5).

#### 2.2.4 Effective Shade

Finally, Effective shade can be estimated for each sampling node using the following formula:

$$Solar_1 = \Phi_{SRB1}$$



$$Solar_2 = \Phi_{SRB4}$$

$$ES = \frac{(Solar_1 - Solar_2)}{Solar_1}$$

Where  $ES$  is equal to the effective shade (%) for the sampling node,  $Solar_1$  is equal to a daily average of the potential incoming direct beam solar radiation (above topographic features) at the sampling node ( $\Phi_{SRB1}$ ) (watts/m<sup>2</sup>) and  $Solar_2$  is equal to a daily average of the direct beam solar radiation received at the stream surface of the sampling node ( $\Phi_{SRB4}$ )(watts/m<sup>2</sup>), after accounting for the solar flux attenuated by topographic features and riparian vegetation combined ( $\Phi_{SRB3}$ ).

### 2.2.5 Model Execution

Shade simulations were set to occur for every minute on August 1<sup>st</sup>, 2012; this date was chosen to represent the time of year when maximum stream heating typically occurs as a result of higher sun altitude and infrequent cloud cover (Chen *et al.* 1998b; DeWalle 2008, 2010). Many other shade modeling studies use similar parameters for the time step (1 minute), or frequency of simulations (Chen *et al.* 1998 a,b; DeWalle 2008; Greenberg *et al.* 2012; Watanabe *et al.* 2005), duration(24 hrs.) (Allen *et al.* 2007; DeWalle 2008; Ryan *et al.* 2013) and time of year (Chen *et al.* 1998 b; DeWalle 2008; Greenberg *et al.* 2012; Ryan *et al.* 2013). At each longitudinal node, the model calculated the amount of incoming solar radiation, or solar flux, attenuated by the vegetation in surrounding polygons once every minute during the specified 24 hour period. The final output provides the daily average of incoming solar radiation that is attenuated by the vegetation within each polygon (henceforth referred to as solar flux attenuation (watts/m<sup>2</sup>)). Based on the net incoming solar radiation at each longitudinal sampling node, the model also calculates the daily average of percent effective shade at each longitudinal sampling node.

It should be noted that the solar flux attenuation estimates associated with each polygon represent the amount of incoming solar radiation prevented from reaching the stream surface at a specific location, which is determined by the location of the longitudinal sampling node the polygon corresponds to. In other words, the model is not estimating the overall solar flux attenuation provided by the vegetation within a polygon; it only estimates the solar flux attenuation provided to a discrete point along the stream. In this way, the overlap that occurs between neighboring polygons (Figure 5) will not result in certain riparian areas being double-counted; overlapping polygons will have completely different solar flux estimates since they will each correspond to two completely different points along the stream.

Each stream was individually modeled under two scenarios; current conditions and a restoration scenario. Both scenarios differed only with respect to vegetation height and density; all other inputs were the same between both current and restored scenarios. Prioritization of taxlots, subwatersheds and jurisdictions was accomplished using model outputs for the average daily solar flux attenuation ( $\text{watts/m}^2$ ) in each polygon. Model outputs for effective shade (%) at each longitudinal sampling node were used for evaluative and quality control purposes only; they were not used in the prioritization scheme.

## **2.5 Effective Shade Analysis**

Effective shade estimates under current and restored conditions were compared to determine where the largest gains, in terms of effective shade, were produced under the restoration scenario. Effective shade estimates under current conditions were subtracted from effective shade estimates under restored conditions to determine the net gain in effective shade (%) resulting from restoration at each longitudinal sampling node. Modeling results for effective shade were spatially joined to all sampling

nodes in ArcGIS and partitioned into various effective shade brackets to produce the maps found in section 3.1.

## 2.6 Restoration Prioritization

Restoration prioritization was performed at three different scales: taxlots, jurisdictions, and subwatersheds. Prioritizing at the taxlot scale identifies valuable prospects for land owner outreach, whereas prioritizing at the jurisdictional or subwatershed scale identifies broader spatial patterns and trends in riparian shade throughout the watershed that will help city and county jurisdictional representatives evaluate their need for action.

Before prioritization at each scale was performed, some minimal post-processing of modeling outputs was required. Solar flux attenuation estimates from current conditions were subtracted from restored condition estimates to determine the net increase in solar flux attenuation per polygon resulting from restoration. This is essentially the amount of solar insolation prevented from reaching the stream surface that is a direct result of restoring all restorable area within that polygon. Additional programming tools (using python scripts) were used to rearrange, or sort, the simulation data results into a table format with the net increase in solar flux attenuation under restored condition listed per polygon.

In order to prioritize taxlots, subwatersheds and jurisdictions for restoration, a series of steps were taken to determine a single value representing the **restoration efficiency** of each individual taxlot, subwatershed, or jurisdiction. Restoration efficiency is defined in this paper as the net increase in solar flux attenuation per acre restored. For each individual taxlot, subwatershed, or jurisdiction, the net increase in solar flux attenuation was found by aggregating all streams (and the polygons therein) within their boundaries and taking the sum of the solar flux attenuation for those streams. This value was then

divided by the acres restored within each unit, to determine the restoration efficiency. The process used for prioritizing at each scale is discussed in further detail below.

### *Prioritizing Taxlots*

Modeling results for all streams were spatially joined to taxlot data and incorporated into a single taxlot shapefile in ArcGIS using the following procedure. Polygons containing solar flux attenuation data were converted to points in ArcGIS (Figure 7) and all points within each taxlot were aggregated resulting in a total sum of potential solar flux attenuation ( $\text{watts/m}^2$ ) for each taxlot. Additionally, the amount of restorable area within each taxlot (vegetation <4m in height and within 15m or stream channel) was calculated using built-in geometry calculation functions in ArcGIS. GIS derived taxlot data was then transferred to an Excel spreadsheet to calculate priority rankings.

Dividing the solar flux attenuation by the acreage restored for each taxlot produced a measure of restoration efficiency within each taxlot that was then used to sort the taxlots from most efficient (greatest solar flux attenuation per acre) to least efficient (least solar flux attenuation per acre). Once sorted, the **cumulative solar flux reduction** was calculated for the entire watershed; the cumulative solar flux reduction is equal to the net increase in solar flux attenuation under a restoration scenario for the entire watershed. A running total of the percent of the cumulative solar flux reduction having been met was tabulated, beginning with the most efficient taxlots (in terms of restoration efficiency) at the top of the list and down to the least efficient at the bottom. Priority rankings were assigned based on the following criteria: taxlots that collectively attain the first 50% of the cumulative solar flux reduction are classified as high priority; taxlots that collectively attain the next 40% (from 50-90%) are classified as medium priority; taxlots that make up the last 10% (from 90-100%) are classified as low priority and finally, taxlots that do not contribute to the cumulative solar flux reduction (increase in solar flux attenuation =0) are classified as “maintain”.

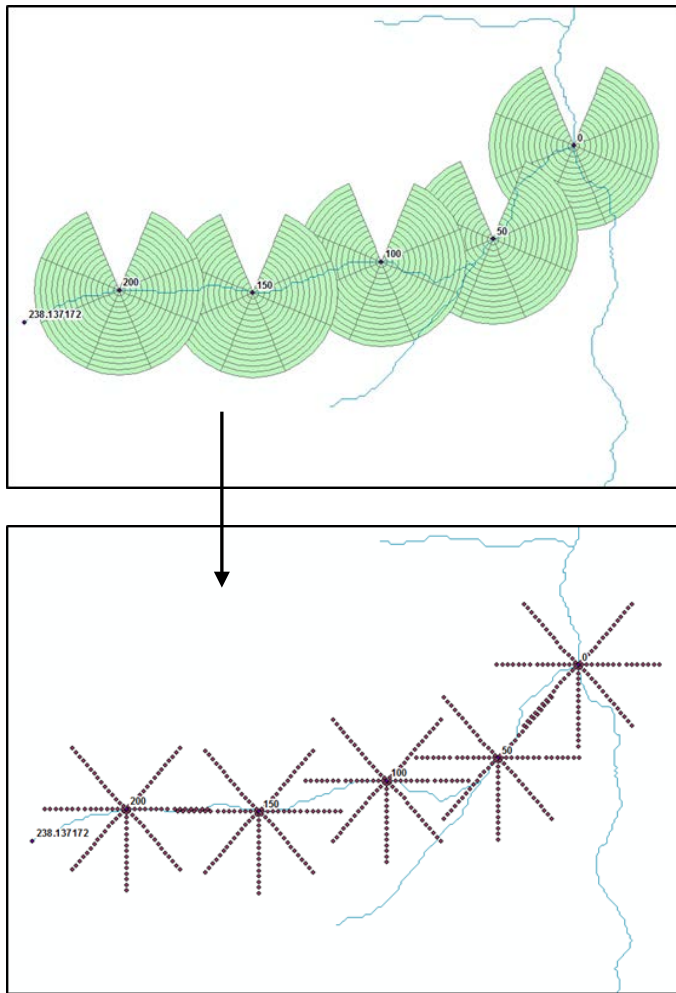


**Figure 8: Polygon-to-point conversion**

*Polygons were converted to points prior to being spatially joined with taxlots. Each point has a value for total daily solar flux reduction ( $\text{watts}/\text{m}^2$ ). All points contained within each taxlot were aggregated to determine the total daily solar flux reduction per taxlot ( $\text{watts}/\text{m}^2$ ).*

### *Prioritizing Subwatersheds and Jurisdictions*

Subwatersheds and jurisdictions were prioritized almost exactly the same way as with taxlots. After solar flux attenuation estimates were aggregated within taxlots, the total solar flux attenuation from all taxlots within each subwatershed or jurisdiction was aggregated, resulting in a total sum of solar flux

attenuation for each subwatershed or jurisdiction. The amount of restorable area in each subwatershed or jurisdiction was calculated using built-in geometry calculation functions in ArcGIS and the data was transferred to an Excel spreadsheet to calculate priority rankings. In Excel, the restoration efficiency within each subwatershed or jurisdiction was calculated and used to sort them from highest restoration efficiency down to least efficient. The cumulative solar flux reduction for subwatersheds and jurisdictions was the same as with taxlots and a running total of the percentage of the cumulative solar flux reduction being met was calculated similarly. Priority rankings were assigned using the same cumulative solar flux reduction thresholds as criteria (first 50%; next 40%; last 10%).

### *Summary Statistics*

All summary statistics were calculated in an Excel spreadsheet or using ArcGIS data summary tools. The number of taxlots, subwatersheds and jurisdictions that fall within each priority ranking were calculated to identify which areas in the watershed will maximize the ecological returns, in terms of shade, of restoration efforts. Furthermore, summary statistics were used to evaluate the relationships between priority rankings and certain taxlot, subwatershed or jurisdictional attributes, such as size, acres of restorable area, or the percent of the restoration buffer that is restorable within each unit.

## **2.7 Quality Control**

### *Testing an Alternative Approach*

In an effort to evaluate the potential impact of *not* accounting for the growth of un-restored vegetation under the restoration scenario, 14 streams were re-modeled using an alternative set of assumptions to define restored conditions. The 14 streams chosen for re-modeling occupy the north-western portion of the Sunshine Creek subwatershed and comprise a cluster of tributary streams that eventually converge with the mainstem of Sunshine Creek; they are not randomly scattered throughout the watershed but rather clustered together. The restored conditions raster was modified from its

original design only with respect to the height of un-restored vegetation. Un-restored vegetation was assumed to contain a similar riparian community as restored vegetation and, as such, the height of all un-restored vegetation currently less than 27m was set equal to 27m under restored conditions. In sum, the restored conditions assumed that in 55 years, the height of all vegetation, weather restorable or un-restorable, would be equal to or greater than 27m. Only vegetation that is currently over 27m tall was assumed to remain at its current height (having already reached its climax life stage) and did not receive additional growth.

Restored conditions were re-modeled for the streams and compared to current conditions to determine the net change in solar flux attenuation as a result of both restoration *and* the natural growth of vegetation. Spatially assigning solar flux attenuation estimates to taxlots was done exactly the same way as previously described in Section 2.6. A total of 51 taxlots intersected the subset of re-modeled streams.

Priority rankings were assigned to each taxlot using the same general approach outlined in Section 2.6, however, only the subset of taxlots that intersected the re-modeled streams were included in the prioritization scheme (i.e. the priority rankings did not reflect their ranking in the entire watershed, but only within the streams that were re-modeled). The cumulative solar flux reduction was determined by summing up solar flux attenuation estimates for just the 51 taxlots being evaluated. Then, the taxlots were sorted from highest restoration efficiency to lowest and prioritized according to their contribution to the cumulative solar flux reduction. For each taxlot, two priority rankings were determined: the first using the old solar flux estimates, and the second using the new solar flux estimates.

The majority of priority rankings were either the same or only a single ranking removed (i.e. maintain instead of low, or medium instead of high). Over half of the priority rankings (52%) were the same for both model runs, whereas 43% were only a single ranking removed.. There were 2 taxlots that had very

different rankings resulting from each model run; one went from a maintain ranking (original approach) to medium ranking (alternative approach) and another went from a maintain ranking (original approach) to a high ranking (alternative approach).

The taxlot that changed from maintain (using original approach) to medium (using alternative approach) had restorable area within it, but did not contribute any increase (increase was equal to 0 watts/acre) in solar flux attenuation as a result of restoration; thus the maintain ranking from the original approach. Once the un-restorable area was allowed to grow, the observed increase in solar flux attenuation under restored conditions significantly increased. When this new solar flux estimate was divided by the restorable area, it appeared as though a large increase in solar flux attenuation resulted from a very small amount of restoration when in reality the true cause for this increase was actually a combination of un-restored vegetation growing taller *and* restoration efforts. In this situation, dividing the increase in solar flux attenuation by restorable acres does not produce a measure of restoration efficiency since the increase in solar flux attenuation is no longer exclusively the result of restoration efforts. While it would make more sense in this situation to divide the increase in solar flux attenuation by the total acres within each taxlot, as opposed to restorable acres only, this would no longer assist in the prioritization of taxlots based on their potential to produce large gains from restoration efforts; instead, it would prioritize taxlots based on their potential to produce large gains without considering the magnitude of restoration efforts needed.

A similar circumstance can explain how the second taxlot went from maintain (using original approach) to high priority (using alternative approach) as well. While there was restorable area in this taxlot, the increase in solar flux attenuation as a result of restoration was extremely low (~1watt/acre); thus the maintain ranking from original approach. When the un-restorable area was allowed to grow, the observed increase in solar flux attenuation significantly increased while the restorable acres remained



the same. As a result, dividing solar flux attenuation by restorable acres gave the false impression that the restoration efficiency for this taxlot was very high when in reality, the increase in solar flux attenuation for this taxlot was primarily caused by natural background growth, not restoration.

In order to identify taxlots with a high level of restoration efficiency, the effect of un-restored vegetation must be controlled for by keeping it fixed. Furthermore, a major assumption of the alternative approach is that all vegetation is comprised of trees and that the tree species are the same as those planted in restorable areas (height and age at maturity are the same as in restored areas). This is not likely to be true since invasive species, which are often shrubs, are known to be prevalent throughout the watershed (BES, 2001; JCWC 2012).

### *Re-modeling*

To ensure accuracy of modeling results, ~10% of the streams (43 streams) were randomly chosen (using the RANDBETWEEN function in Microsoft Excel) to be re-sampled and re-modeled, using exactly the same sampling and modeling procedures from the original run. Results from second models were compared to the first model results in an attempt to identify recurring errors. Results from the second set of model runs exhibited a 4.6% margin of error when compared to original model outputs. In particular, 2 streams out of the 43 total (i.e. 4.6%) that were randomly chosen to be re-sampled and modeled had output values that differed from their original counterparts. For the remaining 41 streams, model results from first and second runs were 100% identical.

For one of the streams that exhibited modeling errors, the source of the error was determined to be improperly formatted model inputs. To ensure that this error was not widespread, the datasheets containing input parameters for all streams were double-checked for similar formatting errors. No additional formatting errors were found as a result of these efforts and the pervasiveness of this specific error is assumed to be low.

The second stream exhibiting modeling errors was also determined to be a result of operator error. During the second model run for this stream, data concerning current vegetation was mistakenly used when modeling both current and restored scenarios and, as a result, when comparing results for both scenarios the apparent difference in daily solar flux attenuation was zero watts/m<sup>2</sup> for all polygons sampled. This error was also very easily detectable during the post-processing of modeling results (i.e. the output file contains all zeros which are visually obvious) and was not apparent in any of the other streams modeled. As such, this particular operator error is not likely to be prevalent; however, operator errors in general are likely to remain largely undetected and a 4.6% margin of error is assumed to appropriately reflect the level of operator error to be expected within the modeling results presented in this paper.

### *Field Measurements*

In order to evaluate the accuracy of model predictions for current conditions, 24 field measurements of effective shade were collected for comparison; over half (14) were collected in July 2012 and the remaining 10 were collected in November, 2013. Collection of field measurements was originally scheduled to occur during the month of August, in order to match up with the date used for shade simulations. Additional measurements were taken in November to increase the sample size of field measurements and provide a more robust measurement of error.

Using a solar pathfinder (Perusion) adjusted for the appropriate latitude band (45°) and magnetic declination (15°), the sunpath arc for August was used to measure effective shade at these locations during both field surveys. GPS coordinates (UTM) were recorded using a Samsung Galaxy cell phone with the Backcountry Navigator PRO application. Modeling estimates for percent effective shade generally agreed with field measurements; the average difference between measured and modeled percent

effective shade estimates was only ~4% ( $R^2=0.73$ )<sup>7</sup> (Figure 8); typically, values greater than 0.5 are considered acceptable (Moriassi *et al.* 2007; Santhi *et al.*,2001, Van Liew *et al.*, 2003). Possible causes for disagreement stem from outdated LiDAR raster data (2007), solar pathfinder measurement error, modeling error, or because some of the measurements were taken in November after abscission of deciduous trees had begun.

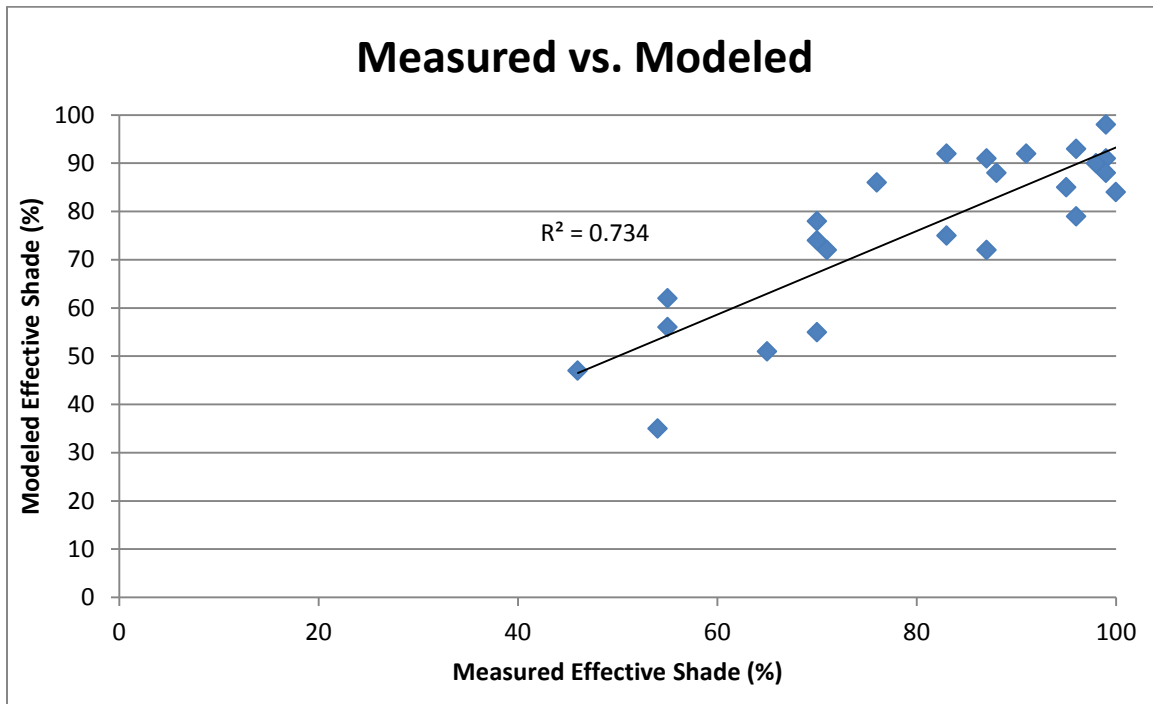


Figure 9: Field measurements vs. modeling estimates of percent effective shade

### 3.0 Results

#### 3.1 Effective Shade

Modeling results for effective shade under current and restored conditions are presented in Table 3 below. The average effective shade for all streams in the watershed is currently estimated at 73% ( $\pm 29\%$ ). Under a restoration scenario, the average effective shade is estimated at 93% ( $\pm 9.6\%$ ).

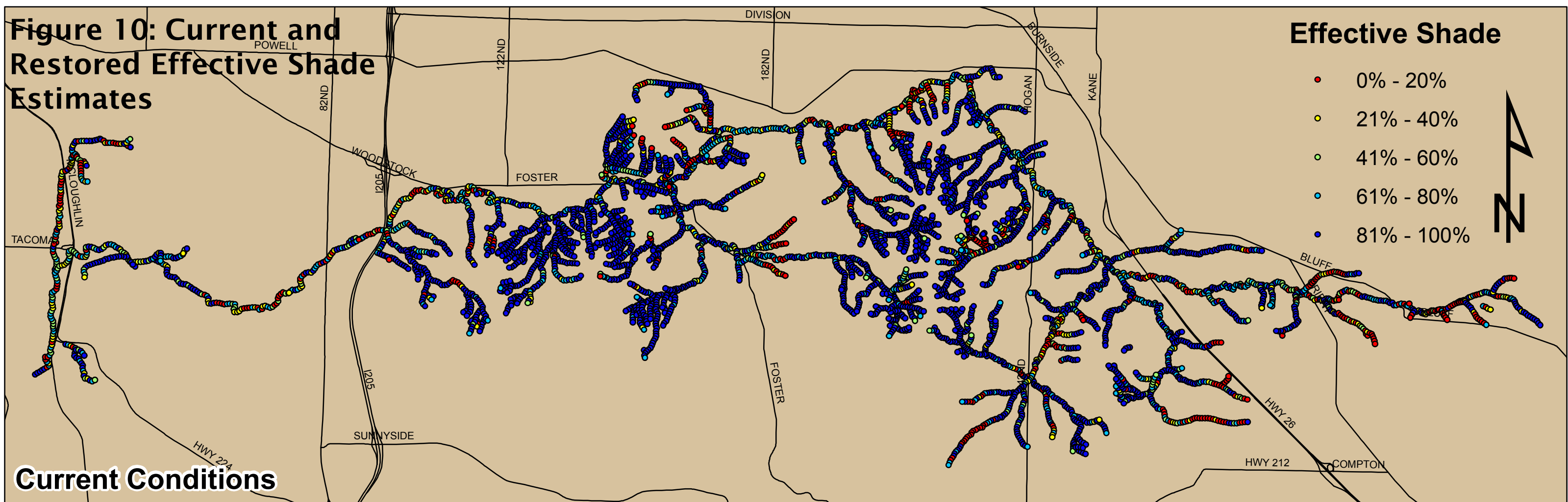
<sup>7</sup> This value was calculated using Excel’s built-in function for a linear regression trendline.

Currently, only 63% of all sampling nodes meet the 80% effective shade target identified for Johnson Creek in the 2006 TMDL whereas 95% of all sampling nodes met this target under a restoration scenario (Figure 10). The average increase in effective shade under restored conditions was 19% ( $\pm 28\%$ ), with the majority of all sampling nodes (73% of total) exhibiting an increase in effective shade between 1-25% (see Figure 11).

**Table 3: Effective Shade Summary Statistics**

|                     | Av. Effective Shade (%) | Std Dev     | Min/Max  | % of sampling nodes $\geq$ 80% Effective Shade |
|---------------------|-------------------------|-------------|----------|--|
| Current Conditions  | 73%                     | $\pm 29\%$  | 0%/100%  | 63%  |
| Restored Conditions | 93%                     | $\pm 9.6\%$ | 13%/100% | 95%  |

**Figure 10: Current and Restored Effective Shade Estimates**



**Current Conditions**



**Restored Conditions**

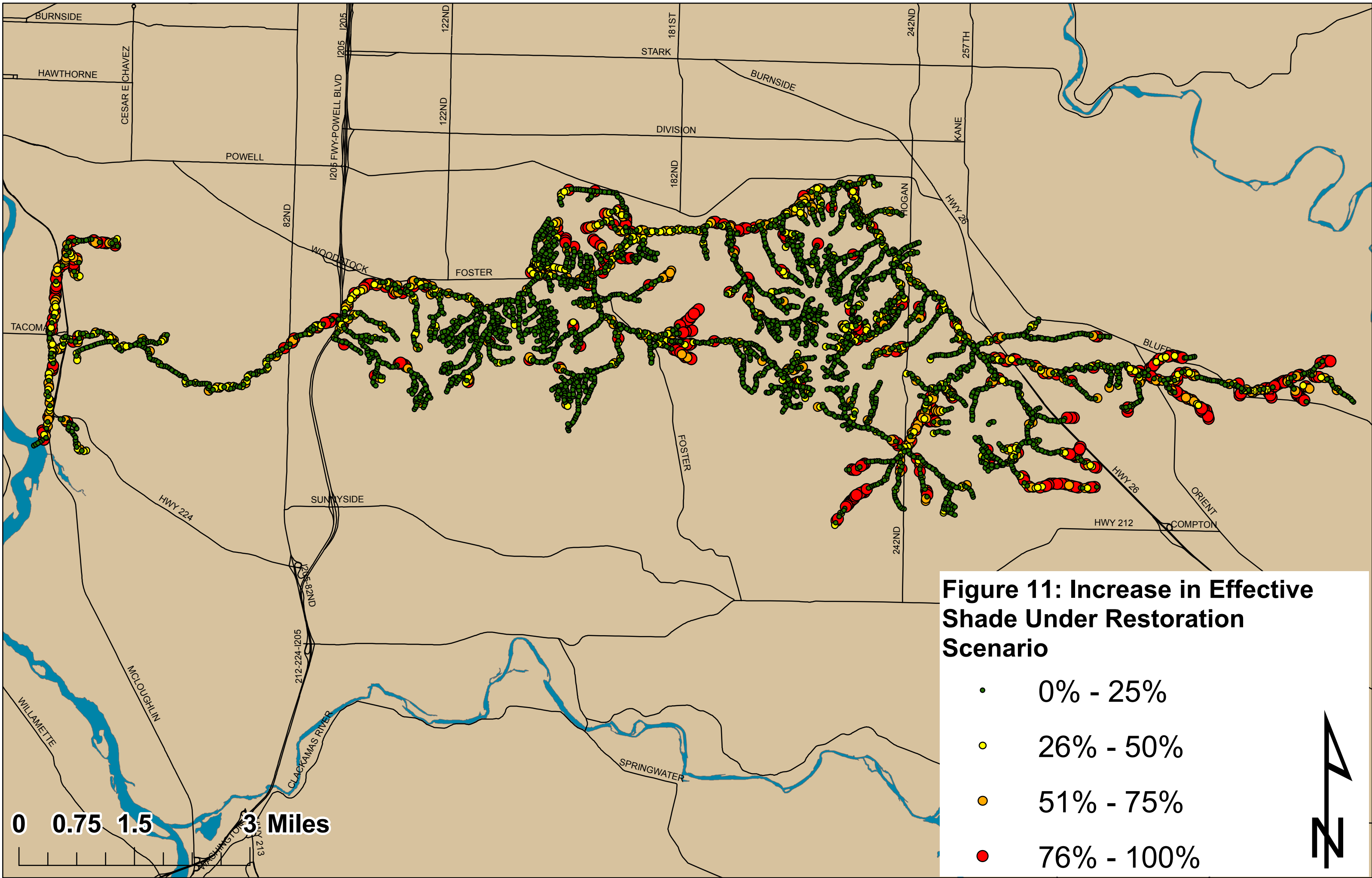


**Figure 11: Increase in Effective Shade Under Restoration Scenario**

- 0% - 25%
- 26% - 50%
- 51% - 75%
- 76% - 100%

## 3.2 Restored Conditions

The cumulative solar flux reduction, or net increase in solar flux attenuation for the entire watershed as a result of restoration, was estimated at 209,118.9 (watts/m<sup>2</sup> /d). The entire restoration buffer, or area extending 15m to either side of the stream channel where restoration activities are likely to occur, encompassed a total area of 8,841.4 acres. The total restorable area, or area with current vegetation < 4m in height within the restoration buffer that *would* be restored under a restored scenario, was estimated at 544.9 acres (6% of the total restoration buffer). The remaining 94% of the restoration buffer either currently supports vegetation ≥4m in height, or is occupied by buildings or roads and *would not* be restored under a restoration scenario. Figure 3 shows the extent and geographic distribution of the total restorable area within the study area.

## 3.3 Priority Rankings by Taxlot

A total of 3,722 taxlots of varying sizes and land uses were found to intersect the restoration buffer within the study area. According to RLIS taxlot data, the primary land uses in these taxlots include: single family residential (54.7% of all taxlots), undeveloped (24.3%), rural (8.1%), agriculture (3.9%), forest (2.6%), commercial (2.4%) and multi-family residential (1.0%). The average area for each taxlot was 2.78 acres, with values ranging between  $8.72 \times 10^{-4}$  to 153.77 acres. The restorable area within each taxlot was, on average, only 9.8% of the entire restoration buffer within each taxlot, yet these values were highly variable ranging between 0 and 100%.

As shown in Figure 12, high priority taxlots collectively achieved 50% of the cumulative solar flux reduction for the watershed. Medium priority taxlots collectively made up another 40% of the cumulative solar flux reduction, bringing the watershed up to 90% of its goal. Low priority taxlots

collectively made up 10% of the cumulative solar flux reduction, bringing the total to 100%. Finally, taxlots categorized as “maintain” did not contribute at all.

High priority taxlots had the largest gain in solar flux attenuation rates as a result of restoration (1719 watts/acre/d on average), medium priority taxlots gained an intermediate amount (438 watts/acre/d on average), low priority taxlots gained even less (102 watts/acre/d on average) and taxlots classified as “maintain” did not exhibit any change in solar attenuation between current and restored conditions (increase of 0 watts/acre/d).

### *Number of Taxlots in Each Ranking*

Of the 3,722 taxlots that were found to intersect the restoration buffer, 831 (22% of all taxlots) were categorized as high priority, 601 (16%) were categorized as medium priority 837 (22%) were categorized as low priority and 1453 (39%) were categorized as “maintain”. Table 4 provides summary statistics for each priority ranking group. In addition, Figure 12 illustrates the percentage of all taxlots that fall within each prioritization ranking group. Figure 13 and Figure 14 provide detailed maps of taxlot rankings throughout the watershed.

### *Restorable Acres in each Ranking*

Based on prioritization rankings made at the taxlot scale, 113.7 acres of the total 544.9 restorable acres within the study area (21% of total restorable acres) fell within high priority taxlots, 184.8 acres (34%) fell within the medium priority taxlots, 189.2 acres (35%) fell within low priority taxlots and 57.0 (10%) occurred in taxlots categorized as “maintain” (Table 4 and Figure 12).



**Table 4: Summary statistics for taxlot priority rankings**

*Please refer to the Glossary for clarification of any terminology used in this Table. The average percent of restoration buffer deemed restorable is essentially the number of restorable acres, divided by the un-restorable acres within each taxlot (converted to a percentage).*

| <b>Priority</b> | <b># Taxlots</b> | <b>% of all taxlots</b> | <b>Restorable acres</b> | <b>% of total restorable acres</b> | <b>Av. taxlot area (acres)</b> | <b>Av. % of restoration buffer deemed restorable</b> | <b>Av. Daily Increase in solar flux attenuation/acre restored</b> |
|-----------------|------------------|-------------------------|-------------------------|------------------------------------|--------------------------------|--|---|
| High            | 831              | 22%                     | 113.7                   | 21%                                | 1.6                            | 15%  | 1719  |
| Medium          | 601              | 16%                     | 184.8                   | 34%                                | 4.0                            | 14%  | 438   |
| Low             | 837              | 22%                     | 189.2                   | 35%                                | 5.2                            | 10%  | 102   |
| Maintain        | 1,453            | 39%                     | 57.0                    | 10%                                | 1.5                            | 5%   | 0   |
| <b>Total</b>    | <b>3722</b>      | <b>100%</b>             | <b>544.9</b>            | <b>100%</b>                        |                                |  |   |

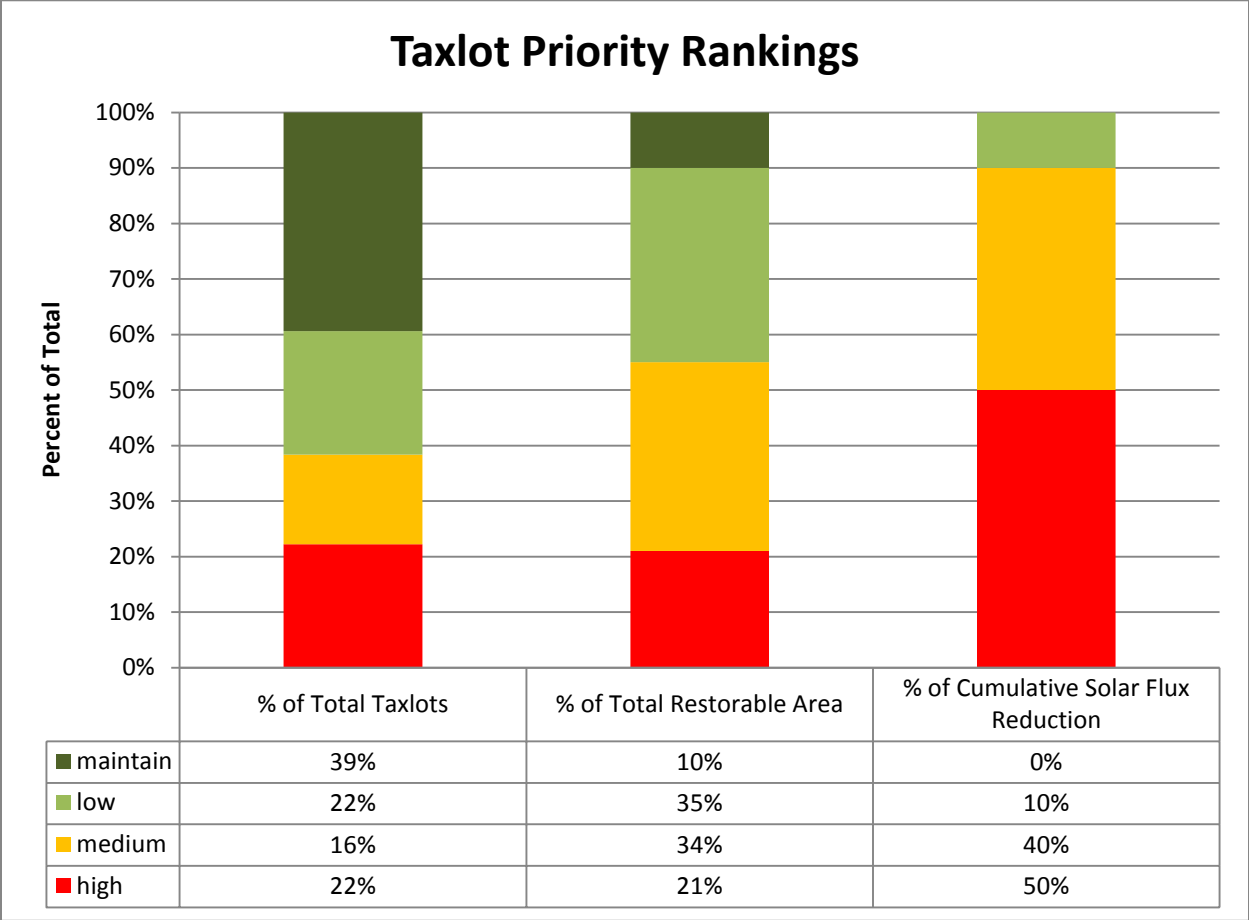
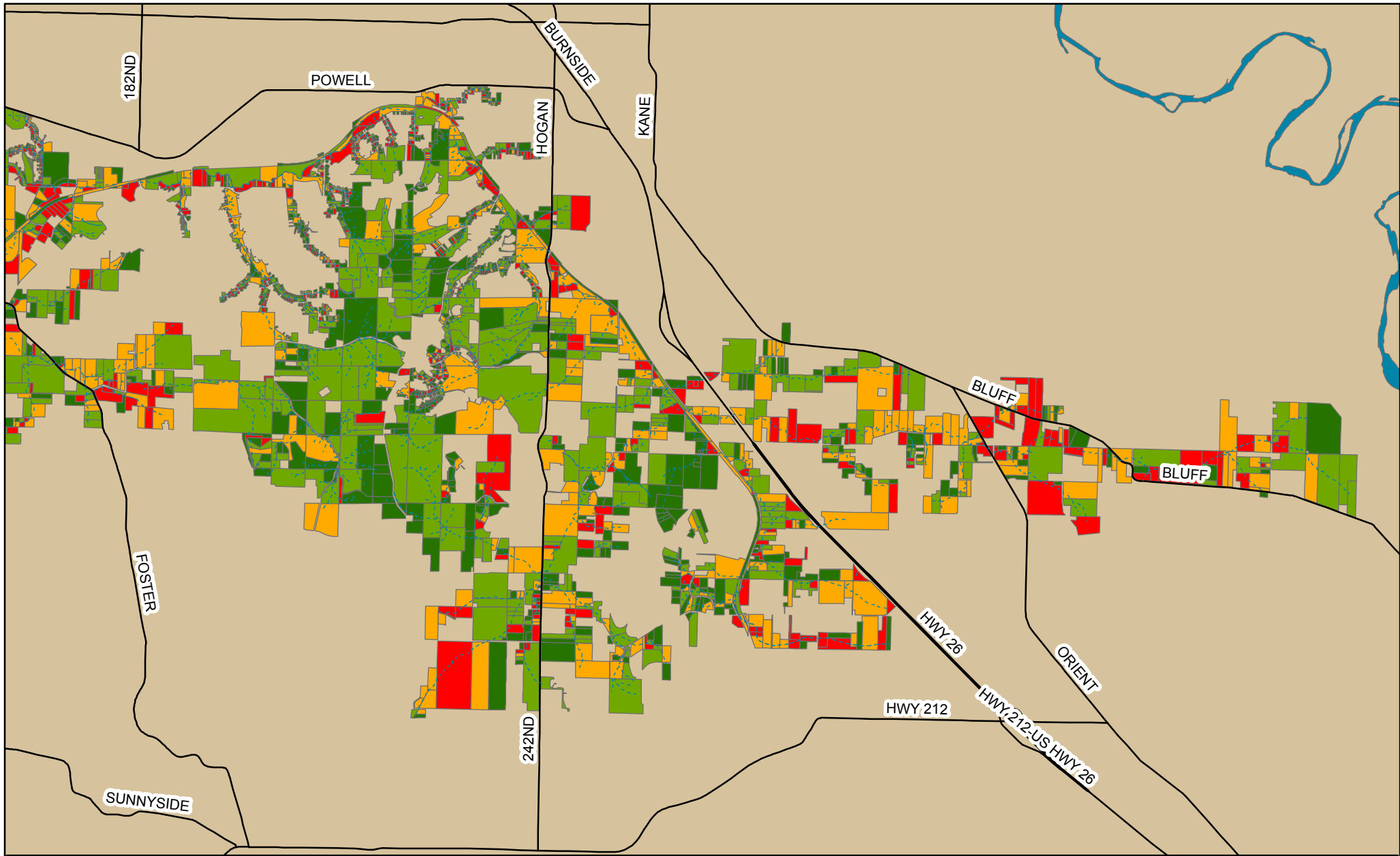


**Figure 12: Taxlot priority rankings chart**

*Taxlot priority rankings are evaluated in terms of various spatial metrics. The cumulative solar flux reduction is the net increase in solar flux attenuation for the entire watershed resulting from restoration (209,118.9 watts/m<sup>2</sup>/d). The total amount of restorable acres is the total acreage in the watershed that would be restored under a restoration scenario (544.9 acres). The total number of taxlots in the watershed that intersected the restoration buffer was 3,722.*



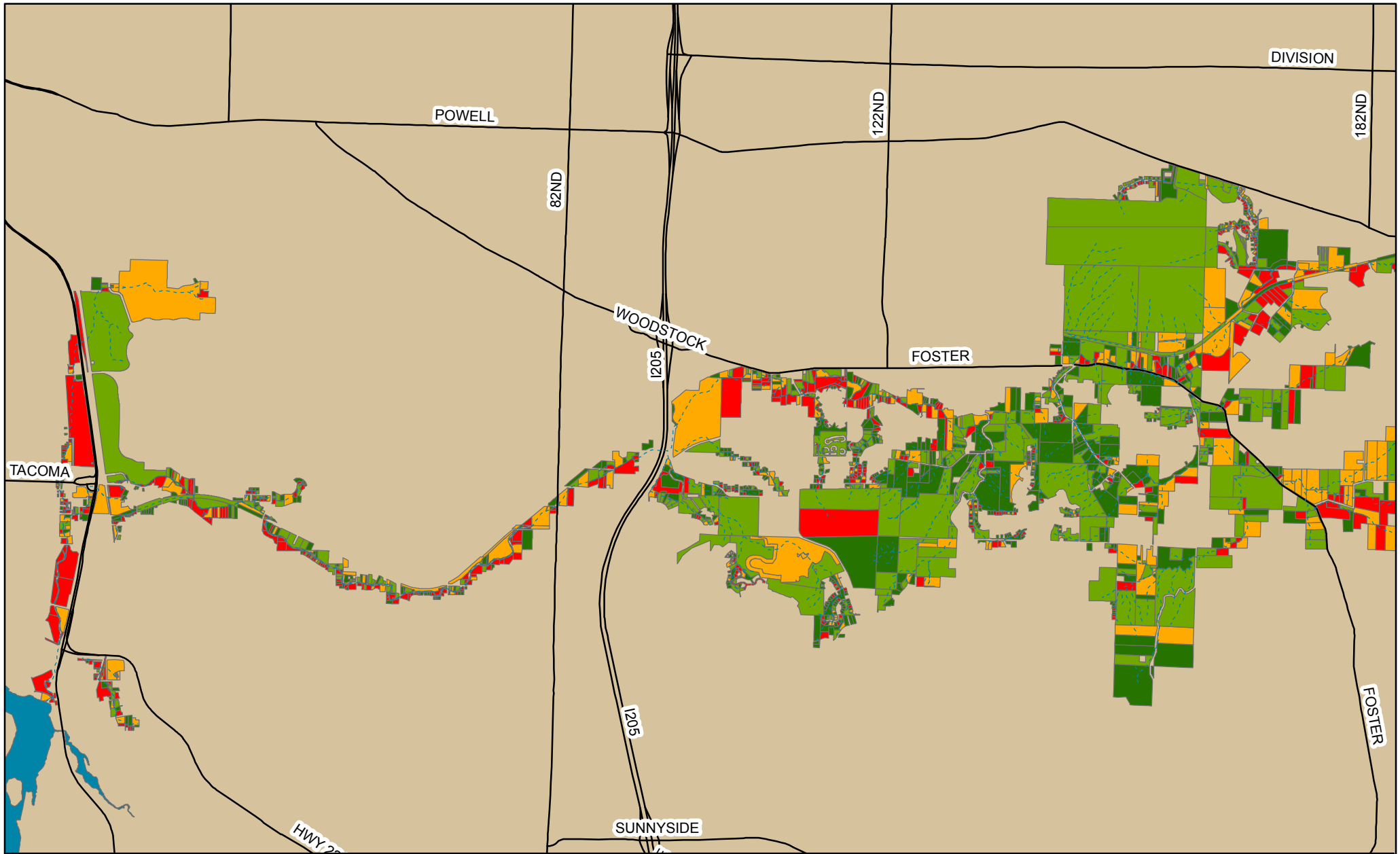
**Priority**

- high
- medium
- low
- maintain



**Figure 13: Taxlot Priority Rankings**  
**Eastern Half of Watershed**

March, 2014



**Priority**

- high
- medium
- low
- maintain



**Figure 14: Taxlot Priority Rankings**  
**Western Half of Watershed**

March, 2014

### 3.4 Priority Rankings by Subwatershed

A total of 36 subwatersheds intersected the restoration buffer and were considered in the prioritization scheme. The same prioritization scheme used for taxlots was applied at the subwatershed scale, where subwatersheds that collectively attain the first 50% of the cumulative solar flux reduction are high priority, the next 40% are medium priority, the last 10% are low priority, and those that do not contribute at all are classified as "maintain". Table 5 provides summary statistics for each priority ranking group in terms of subwatershed allocations.

#### *Number of Subwatersheds in each Ranking*

Of the 36 subwatersheds, 18 (50% of all subwatersheds considered) were categorized as high priority, 7 (19%) were categorized as medium priority 9 (25%) were categorized as low priority and 2 (6%) were categorized as "maintain". Figure 15 illustrates the percentage of all subwatersheds that fall within each prioritization ranking group. In addition, Figure 16 depicts the priority ranking assigned to each subwatershed in the study area.

#### *Restorable Acres in each Ranking*

In terms of restorable acres, high priority subwatersheds collectively comprised 38% of all restorable acres in the study area, medium priority subwatersheds comprised 29%, low priority subwatersheds comprised 31% and subwatersheds classified as "maintain" comprised 2% of all restorable acres (Figure 15).

Due to differences in the size of each subwatershed, the amount of restorable area within them was highly variable, ranging from 0 to 110 acres (Figure 17). The percentage of restorable area within each subwatershed's entire restoration buffer is variable, ranging between 0-11% (Table 5 and Figure 18).

**Table 5: Summary statistics for subwatershed priority rankings**

*Please refer to the Glossary for clarification of any terminology used in this Table. The average percent of restoration buffer deemed restorable is essentially the number of restorable acres, divided by the un-restorable acres within each subwatershed (converted to a percentage).*

| <b>Priority Ranking</b> | <b># of subwatersheds</b> | <b>% of all subwatersheds</b> | <b>Restorable acres</b> | <b>% of total restorable acres</b> | <b>Av. subwatershed area (acres)</b> | <b>Av. % of restoration buffer that is deemed restorable</b> | <b>Av. Daily Increase in solar flux attenuation/acre restored</b> |
|-------------------------|---------------------------|-------------------------------|-------------------------|------------------------------------|--------------------------------------|--|---|
| high                    | 18                        | 50%                           | 204.7                   | 38%                                | 1189.7                               | 7%   | 542.0   |
| medium                  | 7                         | 19%                           | 158.8                   | 29%                                | 817.3                                | 6%   | 362.3   |
| low                     | 9                         | 25%                           | 169.7                   | 31%                                | 517.1                                | 7%   | 263.1   |
| maintain                | 2                         | 6%                            | 11.6                    | 2%                                 | 182.5                                | 2%   | 75.7  |
| <b>Total</b>            | <b>36</b>                 | <b>100%</b>                   | <b>544.9</b>            | <b>100%</b>                        |                                      |  |   |

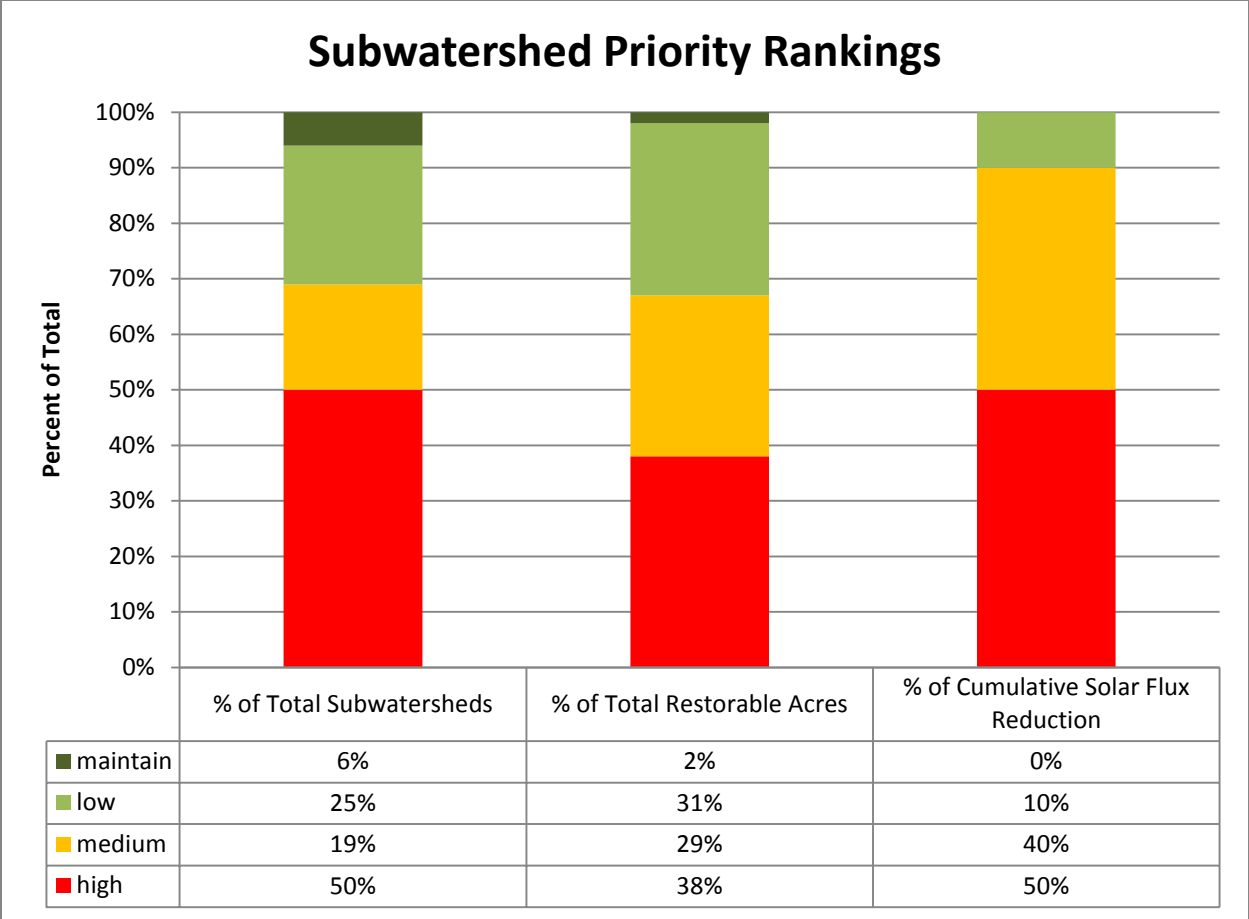
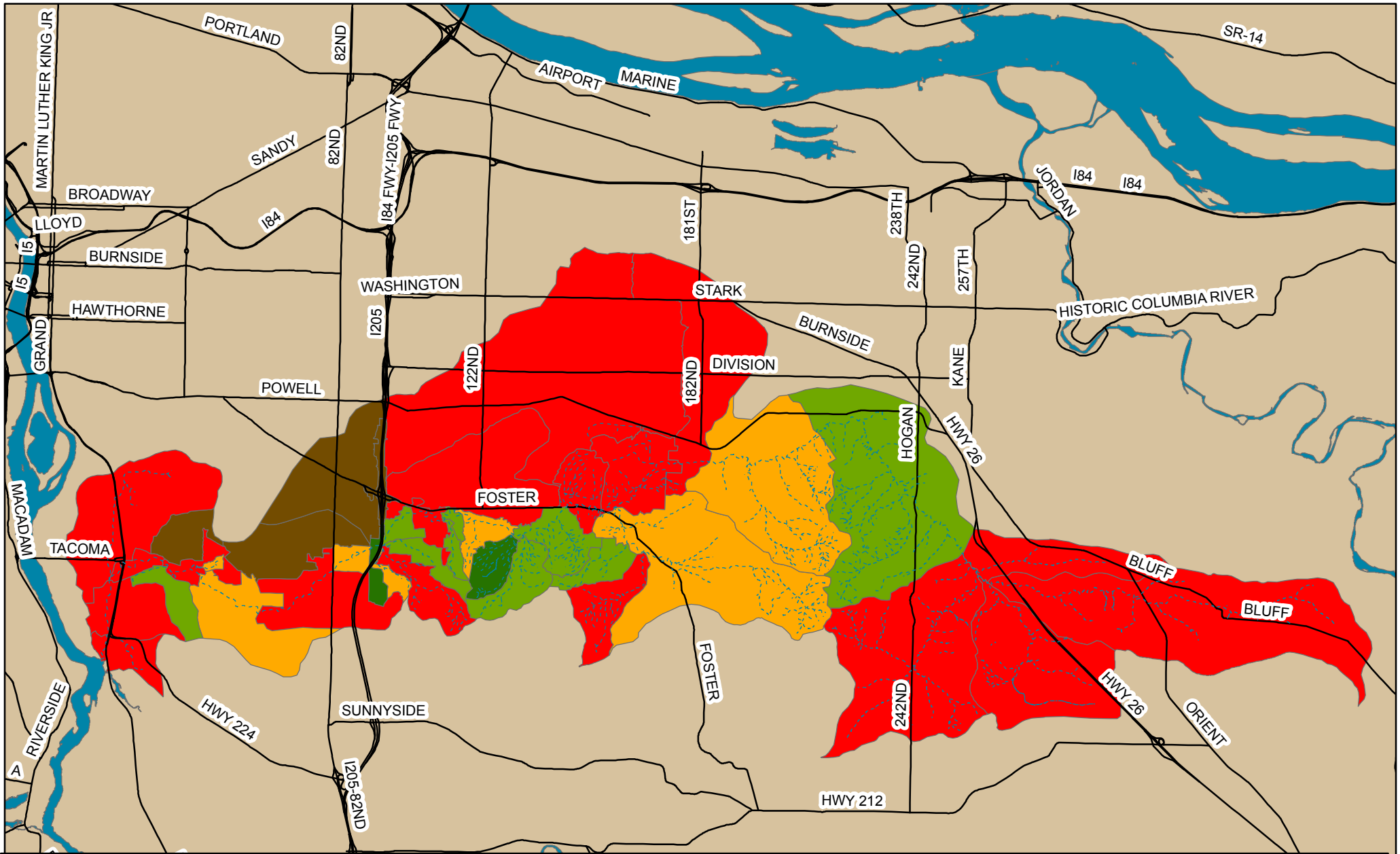


**Figure 15: Subwatershed priority rankings chart**

*Subwatershed priority rankings evaluated using various spatial metrics. The cumulative solar flux reduction is the net increase in solar flux attenuation for the entire watershed resulting from restoration (209,118.9 watts/m<sup>2</sup>/d). The total amount of restorable acres is the total acreage in the watershed that would be restored under a restoration scenario (544.9 acres). The total number of subwatersheds that intersected the restoration buffer was 36.*



**Priority**

- high
- medium
- low
- maintain
- does not intersect restoration buffer



0 1 2 4 Miles

**Figure 16: Subwatershed Priority Rankings**



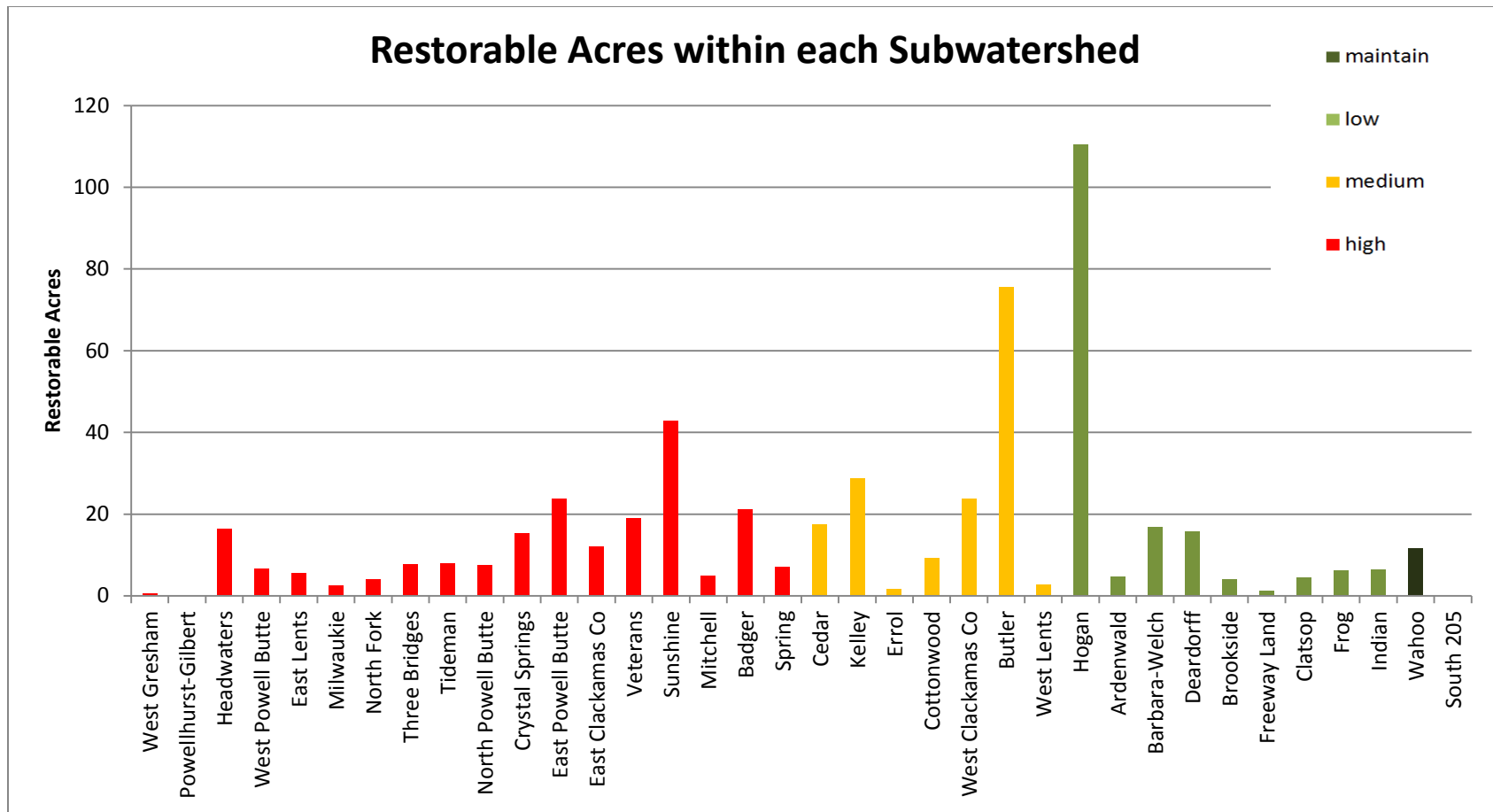


**Figure 17: Restorable acres within each subwatershed**

*The priority ranking of each subwatershed is indicated by its color. While some subwatersheds are bigger in size than others, it is important to consider the percentage of total acres within each subwatershed that are restorable when interpreting this chart and evaluating the restoration potential of each (see Figure 18).*

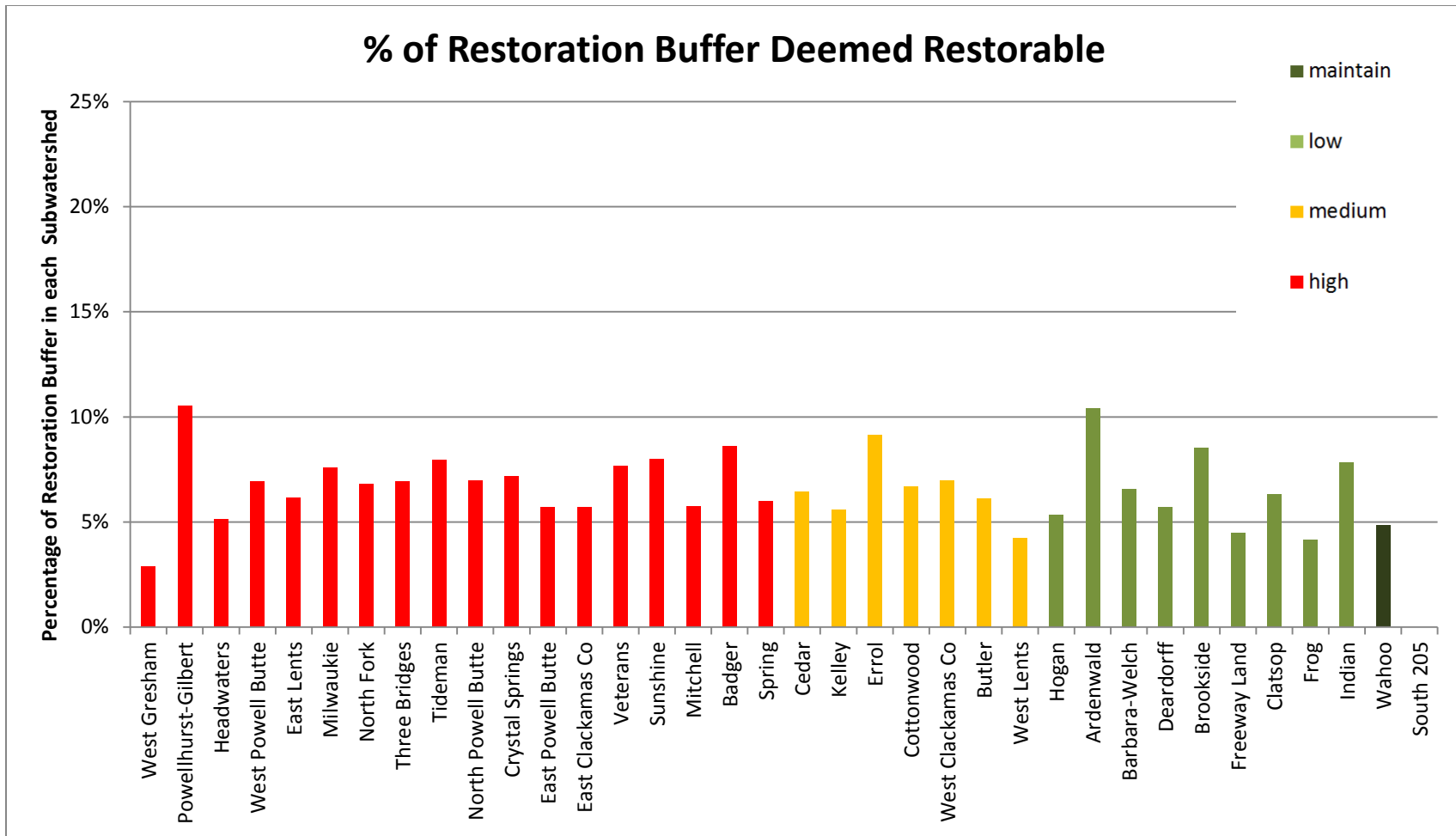


**Figure 18: Percent of each subwatershed's restoration buffer deemed restorable**

*The restoration buffer extends 15m out from the stream channel and represents the area in which restoration activities are likely to occur.*

*Restorable acres are those that fall within the restoration buffer and contain vegetation currently <4m in height.*

### 3.5 Priority Rankings by Jurisdiction

A total of 7 jurisdictions occur within the watershed, they are: the cities of Portland, Gresham, Milwaukie, Happy Valley and Damascus and Clackamas and Multnomah counties. The same prioritization scheme used for taxlots was applied at the jurisdictional scale, where jurisdictions that collectively attain the first 50% of the cumulative solar flux reduction are considered high priority, the next 40% are medium priority, the last 10% are low priority, and those that do not contribute at all are classified as "maintain". Table 6 provides summary statistics for each priority ranking group in terms of jurisdictional allocations.

#### *Number of Jurisdictions in Each Ranking*

Of the 7 total jurisdictions, 3 (43% of all jurisdictions considered) were categorized as high priority, 2 (29% of the total) were categorized as medium priority and 2 (29% of the total) were categorized as low priority. Figure 19 illustrates the percentage of all jurisdictions that fall within each prioritization ranking group. In addition, Figure 20 depicts the priority ranking assigned to each jurisdiction in the study area.

#### *Restorable Acres in Each Ranking*

In terms of restorable acres, high priority jurisdictions collectively comprised 41% of all restorable acres in the study area, medium priority jurisdictions comprised 46%, and low priority jurisdictions comprised 13% (Figure 19).

Due to differences in the size of each jurisdiction, the amount of restorable area within them was highly variable, ranging from 9 to 145 acres (Figure 21). The percentage of restorable area within each jurisdiction's entire restoration buffer is slightly variable, ranging between 4-10% (Figure 22).

**Table 6: Summary statistics for Jurisdictional rankings**

*Please refer to the Glossary for clarification of any terminology used in this Table. The average percent of restoration buffer deemed restorable is essentially the number of restorable acres, divided by the un-restorable acres within each jurisdiction (converted to a percentage). Average jurisdiction area is calculated from the acres of each jurisdiction that fall within the boundaries of the watershed only; it does not account for the area outside the boundaries of the watershed.*

| <b>Priority</b> | <b># Jurisdictions</b> | <b>% of total jurisdictions</b> | <b>Restorable acres</b> | <b>% of total restorable acres</b> | <b>Av. jurisdiction area (acres)</b> | <b>Av. % of restoration buffer deemed restorable</b> | <b>Av. increase in solar flux attenuation/acre restored</b> |
|-----------------|------------------------|---------------------------------|-------------------------|------------------------------------|--------------------------------------|--|---|
| High            | 3                      | 43%                             | 222.54                  | 41%                                | 3406.3                               | 7.4%   | 481.4   |
| Medium          | 2                      | 29%                             | 251.72                  | 46%                                | 5523.3                               | 6.5%   | 366.7   |
| Low             | 2                      | 29%                             | 70.63                   | 13%                                | 828.8                                | 4.6%   | 318.4   |
| <b>Total</b>    | <b>7</b>               | <b>100%</b>                     | <b>544.9</b>            | <b>100%</b>                        |                                      |  |   |

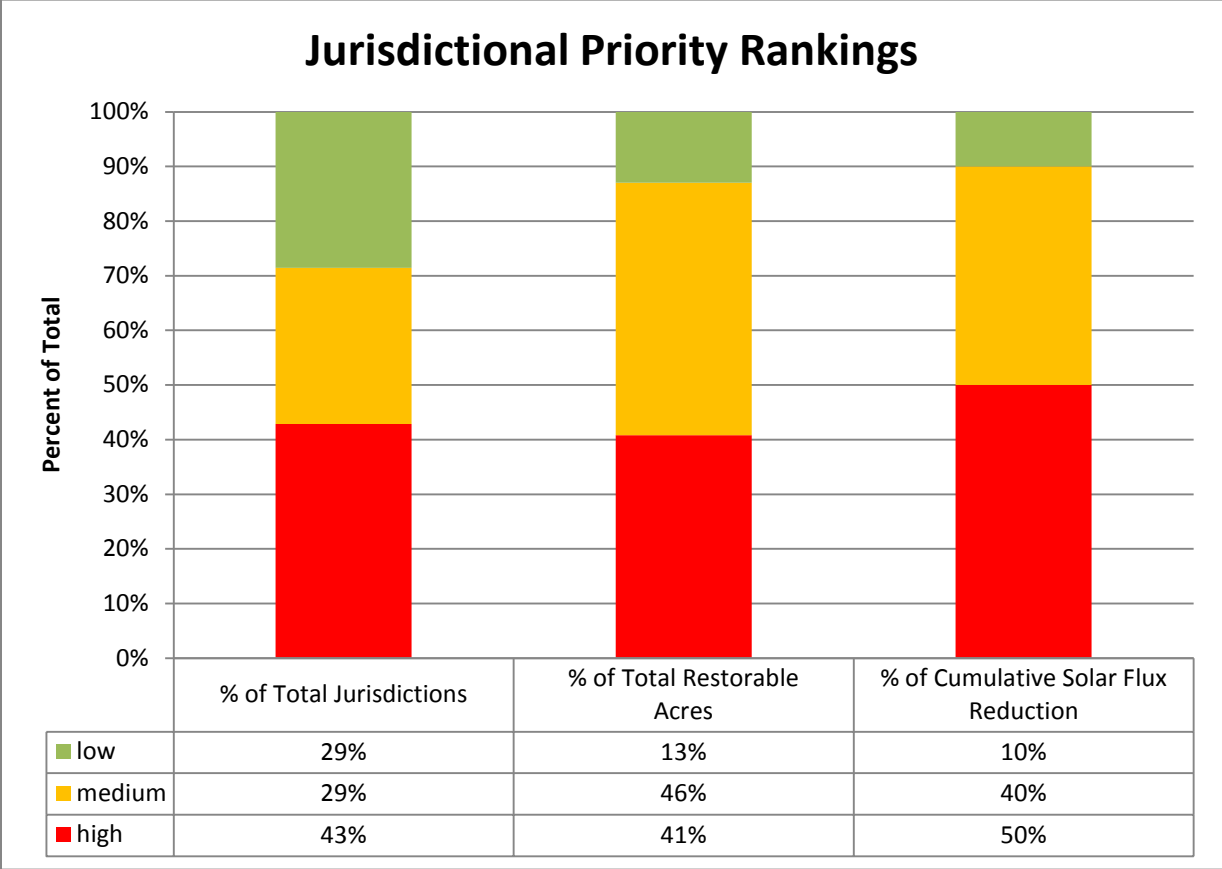
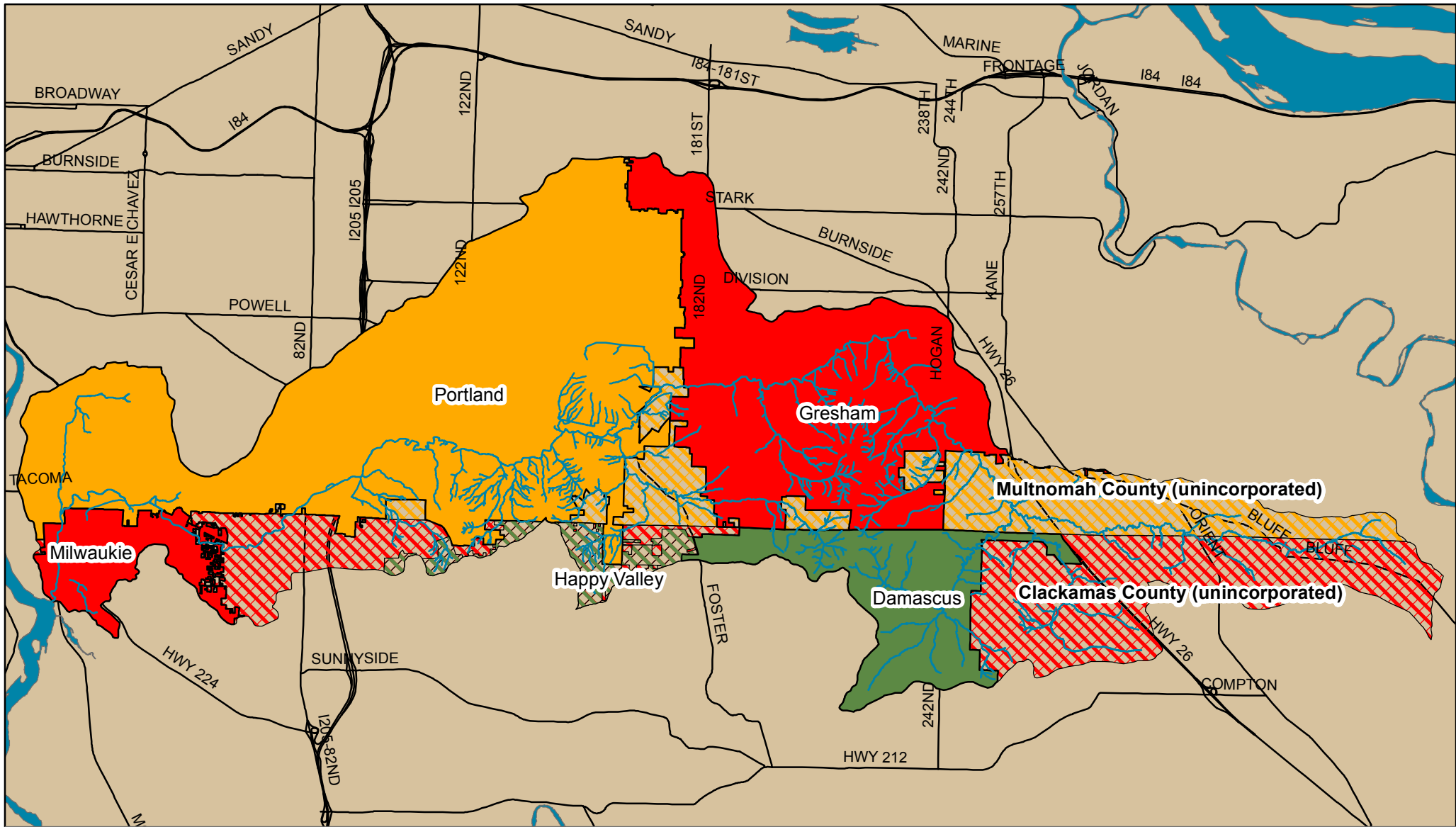


**Figure 19: Jurisdictional priority rankings chart**

*Jurisdictional priority rankings evaluated using various spatial metrics. The cumulative solar flux reduction is the net increase in solar flux attenuation for the entire watershed resulting from restoration (209,118.9 watts/m<sup>2</sup>/d). The total amount of restorable acres is the total acreage in the watershed that would be restored under a restoration scenario (544.9 acres). There are a total of 7 jurisdictions in the watershed.*



**Priority**

 High

 Medium

 Low

0 1.25 2.5 5 Miles

**Figure 20: Jurisdictional Priority Rankings**

March, 2014



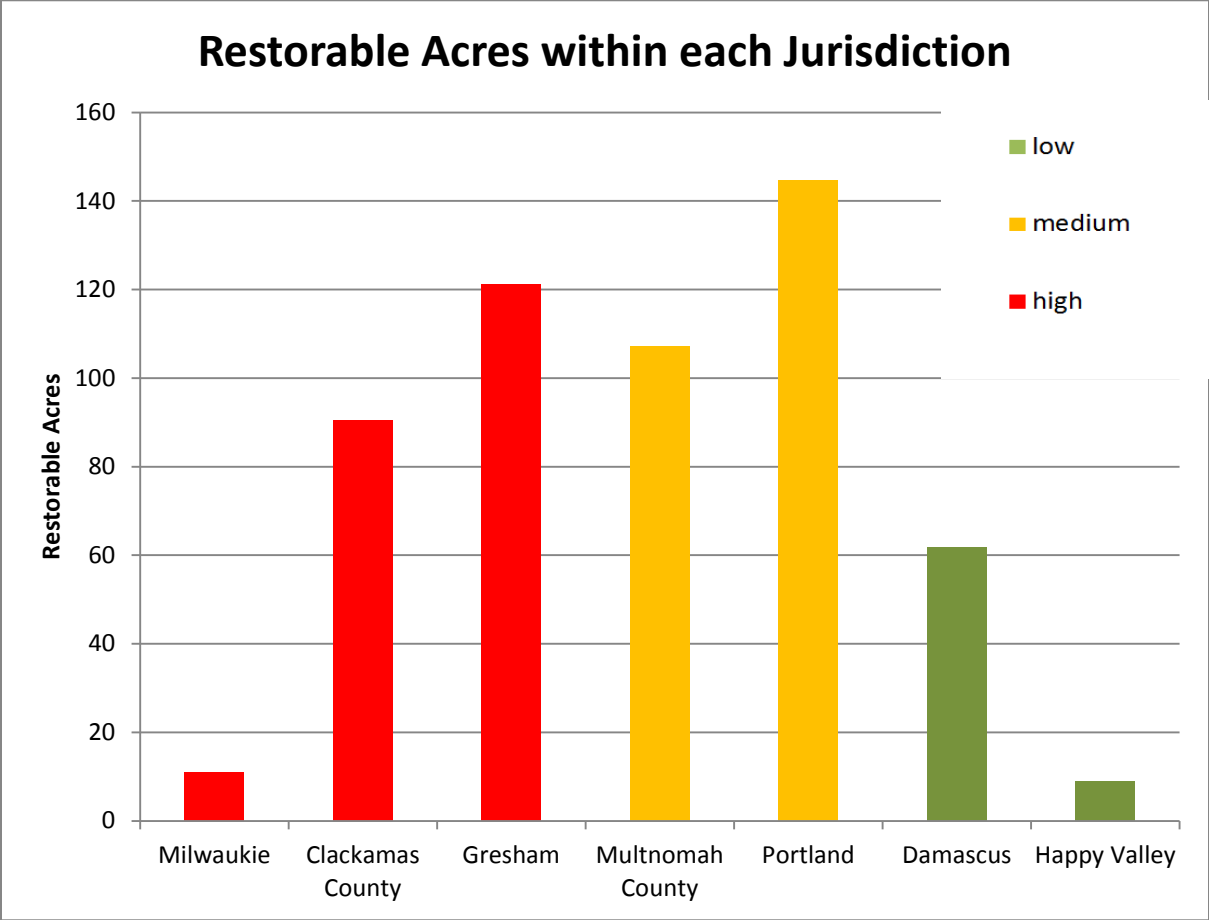


**Figure 21: Restorable acres within each jurisdiction**

*Priority ranking for each jurisdiction is indicated by color. Restorable acres are those that both fall within the restoration buffer and contain vegetation currently <4m in height. While some jurisdictions are bigger in size than others, it is important to consider the percentage of each jurisdiction’s restoration buffer that is deemed restorable when interpreting this chart (see Figure 22).*

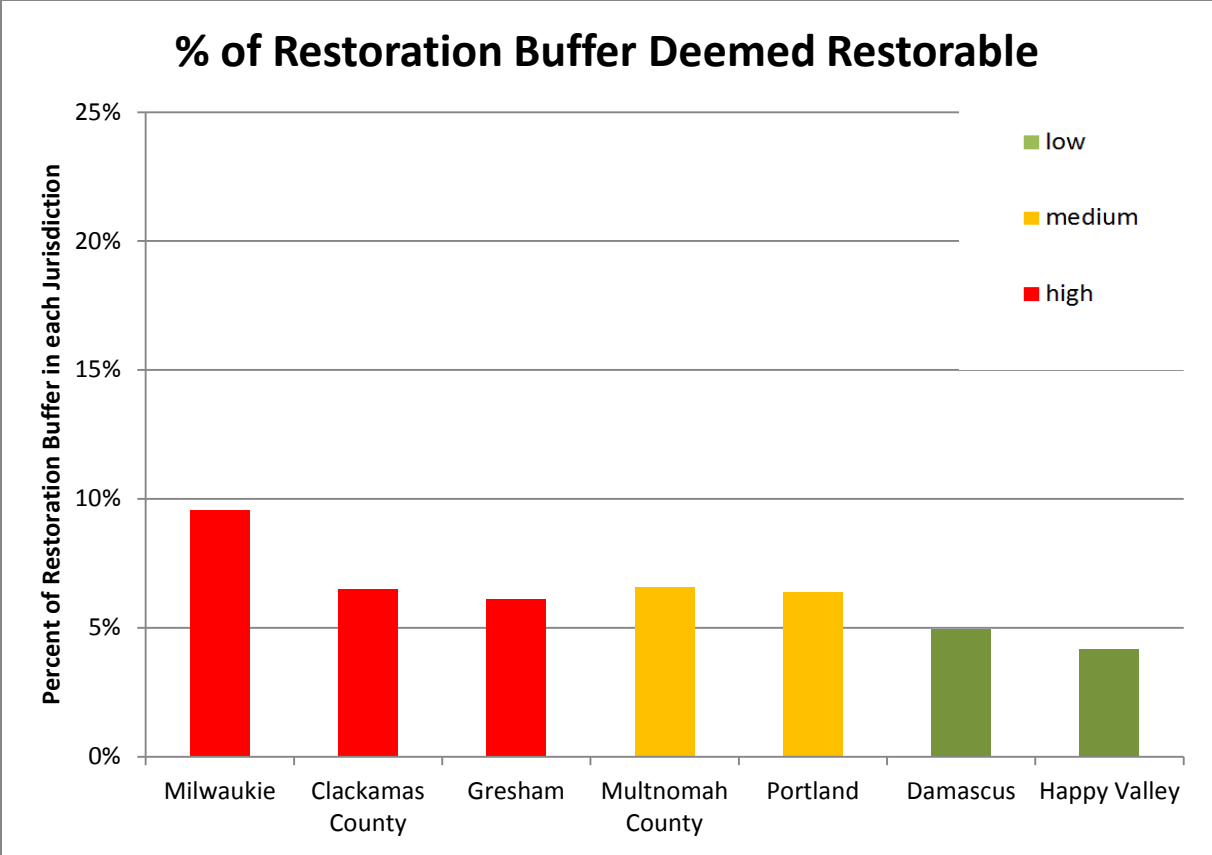


**Figure 22: Percent of each jurisdiction’s restoration buffer that is deemed restorable.**

*Priority ranking for each Jurisdiction is indicated by color. The restoration buffer extends 15m out from the stream channel and represents the area in which restoration activities are likely to occur. Restorable acres are those that both fall within the restoration buffer and contain vegetation currently <4m in height. For each jurisdiction, the percentage of their own restoration buffer that was deemed restorable is presented in this chart; higher priority jurisdictions tend to have a larger percentage of their own restoration buffer deemed restorable.*



## 4.0 Discussion

### 4.1 Summary of Findings

Effective shade was modeled under current and restored conditions as a function of geographic location, solar position and limited riparian vegetation and stream morphology attributes. Currently, effective shade in the watershed is 73% on average, with only 63% of all sampling nodes meeting the effective shade target of 80%. Under restored conditions the average effective shade is 93% and 95% of all sampling nodes met the effective shade target of 80%. Within each stream, a substantial amount of longitudinal variability, in terms of effective shade, exists. This means that prioritizing at a spatial scale smaller than a single stream may be appropriate since each stream has localized areas of both low and high percent effective shade. Furthermore, occasional clusters of sampling nodes exhibiting large increases in effective shade as a result of restoration also occur, meaning prioritization at a spatial scale of taxlots, subwatersheds, jurisdictions may be able to capture these “hot spots”, or clusters, of areas with greatest potential. Overall, areas exhibiting the largest gains under restored conditions, in terms of effective shade, and that currently have very low levels of effective shade (0-40%) also tend to occur within taxlots, subwatersheds or jurisdictions classified as high or medium priority.

Taxlots, subwatersheds and jurisdictions were prioritized according to the increase in solar flux attenuation they would provide if all vegetation within 15m of the stream channel that is currently less than 4m in height were restored. Prioritization at the taxlot scale reveals that restoring only 22% of all taxlots or 21% of all restorable acres in the watershed would achieve 50% of the cumulative solar flux reduction. Similarly, restoring only 55% of all taxlots or 38% of all restorable acres would achieve 90% of the cumulative solar flux reduction. These results suggest that prioritization and implementation of restoration efforts at the taxlot scale has the potential to produce a high rate of returns, in terms of shade enhancement and ultimately, reduced stream temperatures, per acre restored.

Prioritization at the subwatershed and jurisdictional scale reveals that restoring 50% of all subwatersheds or 43% of all jurisdictions in the watershed would be needed to achieve 50% of the cumulative solar flux reduction. Similarly, restoring 69% of all subwatersheds or 72% of all jurisdictions would be needed to achieve 90% of the cumulative solar flux reduction. These results suggest that restoration efforts prioritized and implemented at the larger scale of subwatersheds or jurisdictions is not as efficient, in terms of the benefits produced per unit restored, when compared to prioritization at the taxlot scale. However, priority rankings for subwatersheds and jurisdictions bring attention to some subtle spatial patterns and trends in shade conditions throughout the watershed. Milwaukie, Clackamas county and Gresham exhibited the largest increase in solar flux attenuation under a restoration scenario; however, all jurisdictions had similar percentages of their restoration buffers deemed restorable (4-10%). This means that while some jurisdictions produce larger returns, in terms of shade enhancement, per acre restored, they all have similar ratios of restorable to un-restorable area within them. Milwaukie is the only jurisdiction that stands out as having a disproportionately large amount of restorable acres (see Figure 22).

## 4.2 Model Assumptions

As with all modeling endeavors, the modeling technique used in this study may be limited in its ability to provide accurate estimates of stream shading due to averaged measures of stream morphology, riparian condition and restored conditions, sampling design, or simplification of the stream heat budget (Johnson 2003; Li *et al.* 2012). Many environmental attributes were simplified or excluded from the model in an effort to maintain model simplicity or as a result of financial and technological constraints. Over time, technological advances in satellite image production and processing techniques are expected to allow for data to be more easily extracted from high spatial resolution imagery and incorporated into shade models (Gergel *et al.* 2007).

### *LiDAR Derived Raster data*

Input parameters concerning physical attributes and vegetation height were sampled from raster data collected between 2004 and 2007; the large majority (90%) was collected in 2007. Any changes to bare earth and/or vegetation occurring since 2007 were not considered in the model. The impact of riparian restoration projects that have taken place in the watershed since 2007 on stream shading are not reflected in the modeling results; however, the growth of vegetation since 2007 is not likely to greatly exceed 4 meters based on the average growth rates and establishment periods for the riparian tree species planted (BES 2001; Watanabe *et al.* 2005). Additionally, assuming that the stream channel has not migrated is fairly safe, considering the extent and magnitude of stream channelization that has occurred throughout the watershed. The accuracy of the digitized stream channel was verified using aerial photos from 2010.

### *Heat Budget Simplification*

In this study and many others, model simplicity is maintained by estimating effective shade as a function of solar radiation exclusively (Allen *et al.* 2007; Beschta 1997; DeWalle 2010; Li *et al.* 2012). Although stream temperatures are governed by a variety of heat exchange processes including, but not limited to, short wave direct solar radiation, long wave radiation from the atmosphere or water, evaporative flux, and bed conduction flux (Cristea and Burges 2010; DeWalle 2008; Herb and Stefan 2011), in most cases, direct and diffuse solar radiation is the primary source of heat loading to streams, particularly low-order streams with narrow channel widths (Boyd and Kasper 2003; Chen *et al.* 1998a; Cristea and Burges 2010).

In addition, stream temperature is influenced by hydrologic components such as groundwater inputs and stream flow. Groundwater-fed streams are susceptible to a cooling effect from inflowing groundwater, which could effectively reduce the need for stream shading (Webb *et al.* 2008). Since

effective shade is considered a surrogate measure of stream temperature, additional variables concerning hydrologic components and heat exchange processes were not included in this study to maintain model simplicity. However, certain streams with unique stream flow and groundwater dynamics may exhibit unique shade requirements; in these circumstances, a consideration of stream flow and groundwater inputs would be advisable since they have the potential to significantly influence increase or decrease the need for, and effectiveness of, riparian restoration efforts.

Channel width, vegetation overhang, stream bank shading, and cloudiness are some commonly considered variables in shade modeling endeavors that were not considered in this study. While most shade modeling studies involve some level of simplification and exclusion of variables (DeWalle 2008; Rutherford *et al.* 2010), the specific variables included or ignored by each study tends to vary (Allen *et al.* 2007; Rutherford *et al.* 2010). For example, DeWalle (2008, 2010) and Li *et al.* (2012) modeled riparian shade using simplified, uniformly applied values for vegetation height and overhang, as well as stream width yet ignored the influence of topographic shade. Chen *et al.* (1998a,b) considered channel width, vegetation overhang, topographic shade and cloudiness, but did not consider stream bank shading. Lastly, while many studies have chosen to simulate stream shading under clear-sky, or cloud-free, conditions to represent summer conditions when solar insolation is at its greatest (DeWalle 2008; Greenberg *et al.* 2012; Li *et al.* 2012), many other studies have included cloud cover as well (Chen *et al.* 1998 a,b).

### *Sampling Design*

Most aspects of the sampling design utilized for this study are well-supported in the literature including the longitudinal sampling rate of 50 meters (Chen *et al.* 1998 a,b; Rutherford *et al.* 1997) and buffer width of 30 meters (Chen *et al.* 1998 a,b; DeWalle 2010; Johnson *et al.* 2007). In addition, some aspects of the sampling design tend to exceed the spatial or temporal resolution standards of most

studies including the lateral sampling rate of 2 meters (Chen *et al.* 1998a; DeWalle 2008; Greenberg *et al.* 2012; Li *et al.* 2012) and the number of topographic shade measurements (DeWalle 2010; Li *et al.* 2012; Rutherford *et al.* 2010). However, the main sampling aspect that tends to differ amongst studies is the longitudinal sampling rate. In general, the longitudinal sampling rate should reflect the longitudinal scale of variation in shade (Allen *et al.* 2007; Li *et al.* 2012). If accounting for tree overhang and bank shading, the shadows cast by trees will be very complex and are likely to vary at the scale of tree spacing (4-8m), requiring relatively smaller longitudinal sampling rates from 1-30m (DeWalle 2012; Guoyuan *et al.* 2012). Also, the magnitude of shade variation is related to age-class structure, with young or secondary forests exhibiting much less heterogeneity in canopy structure and light attenuation compared to old growth forests (Warren *et al.* 2013). However, shade models oftentimes employ simplifying assumptions regarding the shape of riparian vegetation by assigning uniform values for height, density, and/or overhang to discrete blocks of vegetation, such as in this study (Boothroyd *et al.* 2004; Chen *et al.* 1998 a,b; Guoyuan *et al.* 2012; Quinn *et al.* 1992). These assumptions regarding the shape of vegetation effectively reduce the scale of spatial variation enabling the use of greater longitudinal sampling rates.

While interest has grown in the study of micro-gradients along stream channels and riparian buffers, research in this topic has generally focused on lateral gradients, radiating out from the center of the stream out to the stream banks, rather than longitudinal, or along-stream, gradients (Goebel 2012; Guoyuan *et al.* 2012; Moore *et al.* 2005; Olson *et al.* 2007; Warren *et al.* 2013; Webb *et al.* 2008). Due to the lack of knowledge surrounding along-stream shade gradients, it remains difficult to determine a proper longitudinal sampling rate a priori (Chen *et al.* 1998b). Use of a smaller longitudinal sampling rate (30m) may have yielded more accurate estimates of effective shade, especially if additional riparian vegetation attributes, such as vegetation overhang or channel width, had been included as modeling inputs (Greenberg *et al.* 2012).

### 4.3 Restored Conditions

Restored conditions were coarsely defined and uniformly applied to all near-stream vegetation throughout the study area. Overall, the main assumptions made in terms of restored conditions that are likely to reduce the accuracy of modeling results relate to the height, width, density and uniform distribution of restored vegetation. In addition, this study did not account for the growth of un-restored vegetation in an effort to isolate the signal, or effect, of restoration efforts on solar flux attenuation from that of naturally occurring growth of riparian vegetation. While the true solar flux attenuation provided by restored vegetation at maturity would be influenced by the surrounding, un-restored vegetation, accounting for the growth of un-restored vegetation would have involved various assumptions regarding species composition and age, which would have introduced additional sources of modeling error. It should be noted, however, that the cumulative solar flux estimate does not account for the future solar flux attenuation provided by un-restored vegetation.

#### *Vegetation Height, Width and Density*

The height, width and density of riparian vegetation required for adequate stream shading will vary according to localized stream conditions such as tree overhang, channel width, orientation, gradient and stream flow (Chen *et al.* 1998b; DeWalle 2008; Guoyuan *et al.* 2012). Many advanced models exist that are capable of determining ideal restored conditions more discerningly, including some of the modules within Heat Source that were not used for this project (Johnson 2003; Li *et al.* 2012). For this study, all streams were assumed to have uniform shade requirements for attainment of desired stream temperatures. While this assumption is likely true for most tributary streams, shade requirements along the mainstem will generally be different from tributaries since the average channel width of the mainstem is greater (Moore *et al.* 2005). Based on the modeling results, the dimensions of restored vegetation under the restoration scenario are sufficient to meet or exceed effective shade targets for

95% of all streams in the watershed, including most of the mainstem. However, this amount of shade may be more than necessary for some streams. For instance, some of the smaller tributaries may require vegetation less than 27 meters in height or restoration buffers less than 15 meters wide, in order to attain stream temperatures in compliance with regulations.

The height of vegetation under restored conditions was derived from the average height at maturity (~55 years) for six of the most common riparian trees species planted in riparian areas. Should the actual tree species planted deviate from this chosen assemblage, the average height at maturity would also be subject to change. For example, a single pixel (3 ft.) of restorable area surrounded by un-restorable area would not realistically be able to support a full grown tree under most circumstances; these areas would likely be planted with smaller herbaceous plants or shrubs (BES 2001). Also, it is assumed that all tree species will be planted in a uniform distribution and will successfully reach a mature age unimpeded by natural processes such as competitive displacement, flooding or erosion. While the *mean* height of vegetation under restored conditions was used rather than the *maximum* height (27m), both under- and over- estimation of heights are possible sources of error.

The height of riparian vegetation required for adequate stream shading varies according to localized stream conditions such as channel width, hydrology, topography and stream orientation (DeWalle 2010; Larson and Larson 1996; Moore *et al.* 2005; Opperman and Merenlender 2004; Webb *et al.* 2008).

Generally, north-south oriented streams will require greater vegetation heights for sufficient shading compared to east-west oriented streams (Chen *et al.* 1998b; DeWalle 2008; Larson and Larson 1996).

Density estimates were derived from a single equation and uniformly applied to all riparian vegetation.

While the density of riparian vegetation is likely to vary with species composition, age, and understory growth, these factors were not considered in density estimates. Also, the effect of riparian shading diminishes with increasing stream width (Cristea and Burges 2010). As such, larger streams may require

riparian buffers as wide as the height of a mature tree (~30m) to meet their shading needs (DeWalle 2010; Fullerton *et al.* 2006; Moore *et al.* 2005). Conversely, smaller streams may require narrower buffers as well (DeWalle 2010).

### *Vegetation Quality*

All vegetation that is currently  $\geq 4\text{m}$  was not considered within the restorable area, with no regard to the species composition or overall quality of habitat provided by this vegetation. In some circumstances, where near-stream vegetation is overrun with invasive species for instance, vegetation currently  $\geq 4\text{m}$  in height would, in fact, be considered worthy of restoration by natural resource managers. Instead, it is assumed that the shade provided by this low quality vegetation would overshadow any sense of urgency in restoring these areas. Conversely, some vegetation currently less than 4m in height may be comprised of native shrubs and herbaceous grasses that would not be directly targeted for removal during restoration efforts. In reality, these areas would still be targeted for restoration in an effort to increase shade, but measures would be taken to avoid disturbing native understory shrubs and grasses.

## **4.4 Priority Rankings**

### *Site Suitability Criteria*

Site suitability criteria are the variables used to identify areas within the spatial extent of a project that are most deserving of riparian restoration. Criteria can be ecologically based or opportunistic, and in many cases a combination of one or more criteria are used in the selection of restoration sites (Fullerton *et al.* 2006; Landers 1997; Opperman & Merenlender 2004; Watanabe *et al.* 2005). For this project, the site suitability criteria used was effective shade, or the amount of incoming solar radiation that is blocked by vegetation before reaching the stream surface. Although effective shade is a commonly used indicator of healthy riparian systems, there are many other criteria that were not considered in this



prioritization scheme that will likely influence the outcome of restoration efforts (Kentula 1997; Webb *et al.* 2008). For example, the continuity of the riparian buffer or proximity to intact riparian habitat, although not included as a site suitability criteria, is believed to enhance the ability of riparian buffers to regulate stream temperature and, as such, is often considered in the prioritization of restoration sites (Fullerton *et al.* 2006). While there is a general lack of consensus regarding lengths of continuous riparian areas necessary for recovery of salmon populations or, more broadly, stream temperature reductions, many studies suggest lengths of continuous riparian habitat between 300-600m are ideal (Fullerton *et al.* 2006; Ryan *et al.* 2013).

Environmental attributes more directly related to climate, hydrology or channel morphology such as hyporheic exchange, stream flow, air temperature, stream width and depth, channel slope, floodplain width and connectivity, frequency of natural disturbances, substrate and soil moisture content are also important variables in stream temperature regulation that were not considered in this study as site suitability criteria (Kentula 1997; Landers 1997; Opperman & Merenlender 2004; Webb *et al.* 2008; WSDOE 2007). Lastly, prioritizing riparian areas for restoration without considering the social, political, and economic aspects will inevitably challenge and constrain the implementation of those projects (Kentula 1997). While socioeconomic criteria were not incorporated into the prioritization scheme for this project, it is assumed that future restoration efforts will be informed by a combination of socioeconomic aspects and ecological knowledge. From a management perspective, it is important to acknowledge and consider these additional factors when interpreting the results and implementing restoration efforts.

Partnering agencies involved with this project have indicated an interest in using the results from this study as one of many site suitability criteria they are likely to examine in their own prioritization schemes. The Johnson Creek Watershed Council for example, intends to incorporate the results from

this study into their 2013 Riparian Restoration Strategy, whereby sites will be prioritized for riparian restoration based on solar flux attenuation estimates as well as buffer continuity, stream flow, stream order, and landowner willingness (JCWC 2013). In sum, the taxlots, subwatersheds and jurisdictions prioritized in this project will be subject to additional screening criteria that will address important factors not considered in the modeling or prioritization process for this study.

### *Taxlot Outcomes*

Restoring a small percentage of all taxlots and restorable acres (~20% for each) resulted in a disproportionately large amount of increased solar flux attenuation (50% of the cumulative solar flux reduction). The restoration efficiency, or the net increase in solar flux attenuation per acre of restored area, is highly variable between taxlots. As such, using taxlots as the minimum restoration unit is not only appropriate but also promotes a high level of efficiency in the allocation of restoration efforts.

Minor differences in the average size and proportion of restorable area within taxlots were observed between different priority rankings (Table 4). High priority taxlots tended to have a comparatively higher proportion of restorable area within them and were smaller in size. By contrast, low priority taxlots had a comparatively low proportion of restorable area within them and were larger in size. Medium priority taxlots fell somewhere in between high and low, while maintain taxlots were both small in size and had a low proportion of restorable area within them. In sum, taxlots that exhibited the largest amount of change between current and restored conditions were those with the highest percentage of their restoration buffer deemed restorable.

### *Subwatershed Outcomes*

Prioritizing at the subwatershed or jurisdictional scale resulted in a lower level of efficiency in the allocation of restoration efforts compared to prioritization at the taxlot scale. Restoring only 22% of all

taxlots achieved the same amount of solar reduction as restoring 50% of all subwatersheds or 43% of all jurisdictions. Similarly, 39% of all taxlots were categorized as “maintain” whereas zero jurisdictions and only 6% of subwatersheds received this same ranking. In part, this is due to a reduced “signal” of landscape heterogeneity that resulted from using a coarser scale, or larger minimum restoration unit. For example, the percent of all restorable acres in each subwatershed ranking was much less pronounced compared to the percent of all restorable acres in each taxlot ranking. Similarly, the percentage of restoration buffer deemed restorable within each subwatershed and jurisdiction is relatively uniform across them all; meaning they all exhibit similar shade conditions and there is less variation to aid in the prioritization of restoration efforts.

When prioritization is performed at the comparatively coarser scale of subwatersheds or jurisdictions, fine scaled variations in the condition of riparian vegetation and stream morphology is lost during the process of aggregating total solar flux attenuation within these large areas. Using the finer scaled restoration unit of a taxlot can increase the efficiency of restoration efforts by highlighting aspects of landscape heterogeneity and using that knowledge to refine the site selection process.

### *Maintain Ranking Group*

The number of taxlots and acreage found to contribute 0 watts/acre to the cumulative solar flux reduction was somewhat unexpected. For some of these taxlots, all near-stream vegetation is currently  $\geq 4\text{m}$  and, as such, there is no difference between current and restored conditions which comes as no surprise. However, the majority (65%) of these taxlots had restorable area that, when restored, did not reduce heat loading to the stream. In other words, 68 acres of restorable area would not contribute to the cumulative solar flux reduction if restoration occurred here; this is most likely due to pre-existing topographic and vegetative conditions that provide sufficient shading to the stream, even when discontinuities in the riparian buffer are present. Furthermore, certain stream orientations (i.e. North

facing streams) require less shade than others, and the benefit of riparian vegetation will be smaller for these streams in terms of solar flux attenuation (DeWalle 2008; Opperman and Merenlender 2004).

While this ranking group was labeled as “maintain” it should not be assumed that restoration in these areas would lack any sort of ecological benefit. In addition to shade, restoring riparian vegetation provides numerous ancillary benefits, including erosion control, flood mitigation, water purification, improved channel complexity, formation of in-stream and riparian habitat and general ecosystem resilience (Chen *et al.* 1998; Gebhardt & Fischer 1999; Holmes *et al.* 2004; Johnson *et al.* 2007; Kentula 2007; Li *et al.* 2012; Niemi *et al.* 2006; ODEQ 2006; Teels *et al.* 2006). Some of these benefits may even lead to reduced stream temperatures indirectly (i.e. LWD recruitment and stream bank stability). In sum, the taxlots classified as “maintain” are currently providing an adequate level of shade but in no way should this determination imply that all other ecological processes that occur within the riparian complex are functioning properly as well.

## 5.0 Conclusion

### *Management Implications*

While the majority of the watershed (63% of all sampling nodes) currently meets the effective shade target of 80%, the remaining areas of concern are spatially diffuse, with individual streams exhibiting substantial longitudinal variability in terms of shade, with occasional clusters of high priority stream reaches. As a result of this spatial heterogeneity, prioritization of riparian restoration efforts is greatly influenced by the spatial scale of restoration efforts. Taxlots, subwatersheds, and jurisdictions within the Johnson Creek watershed have been prioritized for riparian restoration based on the net increase in solar flux attenuation per acre restored. Prioritizing at the scale of taxlots, as opposed to subwatersheds or jurisdictions, is likely to produce the largest returns, in terms of shade enhancement, from restoration

investments. Although the priority rankings assigned to taxlots are indicative of their ability to provide shade to the stream, it is not a measure of their overall worth in terms of habitat or opportunity. All taxlots should be subject to additional screening criteria such as landowner willingness, stream flow, community support, proximity to existing restoration projects, and fundraising opportunities. Taxlots classified as “maintain” may still provide ancillary benefits when restored and, as such, should still be included in additional screening efforts.

Data concerning solar flux attenuation and effective shade estimates and priority rankings can be used, at the discretion of each jurisdiction, to encourage landowner cooperation, community support, or fundraising prospects. In terms of monitoring overall watershed health, this data also provides a snapshot of the current status of riparian shade within the watershed.

### *Suggested Topics for Future Research*

The National Resource Council broadly defines restoration as "...re-establishment of pre-disturbance functions and related physical, chemical and biological characteristics." Given the broad definition of restoration, coupled with the inherent variability and stochasticity of physical, biological, and chemical phenomena, there is no universal formula for successful riparian restoration. To further compound the issue, restoration ecology is a relatively young interdisciplinary field and, as such, the literature tends to lack consensus and resolve on many issues (Johnson 2003; Landers 1997; Palmer 2009). In general, the relative effectiveness of individual prioritization and implementation strategies is both highly debated and difficult to assess given the existing body of literature, making it difficult to choose strategies with confidence (Opperman and Merenlender 2004; Palmer *et al.* 2005; Palmer 2009; Roni *et al.* 2002, 2008, 2010).

Major questions that remain to be answered include: Can smaller headwater streams be sufficiently shaded by short grasses and shrub vegetation? To what extent does tree overhang influence riparian

shade along streams of varying sizes? What are ideal buffer widths for streams of varying sizes and orientations? In sum, when choosing a riparian restoration strategy, a combination of socio-economic and informational limitations demands a careful, calculated consideration of trade-offs. Regardless of which limitations are encountered, restoration efforts are inherently risky endeavors; examples of both successes and failures abound (Beechie & Bolton 1999; Landers 1997; Roni *et al.* 2002, 2008, 2010). Given this high level of uncertainty, natural resource managers are encouraged to take an experimental approach to restoration and acknowledge the value of their contribution, whether a success or failure, to the body of knowledge surrounding restoration ecology (Landers 1997).

To assist natural resource managers in the prioritization of areas for riparian restoration efforts, more research is needed that evaluates the relative effectiveness of restoration techniques and prioritization schemes. Suggested topics for future research include: the influence of stream order, adjacent land use, land ownership, floodplain width, continuity and width of riparian buffers, hydrographic setting, channel slope and substrate, and soil moisture content on the long term effectiveness of riparian restoration efforts. Furthermore, monitoring the response of multiple indicators including macro-invertebrates, fish and wildlife, nutrient and sediment regimes, and even community perceptions will help to advance our understanding of the functional relationships that take place within the riparian complex and will capture more of the benefits received from our efforts. In turn, this knowledge can also help to advance our understanding of the relative effectiveness of restoration techniques and help managers choose their prioritization schemes more wisely.

A growing number of managers have begun to recognize the shortcomings of a piecemeal (ex: uncoordinated efforts or failure to recognize and protect the inter-relationships between ecological processes) approach to riparian restoration and have instead adopted a more refined, holistic approach that acknowledges the importance of many ecological processes at multiple spatial and temporal scales

in maintaining the riparian complex (Chen *et al.* 1998; Beechie & Bolton 1999; Fullerton *et al.* 2006; Harris & Olson 1997; Roni *et al.* 2002, 2008). These types of projects establish objectives that concern both biological resources and hydro-geological processes at broad spatial and temporal scales, such as enhancing regional ecological resiliency and habitat heterogeneity, or restoring the natural processes (i.e. disturbance regime or LWD recruitment) that maintain healthy ecological function of the riparian complex (Beechie & Bolton 1999; Palmer 2005; Roni *et al.* 2002, 2008; Seavy *et al.* 2009). While these holistic approaches, often referred to as "process-based restoration", are gaining in popularity, they can be prohibitively expensive and socio-economically unfeasible (Palmer *et al.* 2005; Seavy *et al.* 2009). In order to facilitate the gradual transition from current restoration strategies to more refined, holistic approaches, it is imperative that socioeconomic and ecological factors are both considered. Identifying effective, workable restoration strategies that can accommodate the socio-economic atmosphere of urban watersheds should be recognized as an important endeavor in the field of restoration ecology.

## References

- Allen, D., Dietrich, W. *et al.* (2007). Development of a mechanistically based basin-scale stream temperature model: Applications to cumulative effects modeling. USDA Forest Service Gen.Tech. Rep. PSW-GTR-194
- Baker, F.S. (1950). "Principles of Silviculture". McGraw Hill, New York
- Beechie, T. and Bolton, S. (1999). An approach to restoring salmonid habitat-forming processes in Pacific Northwest watersheds. *Fisheries*, 24(4), 6-15.
- Beschta, R. (1997). Riparian shade and stream temperature: An alternative perspective. *Society for Range Management* 19(2):25-28.
- Bisson, P.A., Quinn, T.P, Reeves, G.H and Gregory S.B. (1992). Best Management Practices, Cumulative Effects and Long-Term Trends in Fish Abundance in Pacific Northwest River Systems. Pgs 189-232 IN: R.J. Naiman, ed. "Watershed Management: Balancing Sustainability and Environmental Change". Springer-Verlag, New York.
- Boyd, M. and Sturdevant, D. (1997). The Scientific Basis for Oregon's Stream Temperature Standard: Common Questions and Straight Answers. Oregon Department of Environmental Quality. Accessed online at:  
<http://www.deq.state.or.us/wq/standards/docs/temperature/tempstdccibasis1996.pdf>
- Boyd, M. and Kasper, B. (2003). Analytical Methods for dynamic open channel heat and mass transfer: Methodology for heat source model Version 7.0. Accessed online June 2012 at:  
<http://www.deq.state.or.us/WQ/TMDLs/docs/tools/heatsourcemanual.pdf>
- Brokaw, N.V and Grear, J.S. (1991). Forest structure before and after hurricane Hugo at three elevations in the Luquillo Mountains, Puerto Rico. *Biotropica* 23: 386-392.
- Brungs, W.A. and B.R. Jones (1977). Temperature Criteria for Freshwater Fish: Protocol and Procedures. EPA Research Lab, Duluth, Minnesota.
- Bureau of Environmental Services (BES) (2001). Johnson Creek Restoration Plan. Accessed online at:  
<http://www.portlandoregon.gov/bes/article/214367>
- Chen, D., Carsel, R. *et al.* (1998). Stream temperature simulation of forested riparian areas: I. Watershed-scale model development. *Journal of Environmental Engineering*, 124, 304-315.
- Clark, D.A. & Clark, D.B. (1992). Life history diversity of canopy and emergent trees in a Neotropical rain forest. *Ecological Monographs* 62: 315-344.
- Cline, S. P., & McAllister, L. S. (2012). Plant succession after hydrologic disturbance: inferences from contemporary vegetation on a chronosequence of bars, Willamette River, Oregon, USA. *River Research and Applications*, 28(9), 1519-1539.



- Dawkins, H.C. and Field, D.R. (1978). A long term surveillance system for British woodland vegetation. Department of Forestry, University of Oxford.
- Fryer, J.L. and Pilcher, K.S. (1974). Effects of Temperature on Diseases of Salmonid Fishes. EPA, Western Fish Toxicology Lab, Corvallis, Oregon.
- Fujita, A. *et al.* (2003). Canopy structure in a temperate old-growth evergreen forest analyzed by using aerial photographs. *Plant Ecology* 168: 23-29.
- Fullerton, A.H., T.J. Beechie, S.E. Baker, J.E. Hall and K.A. Barnas. (2006). Regional patterns of riparian characteristics in the interior Columbia River basin, Northwestern USA: applications for restoration planning. *Landscape Ecology* 21:1347-1360.
- Gebhardt, K. and Fischer, H. (1999). Using surrogates for stream temperature nonpoint source water quality loading allocation. Proceedings of the Seventh Biennial Watershed Management Conference: Water Resources Center Report No. 98, University of California Davis.
- Gergel, S.E, Y. Stange, N.C. Coops, K. Johansen and K.R. Kirby. (2007). What is the value of a good map? An example using high spatial resolution imagery to aid riparian restoration. *Ecosystems* 10:688-702.
- Goodwin, C., Hawkins, C. and Kershner, J. (1997). Riparian restoration in the western United States: Overview and perspective. *Society for Ecological Restoration* 5(4S), 4-14.
- Harris, R. and Olson, C. (1997). Two-stage system for prioritizing riparian restoration at the stream reach and community scales. *Restoration Ecology*, 5(4S), 34-42.
- Holmes, T.P., J.C. Bergstrom. E. Huszar, S.B. Kask and O. Fritz. (2004). Contingent Valuation, net marginal benefits and the scale of riparian forest ecosystem restoration. *Ecological Economics* 49:19-30.
- Jennings, S.B., Brown, N.D. and Sheil, D. (1999). Assessing forest canopies and understory illumination: canopy closure, canopy cover and other measures. *Forestry* 72(1): 59-73.
- Johnson Creek Watershed Council (JCWC)
- 2012 State of the Watershed Report. Accessed online at: <http://jcw.org/wp-content/uploads/2012/05/2012StateoftheWatershed.pdf>
- 2013 A strategy for riparian restoration in the Johnson Creek watershed. Accessed online at: [http://jcw.org/wp-content/uploads/2013/05/riparian-strategy-poster\\_small.pdf](http://jcw.org/wp-content/uploads/2013/05/riparian-strategy-poster_small.pdf)
- Johnson, S. (2003). Stream temperature: scaling of observations and issues for modeling. *Hydrological Processes* 17:497-499.
- Johnson, T.E., J.N. McNair, P. Srivastava and D.D. Hart. (2007). Stream ecosystem responses to spatially variable land cover: an empirically based model for developing riparian restoration strategies. *Freshwater Biology* 52:680-695.

- Kentula, M.E. (1997). A comparison of approaches to prioritizing sites for riparian restoration. *Restoration Ecology* 5(4S):69-74.
- Landers, D.H. (1997). Riparian restoration: Current status and the reach to the future. *Restoration Ecology* 5(4S):113-121.
- Larson, L. and Larson, S. (1996). Riparian Shade and Stream Temperature: A Perspective. *Rangelands* 18(4):149-152.
- Li, G., Jackson, C. *et al.* (2012). Modeled riparian stream shading: Agreement with field measurements and sensitivity to riparian conditions. *Journal of Hydrology*, 428-429, 142-151.
- Lowry, T., Tidwell, V. and Cardwell H (2008). Evaluating Reservoir operations and other remediation strategies to meet temperature TMDL's in the Willamette Basin, Oregon. World Environmental and Water Resources Congress. ASCE
- Moriasi, D.N. *et al.* (2007). Model evaluation guidelines for systematic quantification of accuracy in watershed simulations. *Transactions of the ASABE* 50(3): 885-900.
- Nakashizuka, T., Katsuki, T. and Tanka, H. (1995). Forest canopy structure analyzed by using aerial photographs. *Ecological Research* 10: 13-18.
- National Marine Fisheries Council (2013). Endangered and Threatened Marine Species. Accessed online November 2013 at: [http://www.nmfs.noaa.gov/pr/pdfs/species/esa\\_table.pdf](http://www.nmfs.noaa.gov/pr/pdfs/species/esa_table.pdf)
- Nehlsen, W. (1997). Prioritizing watersheds in Oregon for salmon restoration. *Restoration Ecology* 5(4S), 25-33.
- Niemi, E., Lee, K., and Raterman R. (2006). Net economic benefits of using ecosystem restoration to meet stream temperature requirements. ECO Northwest.
- Niemic *et al.* (1995). Hardwoods of the Pacific Northwest. OSU Forest Research Laboratory: College of Forestry. Accessed online November 2013 at: <http://ir.library.oregonstate.edu/xmlui/bitstream/handle/1957/7623/RC8.pdf?sequence=1>
- Opperman, J.J and A.M. Merenlender. (2004). The effectiveness of riparian restoration for improving instream fish habitat in four hardwood-dominated California streams. *North American Journal of Fisheries Management* 24(3): 822-834.
- Oregon Department of Environmental Quality (ODEQ)
- 1995 1992-1994 Water Quality Standards Review: Temperature. Accessed online at: <http://www.deq.state.or.us/wq/standards/docs/temperature/19921994wqStandardsReviewTemperature.pdf>
- 2006 Willamette Basin TMDL: Lower Willamette Subbasin Water Quality Summary Ch. 5 (p. 5-103)

- 2011 Temperature Standard Rule. OAR-340-041-0028. Accessed Online November 2013 at:  
[http://arcweb.sos.state.or.us/pages/rules/oars\\_300/oar\\_340/340\\_041.html](http://arcweb.sos.state.or.us/pages/rules/oars_300/oar_340/340_041.html)
- Palmer, M., Bernhardt, E., *et al.* (2005) Standards for ecologically successful river restoration. *Journal of Applied Ecology*, 42, 208-217.
- Palmer, M. (2009). Reforming watershed restoration: Science in need of application and applications in need of science. *Fisheries and Coasts*, 32, 1-17.
- Richter, A. and Kolmes, S. (2005). Maximum temperature limits for Chinook, Coho, and Chum salmon, and Steelhead Trout in the Pacific Northwest. *Reviews in Fisheries Science*, 13, 23-49.
- Roni, P., Beechie, T. *et al.* (2002). A Review of stream restoration techniques and a hierarchical strategy for prioritizing restoration in Pacific Northwest watersheds. *North American Journal of Fisheries Management*, 22(1), 1-20.
- Roni, P., Hanson, K. and Beechie, T. (2008). Global review of the physical and biological effectiveness of stream habitat rehabilitation techniques. *North American Journal of Fisheries Management*, 28(3), 856-890.
- Roni, P., Pess, G. *et al.* (2011). Estimating Changes in Coho salmon and Steelhead abundance from watershed restoration: How much restoration is needed to measurably increase smolt production? *North American Journal of Fisheries Management*, 30(6), 1469-1484.
- Santhi, C, *et al.* (2001). Validation of the SWAT model on a large river basin with point and nonpoint sources. *Journal of American Water Resources Assoc.* 37(5): 1169-1188.
- Seavy, N.E., T. Gardali, G.H. Golet, F.T. Griggs, C.A. Howell, R. Kelsey, S.L. Small, J.H. Viers and J.F. Weigand. (2009). Why climate change makes riparian restoration more important than ever: recommendations for practice and research. *Ecological Restoration* 27(3):330-338.
- Sturdevant, D. (2008). Temperature water quality standard implementation: A DEQ internal management directive. Oregon Department of Environmental Quality.
- Teels, B., Rewa, C. and Myers, J. (2006). Aquatic condition response to riparian buffer establishment. *Wildlife Society Bulletin*, 34(4), 927-935.
- Tompkins, M.R. and G.M. Kondolf. (2000). Integrating geomorphic process approach in riparian and stream restoration: Past experience and future opportunities. 231-239.
- United States Fish and Wildlife Service (USFWS). ( 2013). Listings and Occurrences for Oregon. Accessed online November 2013 at:  
[http://ecos.fws.gov/tess\\_public/pub/stateListingAndOccurrenceIndividual.jsp?state=OR&s8fid=112761032792&s8fid=112762573902](http://ecos.fws.gov/tess_public/pub/stateListingAndOccurrenceIndividual.jsp?state=OR&s8fid=112761032792&s8fid=112762573902)

United States Geological Survey (USGS) (2007). Temperature effects of point sources, riparian shading, and dam operations on the Willamette River, Oregon. In Scientific Investigations Report 2007-5185.

Van Liew, M. W., J. G. Arnold, and J. D. Garbrecht. (2003). Hydrologic simulation on agricultural watersheds: Choosing between two models. *Transactions of the ASABE* 46(6): 1539-1551.

Washington State Department of Ecology (WSDOE) (2007). Modeling the effects of riparian buffer width on effective shade and stream temperature. Accessed Online November 2013 at:  
<https://fortress.wa.gov/ecy/publications/publications/0703028.pdf>

Watanabe, M., R.A. Adams, J. Wu, J.P. Bolte, M.M. Cox, S.L. Johnson, W.J. Liss, W.G. Boggess and J.L. Ebersole. (2005). Toward efficient riparian restoration: integrating economic, physical and biological models. *Journal of Environmental Management* 75:93-104.

## Glossary

**Canopy closure:** the proportion of the sky hemisphere obscured by vegetation when viewed from a single point.

**Cumulative solar flux reduction:** the net increase in solar flux attenuation ( $\text{watts/m}^2/\text{d}$ ) for the entire watershed under a restoration scenario.

**Effective shade:** the percentage of direct beam solar radiation attenuated and scattered by riparian vegetation before reaching the ground or stream surface (ODEQ 2006).

**Restorable area:** all area within the restoration buffer that is currently occupied by vegetation <4 meters in height and is not occupied by roads or buildings.

**Restoration buffer:** the area in which restoration activities are likely to occur. It extends 15m to either side of the stream channel for Johnson Creek mainstem and all tributary streams.

**Restoration efficiency:** the net increase in solar flux attenuation per acre restored (solar flux attenuation/acre).

**Restored conditions:** the condition of riparian vegetation following the implementation of restoration activities that are likely to occur throughout the watershed, with vegetation in restorable areas at a climax life stage and vegetation within un-restorable areas in the same state as current day conditions.

**Restoration scenario:** all restorable area is set equal to 27 meters in height whereas all un-restorable remains unchanged from current conditions.

**Site suitability criteria:** ecological, socioeconomic, or physical attributes used to identify areas that are most deserving of restoration.

**Solar flux attenuation:** the amount of incoming direct beam solar radiation ( $\text{watts/m}^2/\text{d}$ ) that is attenuated by riparian vegetation before reaching the stream surface. Percent effective shade is a commonly used metric for quantifying solar flux attenuation.

**Solar insolation:** The amount of energy received from the sun at the earth's surface; on a clear day  $\sim 1000 \text{ W/m}^2$  reaches a surface perpendicular to the incoming radiation. This energy varies due to the angle of the incoming radiation and cloud cover.

**Un-restorable area:** all area within the restoration buffer that is currently occupied by vegetation  $\geq 4$  meters in height, or buildings or roads.

**Vegetation density:** in this study, vegetation density is defined as an estimate of canopy closure.